Tumor, where good ideas come from, innovation in intervention

K Murphy

Joint Department of Medical Imaging, UHN Mt Sinai WCH, University of Toronto, Toronto, Canada

Metastatic tumors are the most common tumors of bone affecting 10-30% of all cancer patients. Spinal mets are found in 36% of patients who die of cancer. The tumors that most commonly spread to bone are prostate, breast lung kidney and thyroid. These account for 80% of boney mets. The 5 year survival after diagnosis of lung mets is 2% and thyroid is 44%. Pain is the most common presenting complaint and it is usually progressive, unrelenting and poorly controlled. Radiation therapy has been shown to be effective in 75-90% of patients but the benefit is not felt for 2 to 12 weeks after the treatment.

Cord compression from tumor was first described by Elsberg in 1916 in his work "Diseases of the spinal cord and its membranes". 1 in 12700 cancer patients will develop cord compresion. Globally most of these patients will be treated with steroids and radiation. Vast Rad Onc studies of up to 5400 patients have studied the role of IGRT SBRT SABR or HIGRT and other tightly columated spinal radiation therapy to treat spinal mets and cord compresion. The rigour of these NCI NIH CIHR and international studies is admirable. It is clear the role of surgey is limited to the relief of cord compresion causing myelopathy in patients with greater than 1 month life expectancy. Do we as interventionalist have a role in this patient population. Do we have the technology that would allow us have a lower risk minimalist impact on these patients quality of life. Multiple small studies of between 30 and 2 patients would say that we do have s something to offer. Our studies are Cochran level 3 or lower in most cases however. Our interventions are currently paliative and our role is niche. This is unlike our role in Liver primary or secindray disease where RFA TACE Y90 is changing survival, and allowing patients become eligible for liver transplant.

If we are to go beyond the palliative intervention described above and move into to the definitive treatment of patients with oligo metastatic disease ie limited metastatic disease in 5 sites or less we need to apply a new level of rigor and total tumor kill, with by definition marginal obliteration that we currently dont deliver. The application of pre procedural radiation theraphy soft ware planing and dose distribution estimation is critical. The is

the subject of our research for the past 2 year. In this section of this session I will review the state of the literature and discuss our approach to oligo metastatic disease. In addition i will discuss the paucity of innovation in our field since the late 90s and the need for renewed effort.



Modular scaffold engineering for skeletal reconstruction

SJ Hollister

The University of Michigan, Michigan, IL, USA

Large skeletal defects present significant challenges to restoring natural tissue, geometry, and load bearing. Tissue engineering approaches combining scaffolds with osteobiologics (i.e. cells and/or growth factors) have long been proposed to repair such defects when conventional bone grafting or implant therapies fail. However, to date there has been limited large pre-clinical model testing of such approaches, let alone clinical implementation. This can be attributed in part to the significant technical challenges faced in reconstructing large defects and in part to the significant regulatory and commercial challenges that face even a technically successful approach. Clearly, there is no silver bullet for skeletal reconstruction.

The combination of no technical silver bullet with the significant regulatory challenges has led us to propose a modular approach to skeletal tissue engineering (Hollister and Murphy, Tissue Eng., This modular approach not only incorporates integration of multiple structural and biologic components to create a skeletal engineering therapy, but also integrates multiple design and manufacturing processes to achieve these integrated therapies that bridge multiple scales. In this talk, we will address how to design, fabricate, and functionalize skeletal engineering constructs at multiple scales, touching upon how such platform technologies can interface with regulatory requirements.

The ultimate goal is to create an engineering platform that allows design of constructs to reconstruct any complex defect as well as the fabricate capability to such constructs. a platform Furthermore, given that such technology provides a plethora of design choices (e.g. scaffold material, scaffold pore architecture design, scaffold surface modification, osteobiologics) which raises questions as to what choice of modular components will lead to optimal skeletal regeneration, and how do we test such choices for example in vitro, in small animal models or in large pre-clinical animal model. In this talk we will also present results on how choices of material, architecture design and biologic affect bone regeneration in vivo. Open questions and issues resulting from the modular

approach will finally be presented to forge a path going forward.



Biodegradable property of octacalcium phosphate-hyaluronic acid composites as bone substitute materials

K Suzuki^{1, 2}, T Anada², T Miyazaki², N Miyatake², M Hosaka¹, H Imaizumi², E Itoi¹, O Suzuki²

¹ Dept Orthop Serg, Grad Sch Med, Tohoku Univ, Sendai, Japan. ² Div Craniofac Funct Eng,

Tohoku Univ Grad Sch Dent, Sendai, Japan.

INTRODUCTION: Octacalcium phosphate (OCP; Ca₈H₂(PO₄)₆·5H₂O) enhances in vitro osteoblastic differentiation [1,2] and osteoclast formation [3]. OCP is used as a source material for osteoconductive inorganic-polymer composites, such as OCP/gelatine [4]. It is of interest to learn whether OCP can be used as an injectable material in bone defects. We have reported that hyaluronic acid (HyA) works as an agent to combine OCP without losing the osteoconductivity and provide the injectability [5]. However. the effect of HvA biodegradability of OCP and the cellular response in bone formation remains unclear. In the present study, bone tissue response and in vitro osteoclastic response to OCP/HyA were examined.

METHODS: OCP was prepared by a previously reported direct precipitation method [6]. Three sodium hyaluronic acids with different molecular weights were used: 1) 9 x 10^5 , 2) 19 x 10^5 and 3) 60×10^5 . The granules of OCP (300 to 500 µm in diameter) and HyAs were mixed at room temperature. The composites were referred to as OCP/HyA90, OCP/HyA190 and OCP/HyA600 (a chemically-modified sodium hyaluronate derivative). These composites or OCP alone were implanted respectively in polytetrafluoroethylene (PTFE) rings (OD 8 mm, ID 6 mm, 1 mm thickness), and placed onto eight-week old ICR mice until 6 weeks. The rate of the remaining implants was histomorphometrically estimated after decalcification and hematoxylin and eosin staining. The area was calculated using Image J, a public-domain software (NIH Image, USA). Osteoclastic cells were formed by incubating macrophage RAW264 cells with RANKL in the presence or absence of HyAs and OCP. Tartrateresistant acid phophatase (TRAP) staining was used to estimate the effect of the HyAs and OCP.

RESULTS: OCP/HyAs exhibited liquidity (Fig.1) thereby the composites were easily able to inject into PTFE ring at the surgical operation. The bone formation was observed primarily around OCP granules in HyAs until 6 weeks. However, it seems likely that the capability of bone formation differs

much from the type of HyA used for combining OCP: OCP/HyA90 and OCP/HyA600 could be enhancing the osteoconductivity of OCP more than that of OCP alone. Histomorphometric analysis revealed that the biodegradation of the three composites was enhanced with time but the rates were similar with OCP alone. In vitro assay suggested that HyAs may have a role stimulating osteoclast formation if co-existed with OCP.



Fig. 1: Image of an OCP/HyA composite.

DISCUSSION & CONCLUSIONS: The present study confirmed that HyAs provide OCP the injectability in handling at the operation and suggests that HyAs modify the osteoconductivity of OCP through increasing the cellular activity in particular bone formation and/or resorption—related cells. Further study is underway to establish the linkage between the osteoconductivity and the biodegradability of OCP/HyAs composites.

REFERENCES: ¹ O Suzuki, et al (2006) *Biomaterials* **27**:2671-2681. ² T Anada, et al (2008) *Tissue Eng Part A* **14**:965-978. ³ M Takami, et al (2009) *Tissue Eng Part A* **15**:3991-4000. ⁴ T Handa, et al (2012) *Acta Biomater* **8**:1190-1200. ⁵ K Suzuki, et al (2013) *Key Eng Mater* **529-530**:296-299. ⁶ O Suzuki, et al (1991) *Tohoku J Exp Med* **164**:37-50.

ACKNOWLEDGEMENTS: This study was supported in part by Grants-in-aid (23390450, 2363988, 23650282, and 23106010) from the MEXT and JST FS A-STEP.



Osteo-articular pathological calcifications: a physico-chemical point of view

P Gras¹, C Rey¹, S Sarda¹, C Combes¹

¹ CIRIMAT, INPT-UPS-CNRS, University of Toulouse, ENSIACET, Toulouse, France

INTRODUCTION: Osteoarthritis (OA) is the most common form of rheumatic diseases, leading ultimately to chronic pain and disability for the patient. Aggravating factors identified to date include a family history of OA, mechanical overload, older age, and the presence of calciumcontaining microcrystals in the joint. The two main types of calcium-containing crystals found in the joint (synovial fluid and cartilage) are hydrated calcium pyrophosphates (CPP: Ca₂P₂O₇, nH₂O) and calcium phosphates crystals (CaP including octacalcium phosphate, carbonated apatite, etc.) [1]. Although the physico-chemical reactivities of synthetic and biological CaP phases are largely studied in the literature, the formation and dissolution of CPP crystals has been less investigated and not fully understood. Like for CaP crystals, in vitro synthesis of CPP phases appears as an alternative route to progress easier and faster in the understanding of the mechanism of their formation in vivo. The objective of this and study is to synthesize characterize nanocrystalline apatites and CPP phases of biological interest and to study their properties in aqueous medium.

METHODS: Nanocrystalline apatites and various hydrated CPP phases have been prepared by precipitation in aqueous solution at controlled pH and temperature. Some precipitates have been left to mature in the mother solution during various periods of time. The as-synthesized and matured precipitates have been characterized by using powder X-Ray diffraction, FTIR and Raman spectroscopies, thermogravimetry (ATG), scanning electron microscopy (SEM) and chemical analysis. Dissolution tests have also been performed.

RESULTS: The main structural characteristic of biomimetic nanocrystalline apatites, as demonstrated especially by spectroscopic analyses is an association of rather stable apatite domains forming the core of the nanocrystals associated with a surface hydrated layer containing mainly bivalent ions such as Ca²⁺, HPO₄²⁻ or CO₃²⁻ in "non-apatitic" environments. These structural characteristics determine the chemical and biological properties of these compounds:

maturation, ionic exchange and adsorption properties [2].

In the case of CPP phases, we showed that monoclinic and triclinic CPP dihydrates (Ca₂P₂O₇, 2H₂O), the most common polymorphs encountered *in vivo*, are formed only at high temperature and in acidic media with the synthesis system implemented *in vitro*. An amorphous phase was found to form easily in a wide range of pH and temperature. This phase is very stable and do not crystallize even after several years at 37°C. Such a stability of amorphous CPP was also pointed out by Slater et al. in other conditions of synthesis [3].

DISCUSSION & CONCLUSIONS: Several articles have suggested that amorphous phase precursor route was the most common process of minerals formation in vivo [4]. Amorphous CaP or CPP phases can be easily obtained in vitro, whereas the low supersaturation ratio in vivo should not favor the formation of amorphous phases. However, other components in biological fluids can promote their formation and/or stabilize these phases. Physical-chemical studies on calcium phosphate and pyrophosphate phases formation should be developed for explaining the dynamic involved in crystal phenomena osteoarthritis and also for exploring new methods allowing an improvement of the diagnostic.

REFERENCES: ¹ E.S. Molloy and G.M. McCarthy, (2006) *Rheum. Dis. Clin. North Am.* **32**:383-400. ² D. Eichert, C. Drouet, H. Sfihi, et al (2007) Nanocrystalline apatite-based biomaterials: synthesis, processing and characterization in *Biomaterials Research Advances* (ed. J.B. Kendall) Nova Science Publishers, pp 93-143. ³ C. Slater, D. Laurencin, V. Burnell, et al (2011) *J Mater Chem* **21**:18783-91. ⁴ S. Weiner, I. Sagi and L. Addadi (2005) *Science* **309**:1027-8.

ACKNOWLEDGEMENTS: The authors thank the Institut National Polytechnique de Toulouse (PRECIPYCA project – BQR INPT 2011) and the Centre National de la Recherche Scientifique (CalArthros project - "Longévité et Vieillissement 2010" CNRS interdisciplinary program) for supporting this research work.



Hip repair and prophylaxis

J Lane

Hospital for Special Surgery, New York, NY, USA

Osteoporosis is noted for the increased fracture risk, particularly following a low energy fragility fracture. Unfortunately, less than 25% of patients sustaining a low energy fracture actually undergo drug therapy. As a result, for the majority of individuals with fragility fracture there is a five-fold increased risk of vertebral fracture and a two-fold increased risk of hip fracture.

Currently, treatment strategies are primarily directed at systemic interventions including calcium, vitamin D and drugs. The initiation of treatment at the time of the fragility fracture is not only appropriate but clearly understandable to the patient ("perfect storm" concept). An alternative approach would be to utilize local secondary fracture prevention.

The primary target for local prevention would be hip fracture. Fourteen percent of patients undergoing a fractured hip are at risk for the contralateral hip fracture within 5 years. A hip fracture profoundly compromise the patient with 70% losing mobility skills and 24% dying within one year.

To prevent hip fracture the goals could include prophylactic implant fixation, biomechanical enhancement and biological stabilization.

Cannulated screw insertion would only prevent femoral neck fractures and not influence intertrochanteric fractures. Conversely, the insertion of materials to enhance bone mass and improve bone biology throughout the peritrochanteric region would address all forms of hip fracture.

Candidates for rapid bone mass augmentation are centered on injectable ceramics, glasses and polymers. The advantage of ceramics rests in their ability to be integrated and remodeled compared to polymers (PMMA) and glass.

Drugs and biologics include anti-resorptives such as the bisphosphonates, anabolics such as PTH's, and growth factors such as BMPs.

The local insertion of an agent that prevents a secondary fracture is feasible and attractive [1-3]. It could easily be performed under the same anesthesia as the fracture hip repair. By the time the patient has recovered from the primary hip

repair, the contralateral hip would be protected. Systemic drugs require 6+months to work and only decrease the hip fracture rate by 40%. Local treatment would work more rapidly and possibly with greater efficacy. Now is the time to test this avenue of intervention.

REFERENCES: ¹ E. Verron, O. Gauthier, P. Janvier et al (2010) *Biomaterials* **31**:7776-84. ² M. Tanzer, D. Karabasz, J.J. Krygier et al (2005) *Clin Orthop Relat Res* **441**:30-9. ³ B. Peter, D.P Pioletti, S. Laib et al (2005) *Bone* **36**:52-60.

ACKNOWLEDGEMENTS: The support provided by the NIH grant 1 RO1 AR041325 is acknowledged.



Bisphosphonate-combined matrices to prevent osteoporotic fractures

JM Bouler, O Gauthier, J-N Argenson, S Parratte, E Verron, P Janvier, B Bujoli INSERM UMR 791, Dental College, University of Nantes, Nantes, France

INTRODUCTION: The integration of drugs and devices is a growing force in the medical industry. The incorporation of pharmaceutical products not only promises to expand the therapeutic scope of device technology but to design a new generation of true combination products whose therapeutic value stem equally from both the structural attributes of the device and the intrinsic therapy of the drug. In this context, a new calcium phosphate cement-based (CPC) medical device developed, capable of providing mechanical reinforcement and delivering a bisphosphonate (BP) antiresorptive drug locally [1]. While BPs behave as setting retardants, a novel and efficient route was designed for introducing alendronate in a CPC while keeping the main properties of the cement suitable for practical application as a drug combination system, implantable by minimally invasive surgery. We aimed to evaluate both biological (sheep) & biomechanical (human cadavers) consequences of the femoroplasty using this new drug-combination device.

METHODS: An Alendronate-combined CPC has been implanted in proximal femurs of sheep presenting an induced osteopenia for 12 weeks. 3D-µCT analysis was conducted on all implanted and control femurs. Bone volume density (BV/TV), trabecular thickness (TbTh), space between trabeculae (TbSp) and number of trabeculae (TbN) were measured. Twelve paired human cadaveric femora from donors with a mean age of 86.3 years (7 women and 5 men) were included in this study. One femur from each donor was randomly assigned for femoroplasty (Fig. 1) and biomechanically tested for fracture load against their contra-lateral control. A-P and lateral radiographs and DXA scans were acquired before injection. Femoroplasty was performed under fluoroscopic and all femurs were fractured by simulating a lateral fall on the greater trochanter by an independent observer [2].

RESULTS: Osteoporosis induction is confirmed by a 40% decrease of BV/TV (iliac crest). After 12 weeks of implantation a peripheral CPC resorption and significant modifications of the surrounding bone density and micro architecture are observed in all injected proximal femurs. Comparing treated

versus control femurs, $3D-\mu CT$ measurements show significant increases (p<0.05) for BV/TV

(+29.4%), TbTh (+15.4%) and TbN (+21.8%) and a significant decrease for TbSp (-15.3%). These modifications were confirmed by histological and SEM observations. Mean T-score of the tested femurs was -3.4 (SD±1.53). All cadaveric femur presented Kyle II trochanteric fractures. Mean fracture load was 2786 Newton in femoroplasty group (group F) versus 2116 Newton in the control group (group C) (p<0.001). Fracture loads were always higher in the group F: mean 41.6% (mini: 1.2%/maxi:102.1%) (p=0.00024). Effect of femoroplasty was significantly superior for women (+57%) and also correlated to initial BMD (p<0.0001). A positive correlation between BMD and fracture load was observed both in control femurs ($r^2 = 0.74$) and reinforced femurs



 $(r^2 = 0.81)$.

Fig. 1: X-Ray of a cadaveric femur augmented with BP-loaded CPC

DISCUSSION & CONCLUSIONS: This *in vivo* investigation showed a promising ability of an alendronate-loaded cement to resorb while promoting new bone formation and improving bone micro-architecture.

REFERENCES: ¹ V. Schnitzler et al *Acta Biomater* (2011) **7(2)**:759-70. ² P. Heini et al *Clin Biomechanics* (2004) **19**:506

ACKNOWLEDGEMENTS: This work was supported by ANR TecSan (MIADROS Program) and BPI.



Injectable BMP-2 containing hydrogels for bone regeneration

J Hilborn

Chemistry Department – Ångström Laboratory, Science for Life Laboratory, Uppsala University, Uppsala, Sweden.

The gold standard procedure for the treatment of alveolar cleft is autologous transplantation. Although the technique where cancellous bone from the anterior iliac crest is used, gives bone healing in approximately 90% in follow-up studies [1] and is considered safe with complication rates, the procedure is accompanied by donor-site morbidity including pain, scarring, risk of bleeding, infection and nerve injury. [2] To avoid these complications, and to shorten surgery time and hospital stay, bone substitutes including bone morphogenetic protein-2 (BMP-2) have been studied. The BMP-2 efficacy in a clinical setting is however remarkably low and superfysiological milligram doses of the growth factor are required to obtain therapeutic results. Interestingly, the carrier used for BMP-2 delivery has been shown to affect efficassy significantly.

For a number of years, our laboratory has been working with hyaluronic acid (HA)-based hydrogels. These are extremely biocompatible and degraded enzymatically by the endogenous enzyme hyaluronidase. We have successfully evaluated these as carriers of BMP-2 to obtain ectopic and orthotopic bone at the site of injection [3-5] as well as to heal critical-sized cranial defects [6] in large animal models. In addition, tailored versions of these hydrogels may engineer significant amounts of mandibular bone upon subperiosteal injection in rats [4]. The material acts as an expander that defines the space to be substituted by newly formed bone.

Despite the the lowered concentration of BMP-2 and successful outcome in animal trials, trials in humans resulted in unacceptable swelling although adquate bone formation resulted [7]. We have therefore optimized the source of BMP-2, [8] the stability of the hydrogel crosslinks, the handelling of the gel, incoporation of extracellular cell adhesive fragments [9] and used precomplexation with heparin to result in improved bone fomation at lower BMP-2 doses. Using these strategies we are convinced that significant increase in BMP-2 stabilization and release profiles can be achieved.

REFERENCES: ¹ O. Bergland, G. Semb and F.E. Abyholm (1986) Cleft Palate J 23(3):175-205. 2 M.A. Rawashdeh and H. Telfah (2008) Br J Oral Maxillofac Surg 46(8):665-670. 3 K. Bergman, T. Engstrand, J. Hilborn et al (2009) J Biomed Mater Res Part A 91A(4):1111-1118. 4 E. Martinez-Sanz, D.A. Ossipov, J. Hilborn et al (2011) J Contr *Release* **152(2)**:232-240. ⁵ G. Hulsart-Billstrom, Q. Hu, K. Bergman et al (2011) Acta Biomater **7(8)**:3042-3049. ⁶ A. Docherty-Skogh, Bergman, M.J. Waern et al (2010) Plast Reconstr Surg 125(5):1383-1392. 7 E. Neovius, M. Lemberger, A.C. Skogh et al (2013) J Plast Recon Aestic Surg 66(1):37-42. 8 M. Kisiel, M. Ventura, P. Oommen, Oommen et al (2012) J Contr Release **162(3)**:646-653. 9 M. Kisiel, M. Martino, M. Ventura et al (2013) *Biomater*ials **34(3)**:704-712.



Bone reconstruction with a bupivacaine-loaded injectable calcium phosphate cement can reduce postoperative pain after iliac bone graft harvesting procedure in a canine model

O Gauthier^{1, 2}, X Plaetevoet¹, E Verron², BH Fellah¹, P Janvier³, D Holopherne-Doran¹, JM Bouler²

¹Preclinical Investigation and Research Center, ONIRIS College of Veterinary Medicine, Nantes, France. ²INSERM U791, LIOAD, University of Nantes, Nantes, France. ³CNRS, UMR 6230, CEISAM, University of Nantes, Nantes, France.

INTRODUCTION: The aims of our study were:

- To establish an animal model that would reproduce the human iliac crest bone graft harvesting procedure;
- To evaluate the induced pain after such a harvesting procedure;
- To evaluate the benefit in pain relief obtained with a CaP cement loaded with bupivacaine compared to the same cement without any analgesic agent.

MATERIALS AND METHODS: A 2 x 2 cm square bone defect was created with an orthopaedic bur on the iliac wing, mimicking a unicortical posterior iliac bone graft, on 12 adult female beagle dogs, according to European Community guidelines for the care and use of laboratory animals (2010/63/UE) after approval of the Local Animal Welfare Committee. Briefly, with the animal in lateral recumbency, a dorsal approach of the left iliac crest was performed. The middle gluteal muscle attachements were incised dorsally and cranially on the iliac crest, elevated and reflected ventrally together with the deep gluteal muscle to expose the whole iliac wing. The contours of the iliac bone defect were stamped with the bur and the inner iliac trabecular bone was removed with the bur. Each dog was implanted unilaterally with either the bupivacaine-loaded CaP cement [1] or the unloaded control one (Graftys® OUICKSET cement). A few minutes after cement injection, the muscle flap was repositioned over the defect and the middle gluteal muscle attachements were sutured dorsally with absorbable sutures. Subcutaneous and skin sutures were routinely performed. Postoperative evaluations performed 6h, 12h, 24h after cement injection and every 24h until day 7. They included physical and orthopedic examinations that defined a lameness score, a visual analogic scale pain score and a postoperative pain score using the 4A-Vet pain scale. Sensitivity measurements (n=3) with a Von Frey sensor were carried out by application of progressive pressure with a plastic cone on predetermined locations until the animal reacted (between the two first lumbar vertebras, laterally to the tibio-patellar ligament, medially to the iliac crest and on the iliac insertion of the middle gluteal muscle just over the surgical site). Rescue analgesia with morphine was available. Six months after the first surgery, the 6 animals that had received the control unloaded cement underwent the same surgical procedure on the contralateral iliac crest where the created bone defect was left unfilled to provide negative control sites. Osteointegration of the CaP cement was investigated with CT, microCT and histology.



Fig. 1: CT image of the dog pelvis with both cement filled and unfilled iliac crest bone defects

RESULTS: Pain relief after cement bone filling was highly significant regardless the cement used, compared to unfilled surgical site conditions where significant postoperative pain was observed during the first 4 postoperative days. Bupivacaine-loaded CaP cement provided very local and short-term better pain relief compared to the unloaded cement, during the first 6 postoperative hours. CT imaging confirmed the bone reconstruction of the iliac crest by the injected cement that remained in place and showed very good osteointegration on both microCT and histological analysis.

DISCUSSION & CONCLUSIONS: Bone filling of the iliac crest harvesting site with a CaP cement significantly reduced postoperative pain and allowed restoration of the iliac crest bone morphology. The injection of CaP cement may be an effective bone augmentation method to decrease permanent induced local pain and thus long-term morbidity after iliac crest harvesting procedure.

REFERENCES: ¹ E. Verron, O. Gauthier, P. Janvier et al (2000) *J Biomed Mater Res B* **94(1)**:89-96.

ACKNOWLEDGEMENTS: This work was supported by the Graftys® Company.



Discerning the role of the setting reaction on the injection behaviour of tricalcium phosphate pastes

EB Montufar^{1, 2}, Y Maazouz^{1, 2}, MP Ginebra^{1, 2}

¹ Biomaterials, Biomechanics and Tissue Engineering Group, Dept. Materials Science and Metallurgical Engineering, Technical University of Catalonia, Barcelona, Spain. ² Biomedical Research Networking Centre in Bioengineering, Biomaterials and Nanomedicine, Spain.

INTRODUCTION: Understanding the mechanisms of the injectability of calcium phosphate pastes is of interest both for the delivery of calcium phosphate cements via minimallly invasive surgical techniques and for tissue engineering scaffold fabrication by robocasting. In the past, several research articles focusing on injectability of non-self-setting calcium phosphates were published [1]. The aim of the present work was to gain further insight in the role of the setting reaction on the injectability of tricalcium phosphate (TCP) pastes. Pastes prepared with both polymorphs of TCP, alpha (α; self-setting) and beta (β; non-self-setting) were studied. Reaction kinetics were modified either by thermal treatment of the powders or by the addition of nanocrystal seeds or accelerant solution, and their effect on injectability was studied [2].

METHODS: α -TCP and β -TCP were synthetized and milled to obtain powders with two different particle size distributions (PSD), fine and coarse. Powders were used as milled or after calcination at 500 °C for 24 h, and mixed with the liquid phase at L/P ratio of 0.45 ml/g. The injection test was performed at 15 mm/min, to a maximum injection load of 100 N, starting at different times after mixing. The paste was extruded through the 2 mm syringe aperture or through a 0.84 mm diameter cannula. The injectability percentage, yield load and injection load were determined and correlated with the type of polymorph, setting times, PSD, syringe aperture and the use of additives that accelerate the setting reaction, i.e. a 2.5 wt% Na₂HPO₄ solution and/or 2 wt.% of hydroxyapatite (HA) seeds in the powder.

RESULTS: β -TCP pastes were more injectable than α -TCP pastes (Fig. 1). Differences were more marked when small diameter cannulas were used or when the beginning of injection was delayed. Fine powders were more injectable and required smaller injection loads than coarse ones. Powder calcination resulted in an increased injectability due to lower α -TCP reactivity. The addition of setting accelerants

tended to reduce the injectability of α -TCP pastes, especially if adjoined simultaneously with the Na₂HPO₄ solution.

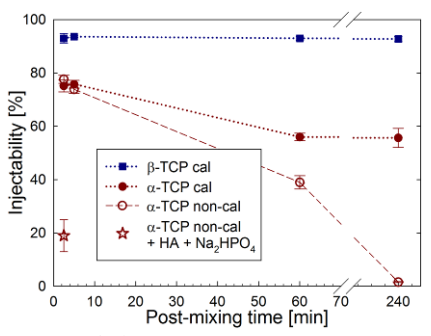


Fig. 1: Injectability as a function of post-mixing time for calcined (cal) and non-calcined (non-cal) TCP fine powders. The pastes were injected through a 2 mm aperture, without additives, unless otherwise stated.

& **CONCLUSIONS:** DISCUSSION The parameters affecting powder reactivity were shown to play a significant role in the injectability of TCP pastes. α -TCP was in general less injectable than β-TCP and required higher injection loads. Whereas powder calcination resulted in an increased injectability, the addition of setting accelerants tended to reduce the injectability of the TCP pastes. As a general trend, faster setting pastes were less injectable; although, some exceptions were found, e.g. in absence of setting accelerants fine TCP powders were more injectable than coarse ones in spite of shorter setting times. When setting accelerants were added the opposite was true.

REFERENCES: ¹ M. Bohner, G. Baroud et al (2005) *Biomaterials* **26**:1553-63. ² E.B. Montufar, Y. Maazouz and M.P. Ginebra (2013) *Acta Biomater* **9(4)**:6188-3198.

ACKNOWLEDGEMENTS: The authors thank the Spanish Government for its financial support through the MAT2012-38438-C03-01 project and FPU scholarship of Y Maazouz. MP Ginebra acknowledges the ICREA Academia prize by the Generalitat de Catalunya.



Injectable BP-loaded cement to reinforce sheep osteoporotic vertebral bodies

E Verron¹, ML Pissonnier¹, J Lesoeur¹, P Mousselard¹, P Pilet¹, O Gauthier^{1, 2}, JM Bouler¹

INSERM U791, LIOAD, University of Nantes, Nantes, France. ² Preclinical Investigation and Research Center, ONIRIS College of Veterinary Medicine, Nantes, France.

INTRODUCTION: Reinforcing osteoporotic bone is a clinical challenge for prevention and treatment of bone fractures. In this context of bone regeneration, we developed a local approach based on the use of calcium phosphate (CaP) bone substitutes that can deliver in situ bisphosphonate (BP) [1-2], an inhibitor of resorption largely used in the treatment of osteoporosis. Our previous study demonstrated the ability of granules of CaP loaded with BP to form new bone and to reinforce existing trabeculae in femur of osteoporotic ewes [3]. In continuation to this *in vivo* study, we have optimized the formulation of CaP by designing an injectable apatitic cement (CPC) that (i) hardened in situ without degrading the BP loaded and (ii) presented immediate mechanical properties more adapted to clinical applications in an osteoporotic environment.

METHODS: CPC was loaded with BP as previously described by Schnitzler et al [4]. Twelve adult female Vendeen sheeps were ovariectomized 9 months earlier to induce osteoporosis. An injection of the CPC loaded or not with BP was performed into lumbar vertebral (L3-L4) to achieve bone reinforcement in the vertebras. After 3 months, ewes were sacrified and vertebras and iliac crests were collected. Bone modifications have been determined histological analysis, 3D-microtomography and SEM analysis performing in 3 regions of interest according to a growing distance from implant (0.8, 1.2 and 1.8 mm) as showed in Fig. 1. Calculation (i) morphological parameters included parameters, mainly bone volume fraction (BV/TV, %), trabecular thickness (TbTh, mm), trabecular separation (TbSp, mm), trabecular number (TbN, mm⁻¹) and total porosity (PO, %), (ii) topological parameters like trabecular bone pattern factor (TbPf, mm⁻¹), structure model index (SMI) and Euler.

RESULTS: As previously demonstrated [3], osteoporosis has been validated in iliac crest in ovariectomized ewes. CPC loaded with BP induced a distance-dependent effect on bone microarchitecture. Moreover, histological data showed the quality of osteointegration of combined-CPC.

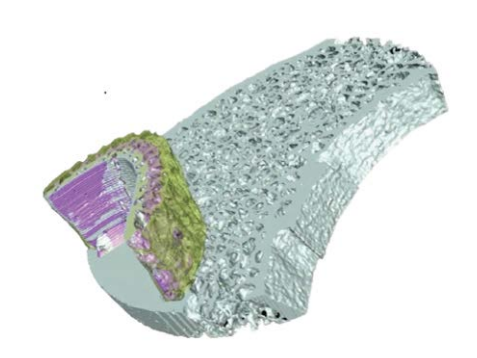


Fig. 1: Reconstruction of 3D image by using CTAnn® software of an implanted vertebra: three regions of interest have been defined according to the distance from implant (0.6, 1.2 and 1.8 mm).

DISCUSSION&CONCLUSIONS: Ewes that followed an ovariectomy have been previously used as a model for post-menopausal osteoporosis [3] and it has been validated as a clinically relevant model of human post-menopausal bone loss. It is the first time that a BP-combined cement has been implanted in vertebrae in ovariectomized ewes. Interestingly, biological effect was distance-dependent that reflects the bone distribution of BP after the release process from cement. Quantitative (micro-architectural parameters) and qualitative (histological staining) analysis demonstrated that implantation of our combined cement in vertebra induced a beneficial impact on microarchitectural properties of trabecular bone.

REFERENCES: ¹ E. Verron, et al (2010) *Drug Discov Today* **15**(13-14):547-52. ² E. Verron, et al (2012) *Acta Biomater* **8**(10):3541-51. ³ E. Verron, et al (2010) *Biomaterials* **31**(30):7776-84. ⁴ V. Schnitzler, et al (2011) *Acta Biomater* **7**(2):759-70.

ACKNOWLEDGEMENTS: The authors thank Dr N. Rochet, X. Mouska and Dr C. Sattonnet for their technical contribution relative to μCT imaging. This work was supported by ANR (Gabiphoce Program), FUI (Spineinject program).



Nanocrystalline calcium phosphate cements in tibial plateau fractures: Implant augmentation designs derived from clinical studies

TA Russell

Professor Emeritus, University of Tennessee, Elvis Presley Trauma Center, Memphis, TN, USA

Nanocrystalline Calcium Phosphate Cements developed in Cambridge, MA by ETEX, founded by Dr. D. Lee have been extensively studied in animal and human models. A level I prospective randomized multi-center study on tibial plateau comparing Alpha-BSM Cambridge, MA) to autogenous iliac bone graft with standard reduction and internal fixation techniques published in JBJS (A) in 2008 documented a decreased articular subsidence rate with this ceramic cement compared to cancellous graft [1]. The study mirrored the findings by Welch et al reported in JBJS 2004 showing the improved healing of trabecular bone with Alpha-BSM compared to autogenous bone graft [2].

The technical problems associated with proper placement of ceramics in fracture defects have hindered the widespread clinical adoption of these materials in general practice. The optimal combination of surgical implants with these ceramic materials would permit placement of the ceramics in intimate proximity to the fracture cavity, in adequate volume, without significant dilution by blood and fluids in the fracture cavity. Also, the fracture implant would require modified optimize strength, designs to hydraulic modifications for cement intrusion without excessive force and a method of extraction of the implant after fracture healing without associated damage to the regenerated bone.

The N-Force Fracture Fixation (InnoVision, Inc., Memphis, TN, USA) received USFDA clearance in the fall of 2011, and was commercially released in the USA in 2013 [3]. It is a titanium alloy screw with the initial offering of a 4.0mm headless screw design with strength equivalent to non-fenestrated 4.0 Cannulated screws. It is cleared for cement delivery of ETEX proprietary Beta-BSM and CarriGen materials only at this time due to requirements by the FDA [4]. It is capable of nondestructive removal by hand force after fracture healing. The hurdles faced in obtaining the first clearance in the USA of a combination implant and biomaterial delivery system centered about safety issues raised by the FDA.

Initial clinical studies have begun in fracture surgery and selected cases will be presented. This system opens the door for future combination implants and orthobiologic materials delivered by the implant to optimize function and placement of both materials.

REFERENCES: ¹ T.A. Russell and R.K. Leighton (2008) *J Bone Joint Surg* **90**:2057-61. ² R.D. Welch, H. Zhang and D.G. Bronson (2003) *J Bone Joint Surg Am* **85**:222-31. ³ N-Force Fixation System. Innovision, Inc. www.innovisionus.com. ⁴ FDA 510(k) K102528, July 29, 2011.

ACKNOWLEDGEMENTS: The author thanks ETEX Corporation, Cambridge, Massachusetts, USA (www.etexcorp.com) for its support.



Designing augmentation systems -from cement to application a hard road

P Procter^{1,2}, G Insley³, A Greter ⁴

¹Stryker Osteosynthesis, Selzach, CH.² Brunel University, Uxbridge, UK. ³ PBC Ldt. Ireland ⁴Medmix AG, Rotkreutz, CH.

INTRODUCTION: Cement makers usually provide one or two cannulae for their "void filler" cement thinking that the job is done. Reality is that the limited approvals, the lack of suitable application specific properties and delivery cannula have limited the applicability of these cements. The authors present a case study to illustrate how an application specific approach is needed and what the cement maker needs to take into account in the design of delivery devices. Hip fractures are a great example as there is such a diversity of designs addressing the same clinical problem.

The first two authors were involved with the development of a commercially available bony void filler cement. The approval to use with screws was obtained in EU. A key application is to augment screws in the proximal femur. Despite customers asking for this application there was no cannula available. At this point we turned to a professional group (Medmix) for help. We thought that any form of long cannula could be used and a series of trials that initially failed showed that the cannula had to meet certain criteria to be successful in this application. Furthermore it was learned that the operative technique was a critical part of the successful application and as the CaP cement only had a working time of 2 minutes it was essential to come up with a safe and effective application method.

A clinical simulation model was developed using Sawbones with the implant and instruments. It was determined (clinical interviews) that surgeon preference was to inject the cement through the cannulation of the screw. This meant that the minimum cannula length was now fixed by the length from the outer guide sleeve through to the femoral head. (This implies that for each manufacturer's hip screw a length and a cannula diameter would be to be determined). The technique finally adopted was drilling the screw minor diameter. Insertion of the lag screw over the guide wire until 2 cm from the end, removal of the guide wire and insertion of the cannula until it is in the remaining 2 cm space. Back fill the 2 cm space and then remove the cannula and tighten the lag screw. An in-vitro handling test demonstrated that it is

feasible for a single metal cannula to safely and effectively deliver 1-2 ccs of CaP cement using the existing surgical technique with minor modifications. Reported in an MSc project U. Lübeck DE [1].

implant specific cannula solution successfully proven in an in vitro model. The cannula must now be CE marked. Despite the later excellent feasibility, 1.5 years manufacturer has taken no steps to commercialise this application. This is attributed mainly to the lack of an approved screw augmentation application in the US. The FDA has expressed concerns that the CaP may resorb/remodel with time and that the augmented screw might migrate or loosen over time. Synthes has taken a first step into the clinical use of augmentation of hip devices but using a PMMA like cement and it remains to be clinically tested whether this or CaP augmentation will prove the better choice.

The authors conclude that if the cement makers wish to more widespread adoption of their products that they will have to take the larger part of the financial burden of delivering clinical evidence that CaP augmentation in bone works. Prospective randomised studies are needed to prove out the clinical benefit of CaP vs PMMA.

REFERENCES: ¹ B Nieber (2012) MSc Project Fachhochschüle Lübeck. Konzepterstellung und Funktionalitätsprüfung eines Applikationssystems für die Knochenzement-Augmentation – Am Beispiel der Schenkelhalsschraube.

ACKNOWLEDGEMENTS: The authors thank Stryker Corporation for the studentship provided for some work presented here.



Developments in CaP Injectable Cement for Screw Augmentation

CJ Brown¹, P Bennani¹, C Hughes¹, A Piper¹, P Procter ^{1,2}

¹ Brunel University, Uxbridge, UK. ²Stryker Osteosynthesis, Selzach, CH.

INTRODUCTION: The use of CaP injectable cement for screw augmentation has been described at GRIBOI [1]. The current paper presents some developments in the modelling of cements using finite elements. Techniques that have proved successful, along with some others that are more problematic, are outlined. Further results from the parallel test series are presented.

METHODS: The experiments were carried out on two densities of Sawbones® open-pored bone materials. HydroSet® substitute calcium phosphate bone cement was used to fill pre-drilled holes, and 4mm bone screws inserted. Pull-out tests were undertaken, and the specimens cut to examine the distribution of cement that had been A series of tests with and without achieved. gelatine, and with or without cement has been carried out. The gelatine is used to provide a resistance to the injectable cement representing fluids in the pore space.

Finite element models of cement-augmented cancellous bone with and without cortical layers have been developed using ANSYS commercially available software. The use of real bone geometry has been abstracted and developed from CT scans; the CT scans have been processed using MIMICS software. Subsequent methods for processing models have proved to be important.

RESULTS: The results of pull-out tests (Fig. 1) would indicate that the use of cement always increases the pull-out force required for screws in Sawbones® material. The use of gelatine as a fluid filler in the pores of the polymer bone substitute means that cement penetration is limited to more practical amounts (Fig. 2). Nevertheless, the amounts of cement injected with the use of a bone substitute — even with the gelatine — are considerable. Finite element models (Fig. 3) show the variability of pull-out force with position of the screw in the bone [2].

DISCUSSION & CONCLUSIONS: The variation in pull-out force from position alone can be significant, but the cement may have the effect of removing some of this variability. The use of gelatine to restrict the radial flow of cement is demonstrated in Sawbones material.

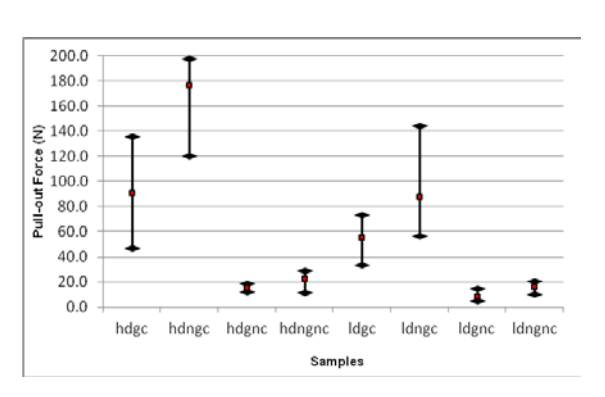


Fig. 1: Variation of pull-out force with cement (c) or no cement (nc), gelatine filled (g) or not gelatine filled (ng), for low density (ld) and high density (hd) Sawbones material.



Fig. 2: (left) Screw and attached cement after pullout from sample shown (right).

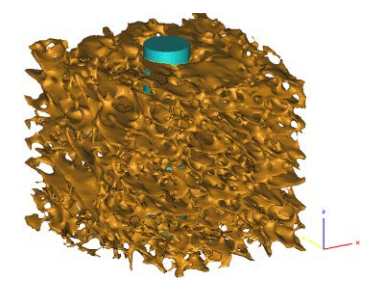


Fig. 3: Finite element model of a screw in the bone

REFERENCES: ¹ C.J. Brown et al (2012), Eur Cell Mater **23(S3)**:17. ² C.J. Brown, et al (2013) Comput Methods Biomech Biomed Engin **16(4)**:443-450.

ACKNOWLEDGEMENTS: Some work presented has been funded by studentships from the Stryker Corporation.



Macroporous ceramics of carbonated hydroxyapatite for bone grafting applications

N Douard, D Marchat, C Laurent, D Bernache-Assollant Ecole Nationale Supérieure des Mines de Saint-Etienne, CIS-EMSE, CNRS LGF 5307, Saint-Etienne, France.

INTRODUCTION: Calcium phosphate based materials, specifically hydroxyapatite (HA) and tricalcium phosphate (TCP), have been extensively used as bone graft substitutes for various applications (e.g. bone augmentation procedure). They temporarily substitute for bone while simultaneously supporting regeneration. its However, they present inappropriate resorption rate. Indeed, ideally a bone substitute should degrade only after the regenerated tissue has been remodelled at least once in the natural remodelling cycle [1]. Thus, the solubility of HA is too slow and that of TCP too fast to foster successful bone re-growth. To further improve the properties of calcium phosphate ceramics, ionic substitutions could be used. One way to modulate their resorption rate would be to substitute carbonate ions (CO₃²⁻) for phosphate ones (PO₄³⁻) into the HA structure [2]. Thus, the aim of the present work was to elaborate interconnected macroporous scaffold of pure carbonated hydroxyapatite (CHA).

METHODS: CHA powders were synthesised by an aqueous precipitation method using calcium, phosphate and carbonate salts solutions. The amount of reagents was calculated according to the $Ca_{9,2}(PO_4)_{5,2}(CO_3)_{0,8}(OH)_{1,2}$. formula: Green materials with controlled macroporous architecture were then shaped via a template casting process [3]. The ceramics scaffolds were finally obtained after sintering at 1100°C under controlled atmosphere. To assess the phase composition of the materials, X-Ray Diffraction (XRD) and Fourier Transformed Infra-Red (FTIR) analysis were performed. Calcium, phosphorous and carbonate content of the scaffolds were determined by elemental analyses (e.g. inductively coupled plasma atomic emission spectroscopy). The architecture of the ceramics was also observed by means of Scanning Electron Microscopy (SEM).

RESULTS: The XRD pattern of the sintered material shows only hydroxyapatite diffraction peaks; no secondary crystalline phase is observed (data not shown). The FTIR spectrum of the CHA ceramic is in accordance with the hydroxyapatite

structure (data not shown). Moreover, spectrum exhibits characteristics bands carbonate groups from both A and B sites. The carbonate content of the material was evaluated at 4.9 wt. %, amount which is very close to the theoretical value of 5.2 wt. %. The architecture of sintered material (Fig. 1) reveals structure interconnected macroporous macropores of $400 \pm 50 \,\mu m$ and interconnections of $150 \pm 30 \, \mu m$.

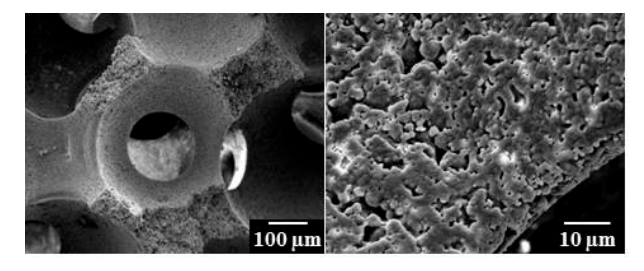


Fig. 1: Macroporous architecture of CHA ceramics obtained via a template casting process (left) and detail of the microstructure (right)

DISCUSSION & CONCLUSIONS: The physicchemical analysis of the sintered ceramic (XRD, FTIR and elemental analysis) confirmed the incorporation of carbonate into the HA structure in and A sites during, respectively, precipitation and the heat-treatment. The thermal under controlled treatment atmosphere $(p_{CO2} = 1 \text{ bar})$ allowed to prevent undesired decarbonation of the material that occurs around 700°C under air atmosphere. With the template casting process adapted to CHA powders, it was possible to control the architecture of the final ceramic. To conclude, interconnected macroporous materials made of carbonated hydroxyapatite free secondary phase has been successfully manufactured. To fulfil the characterization of this scaffold, solubility product measurements are under progress as well as in vitro and in vivo biological assays.

REFERENCES: ¹M.K. Heljak et al (2012) *Int J Numer Meth Biomed Eng* **28**:789–800. ²Y. Doi et al (1998) *J Biomed Mater Res* **39**:603-610. ³M. Descamps et al (2008) *J Eur Ceram Soc* **28**:149-157.



PMMA-hydroxyapatite composite material increases lifetime of augmented bone and facilitates bone apposition to PMMA: Biomechanical and histological investigation using a sheep model

M Arabmotlagh, M Rauschmann

Department of Spine Surgery, University Hospital Frankfurt, Frankfurt, Germany

INTRODUCTION: The most commonly used filler material for vertebral body augmentation is polymethylmethacrylate (PMMA), but its mechanical properties differ from that of cancellous bone [1]. This difference may result in fracture in the adjacent bone [2, 3]. The purpose of this study was to investigate the approximation of mechanical properties of PMMA to cancellous bone by addition of nanocrystalline hydroxyapatite (HA) (Nanostim®, Medtronic) to PMMA. Lifetime and fatigue failure of surrounding bone tissue under cyclic compression and the histological reaction of bone tissue to the material were investigated.

METHODS: Composite material (30% volume fraction HA) was implanted in one medial condyle of sheep femur and plain PMMA in the other as control. 18 adult female sheep were divided in two groups. One group was followed-up for three months and the other for six months. After the period the animals were killed and specimens containing the implant material and surrounding bone were cut out. Three samples were assigned for histological examination and from six for mechanical testing. Before light microscopy evaluation, the sections were stained with hematoxylin and eosin as well as with toluidine blue. The mechanical testing was performed under cyclic compressive loading. Failure was defined as a 10 % reduction of the initial modulus E_0 . The applied stresses (σ/E_0) were plotted as a function of the number of cycles (Nf), at which failure was reached. Lifetime curves were calculated. The significance of differences between the lifetime curves of groups and the follow-up periods was calculated by analysis of covariance ANCOVA.

RESULTS: Composite implants had a direct surface contact with the bone tissue throughout the whole circumference. PMMA implants were covered by a layer of fibrous connective tissue and thus, separated from surrounding bone. At 3 and 6 months, the composite specimens showed a significant higher lifetime curve than the respective PMMA specimens (p = 0.0031 and p = 0.04, respectively). A significant increase of specimen lifetime was observed for PMMA (p = 0.0013) and

composite (p = 0.0015) implant groups from three to six months follow up.

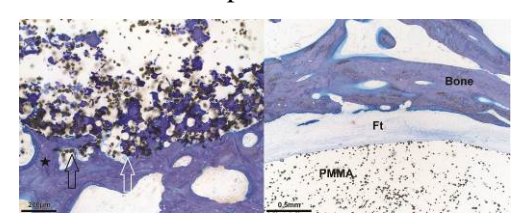


Fig. 1: Histological section of distal femur containing composite material (left) and PMMA (right) six months after implantation.

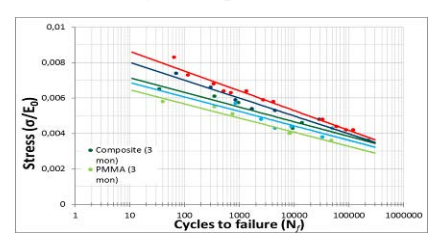


Fig. 2: Applied stresses (σ/E_0) to bone, augmented bone with PMMA and composite material as a function of cycle number until failure.

results suggest that the addition of HA to PMMA enabled bone apposition to the material. PMMA alone became encapsulated by fibrotic connective tissue. A significant bone ingrowth into the porous structure of the composite material was not observed. Specimens augmented with composite material, and a compressive elastic property close to cancellous bone, exhibited better mechanical performance and lifetimes versus plain PMMA groups. Addition of HA to PMMA retarded fatigue failure of augmented bone. This is of interest for augmentation of osteoporotic vertebral body compression fracture where adjacent vertebral body is at high fracture risk.

REFERENCES: ¹ X. Banse T.J. Sims and A.J. Bailey (2002) *J Bone Miner Res* **17**:1621-1628. ² A.T. Trout, D.F. Kallmes and T.J. Kaufmann (2006) *Am J Neuroradiol* **27**:217-223. ³ A. Boger, P. Heini, M. Windolf et al (2007) *Eur Spine J* **16(12)**:2118-25.

ACKNOWLEDGMENT: Funding for this research was provided by any Biomaterials



Architecture control and characterization in injectable bone graft substitutes

MP Ginebra^{1,2}

¹Biomaterials, Biomechanics and Tissue Engineering Group, Dept. Materials Science and Metallurgical Engineering, Technical University of Catalonia, Barcelona, Spain. ²Biomedical Research Networking Centre in Bioengineering, Biomaterials and Nanomedicine, Spain

Synthetic materials emerge as an alternative to bone grafts, since in recent years it has been shown that they can effectively foster bone regeneration while simultaneously avoiding some of the limitations associated with bone grafts such as limited availability, morbidity or disease transmission.

Bone graft substitutes must satisfy various requirements to act as a guide for new bone formation, stimulating tissue repair at the site of implantation. Besides the prescriptive biocompatibility, bioactivity and adequate resorbability, porosity appears as one of the key requirements for the material to act as a substrate for bone regeneration.

Moreover, nowadays, when the use of minimally invasive surgical techniques represents a major achievement in orthopaedic surgery, there is a growing need for injectable biomaterials. We have shown that it is possible to obtain injectable calcium phosphate foams, which are able to set in vivo and retain macroporosity after injection [1, 2]. Different surfactants can be used, either from natural or synthetic origin, to control not only the amount and size of macropores introduced in the material, but also the level of interconnectivity of these macropores. In these materials. macroporosity is superimposed to the intrinsic nano/microporosity of calcium phosphate cements, which can in turn be tailored by adjusting specific processing parameters. Therefore, a complex architecture is obtained, with interconnected pores covering from the nano to the macroscale, which can be of interest also when designing tissue engineering scaffolds or drug delivery matrices for the musculoskeletal system [3].

Porosity is a multifaceted property that cannot be characterized with a single parameter. Apart from total porosity, other features like pore architecture, pore size distribution, pore shape, pore interconnectivity and tortuosity, are also aspects that affect the interaction with the living organism

at different levels and therefore condition material performance in multiple scenarios. The spatial configuration provided by macroporosity plays an important role in guiding new tissue ingrowth within the material, so that cell colonization and angiogenesis events can take place. Moreover, not only macroporosity but also microporosity will influence the kinetics of resorption of the material. In addition, micro/nanoporosity results in larger surface area that contributes to higher protein adsorption and ionic exchange; and pore architecture at this level can also lead to protein concentration/entrapment, creating microenvironments. For all these reasons, a careful characterization of material's architecture and textural properties, from the nano- to the macroscale, is required to understand mechanisms of interaction between the material and the biological environment, and their influence on the events leading to bone formation [4].

At present there is no single technique that allows a comprehensive characterization of architectural features of this type of materials, at all the levels that are relevant for the biological response. For this reason it is important to combine the complementary information provided by imaging techniques like scanning electron microscopy or microcomputed tomography, and physicochemical techniques like mercury intrusion porosimetry, gas adsorption or thermoporometry.

REFERENCES: ¹ S. del Valle et al (2007) *J Mater Sci Mater Med* **18**:353–61. ² E.B. Montufar et al (2010) *Acta Biomater* **6**:876–85. ³ M.P. Ginebra et al (2012) *Adv Drug Del Rev* **64**:1090-110. ⁴ M. Bohner et al (2011) *Acta Biomater* **7**:478-84.

ACKNOWLEDGEMENTS: The author thanks the Spanish Ministry of Economy and Competitiveness for the financial support through project MAT 2009-13547.



Multiscale cell seeding in CaP scaffolds containing controlled macro and microporosity

AJ Wagoner Johnson¹, SJ Polak¹, GM Genin², M Talcott³, LE Rustom¹

¹Department of Mechanical Science and Engineering, University of Illinois at Urbana-Champaign, Urbana, IL, USA. ²Department of Mechanical Engineering and Materials Science, and Department of Neurological Surgery, Washington University School of Medicine, Washington University, St. Louis, MO, USA. ³Division of Comparative Medicine, Washington University, St. Louis, MO, USA

INTRODUCTION: The most severe, complex and/or critical size bone defects do not heal with current treatments of allo-, auto-, or synthetic graft. Research in scaffold-based bone repair focuses on the use of calcium phosphates (CaPs) and other materials to repair these defects that can cause disfigurement and loss of function. One major challenge in the repair of critical size bone defects is ensuring efficient and rapid cellular ingress into the scaffold. Forced cell seeding in porous ceramic scaffolds has been shown to enhance bone regeneration [1]. This study demonstrates a cell localization and self-seeding mechanism driven by capillary forces in porous, 2D CaP substrates in vitro. The approach shows promise for populating scaffolds with cells in vivo in a tunable manner.

METHODS: 2D CaP substrates were fabricated as in previous work. PMMA beads in the colloidal suspension serve as sacrificial porogens and allow for precise control over the micropore size and fraction. Cell localization on 2D substrates in the presence of capillary forces was measured for substrates with and without porosity (MP, NMP), for dry substrates, and for PBS-soaked substrates (wet). Cells stained with Cell-Tracker Green were placed on top of the substrates and cell density measured using a fluorescent microscope. For cell penetration experiments, the cell suspension lined a glass slide, and then was brought into contact with a dry MP substrate (Fig. 2a). Cell penetration distance was measured for MC3T3-E1, MSC, and D1 cells.

RESULTS: The pore fraction in MP samples was 46% and fully interconnected [2]. Pore size, measured by MIP², was nominally 5μm. Dry, MP substrates showed the greatest cell localization and the other conditions were all statistically similar (Fig. 1). NMP samples had negligible porosity and therefore low capillary pressure (Fig. 1a). In wet samples, PBS filled pores and eliminated capillary forces (Fig. 1b, c). These factors explain the differences observed. Cell penetration distance (Fig. 2b, c) depended on cell type, *i.e.* size and stiffness,

and their ability to deform and squeeze through the pores and interconnections.

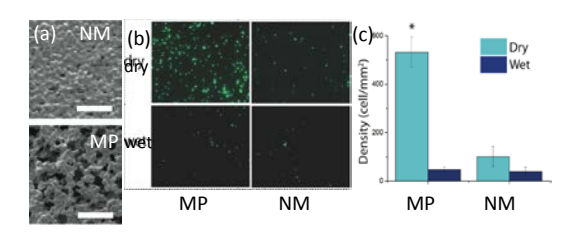


Fig. 1: (a) SEM images of MP, NMP microstructures. Scale bar: 50µm. (b) Images show cell localization on top of substrates. (c) Cell density for MP/dry was significantly higher than all others.

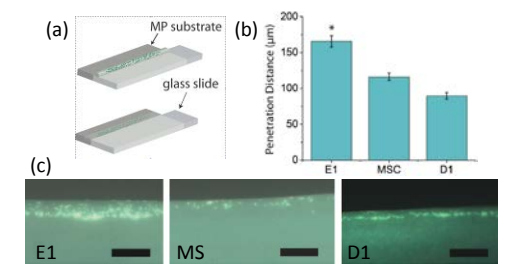


Fig. 2: (a) Schematic of cell penetration experiments. (b) MC3T3-E1 cells penetrated significantly further than MSCs or the D1s. (c) Fluorescent images show cell penetration. Scale bar: 500µm.

DISCUSSION & CONCLUSIONS: This paper shows a novel, simple mechanism to self-seed CaP scaffolds and substrates. Cell localization and self-seeding depends both on the presence of capillary forces, determined by the microstructure (MP, NMP) and the state of the pores (wet, dry), and the cell type. Optimization by tuning micropore and pore interconnection size and pore fraction size could lead to efficient and deep cell penetration into 3D scaffolds. This will improve their efficacy for healing and repair of large bone defects.

REFERENCES: ¹T. Stoll et al. (2004) *Mat wiss u Werkstoff-tech* **35**(4):198-202. ² J.M. Cordell et al (2009) *J Mech Behav Biomed Mat* **2**:560-570.

ACKNOWLEDGEMENTS: The work was supported by NSF DMR (No. 1106165).



Development of an intra-operative artificial tissue fabrication approach for reconstruction of large tissue defects

ML Liebschner^{1,2,3}, A Srivatsan², K Chun¹, B. Ehni^{1,2}

¹ Bio-Innovations Laboratory, Baylor College of Medicine, Houston, TX. ² Michael E. DeBakey VA Medical Center, Houston, TX. ² Biomedical Practice, Exponent Failure Analysis, Houston, TX.

INTRODUCTION: Current technologies for large tissue defect reconstruction are imperfect solutions that come with heavy burdens for patients and an enormous economical cost [1]. Engineered biological tissue that is customizable and immune-compatible can potentially make a significant difference in the lives of patients. Furthermore, on-demand scaffold and tissue fabrication has the promise for broad applicability towards many medical maladies and to allow fabrication of complex in-vitro tissue models, thereby facilitating discovery of novel drugs and diagnostic tests [2]. We are developing a concept for intra-operative fabrication of custom implants utilized in reconstructive surgery. The main application will be for the treatment of non-unions after tumor resection or injury, an unsolved clinical problem.



Fig. 1: Patient requiring complex 3D reconstruction after tumor resecction.

In this phase of development we focused on 1) building block manufacturability; 2) developing a robotic platform for concept validation; and 3) integrating tissue engineering concepts into blocks.

METHODS: Unit block polyhedral were generated using Rhinoceros 3D with a bounding box of 3x3x3mm. A common interface between building blocks was designed. Several different architectures representing the in-homogeneity found within human bone tissue were designed and subsequently fabricated using additive fabrication. Dimensional accuracy and mechanical properties were evaluated. We built a robotic test platform for our block assembly system that is based on the Adept Quattro high-speed parallel robot. A test setup was generated to investigate robot path optimization. We examined 6 different strategies for fluid flow perfusion through an array of building blocks. An analytical model following

Hagen-Poiseuille equation was established for comparison of the different flow perfusion strategies.

RESULTS: Geometric errors between designed and fabricated building blocks were less then 1.5% for overall dimensions and around 10% for the smallest of all features. The stiffness of the building blocks was not significantly affected by the removal of the fluid pathways, 44.9 ± 7.7 MPa w/o fluid channels versus 48.8 ± 8.7 MPa with fluid channels. The overall strength of the building blocks was higher for the building blocks with fluid pathways $(41.4 \pm 1.9 \text{ MPa})$ compared to building blocks that were empty $(26.5 \pm 3.1 \text{ MPa})$.



Fig. 2: Building blocks at 4 different scales

The six different flow strategies exhibited vastly different flow conditions. There was a 10-fold difference in magnitude between the construct with the least and the highest pressure loss.

As expected, adding transverse flow channels did not improve pressure loss. However, it is expected that during *de-novo* tissue growth transverse channels provide redundant pathways for flow perfusion.

DISCUSSION & **CONCLUSIONS:** We successfully developed a viable concept for the evaluation of robotic intra-operative scaffold fabrication. The micro-architecture of building blocks can be engineered to balance mechanical and fluid perfusion properties parameters independently. Engineering artificial flow channels into a scaffold construct may allow perfusion at the time of surgery.

REFERENCES: ¹ S.J. Hollister, C.Y. Lin, R.D. Saito, et al (2005) *Orthod. Craniofac. Res.* **8(3)**:162-73. ² A.M. Tarawneh, M. Wettergreen and M. Liebschner (2012) *Computer-Aided Tissue Engineering* (ed. M. Liebschner) Springer Protocols, pp 1-26.



Dynamic cell culture on glassy crystalline calcium alkali orthophosphates scaffolds

MA Lopez-Heredia¹, R Gildenhaar², G Berger², U Finow², C Gomez², A Houshmand¹, M Stiller¹, C Knabe-Ducheyne¹

¹Dept of Experimental Orofacial Medicine, Philipps University, Marburg, Germany ² Federal Institute for Materials Research and Testing, Berlin, Germany.

INTRODUCTION: Calcium phosphate (CaP) materials are well documented synthetic bone substitutes. The standard CaP materials include hydroxyapatite and/or α/β -tricalcium phosphates as main components [1]. A new kind of CaP was developed in the mid-90's; these CaPs are composed of glassy crystalline calcium alkali orthophosphates (CAOPs) [2]. The aim of the present work was to study the feasibility and outcome of dynamic cell culture on CAOP scaffolds.

METHODS: The properties and preparation of the CAOP used, i.e. GB14, have been described previously [2]. This material is commercially available as Osseolive ® (Curasan, Germany) and has CE and FDA approval. Cylindrical scaffolds (Fig 1) were obtained by rapid prototyping (RP) and by investment casting (IC) methods. Briefly, RP scaffolds, with controlled architecture and porosity, were built by injecting a CAOP slurry via a printing machine (RX Series, Prometal, Germany). IC scaffolds were obtained by embedding a polyurethane foam with a CAOP slurry and burning out the polyurethane. MC3T3-E1 cells (ATCC, USA) were used. Seeding media consisted of **DMEM** (PAA, Germany) supplemented with 10% FBS (PAA, Germany), 2mM L-Glutamine (Gibco, Germany), 5mM β Glycerophosphate (SigmaAldrich, Germany) and 50µg/ml of Penicillin-Streptomycin Germany). Culture media was seeding media with additional $50\mu g/ml$ ascorbic of (SigmaAldrich, Germany). Cell densities of 1.5 and 3.0 E6 cells/ml were used. Dynamic cell seeding and culture was performed in a Bioreactor (TEB100; Ebers, Spain). Scaffolds were seeded under dynamic revesible perfusion for 24 h at 0.25 ml/min. Dynamic culture was performed for 7 days at 0.5 ml/min. After 7 days, samples were fixed in HistochoiceTM (Amresco, USA), dehydrated and embedded in PMMA/BMA for histological observation [3]. 50 µm-thick sections were cut using a sawing microtome (SP1600; Leica, Germany). Sections were Giemsa stained and analyzed for histology.

RESULTS: Histological analysis demonstrated that, under dynamic seeding and culture, cell attachment and invasion was possible in both scaffolds. However, cell presence was more prominent at 3.0 E6 cell/ml than 1.5 E6 cell/ml, for the RP scaffolds, as compared to the IC ones. After 7 days of culture a change of the scaffold behaviour was observed.

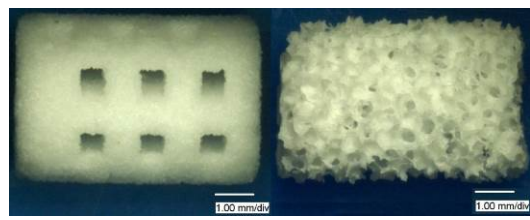


Fig. 1: Images of representative rapid prototyping (left) and investment casting (right) scaffolds.

DISCUSSION & CONCLUSIONS: Depending on the scaffold architecture and cell density, a more advantageous cellular interaction could be observed with the RP scaffolds. This behavior is related the initial cell availability and to the fluid dynamics created within the scaffold, which affect nutrient supply to the cells [4-5]. However, further tests and quantification are needed to confirm this observation. After 7 days, both scaffolds presented a squeezable behavior when handled with tweezers. Without cells, the CAOP becomes fragile due to its dissolution. Hence, this behavior is due to the cell-material interaction. This study opens the possibility for further study of these scaffolds as elements for tissue engineered interbody fusion cages.

REFERENCES: ¹ M. Bohner (2000) *Injury* **31(4)**:D37-D47. ² G. Berger, R. Gildenhaar and U. Ploska (1995) *Biomaterials* **16(16)**: 1241-1248. ³ C. Knabe et al (2006) *Biotech Histochem* **81(1)**:31-39. ⁴ Kruyt et al (2008) *Tissue Eng Part A* **14(6)**:1081-1088. ⁵ Grayson et al (2008) *Tissue Eng Part A* **14(11)**:1809-1820.

ACKNOWLEDGEMENTS: Authors thank the DFG (Grant KN 377/8-1) for its financial support and the technical assistance of Mrs. A. Kopp.



Wet-chemical process to synthesis the biphasic calcium-phosphate powder

M Habib¹, M Loszach², F Gitzhofer², G Baroud³,

¹Mechanical Engineering Dept., Al-Azhar University, Cairo, Egypt. ² CREPE, Universite de Sherbrooke, Sherbrooke, Quebec, Canada. ³Biomechanics Laboratory, Universite de Sherbrooke, Sherbrooke, Quebec, Canada.

INTRODUCTION: Wet-process is mainly used for the synthesis of calcium deficient HA. However and recently, it can be used in direct processing of biphasic calcium-phosphate ceramics HA/TCP [1-3]. When compared to both α - and β -TCP, HA is a more stable phase under the physiological conditions, as it has a lower solubility and, thus, slower resorption kinetics. Therefore, the biphasic calcium-phosphate BCP concept is determined by the optimum balance of a more stable phase of HA and a more soluble TCP [2]. Due to a higher biodegradability of the α - or β -TCP component, the reactivity of BCP increases with increasing TCP/HA ratio. Therefore, in vivo bioresorbability of BCP can be controlled through the phase composition. This study examined the use of wet-chemical process to synthesis the (BCP) powders and the effect of the aging on the phase composition.

METHODS: Ca(NO₃)₂.4H₂O and (NH₄)2HPO₄ precursors, as a starting materials, were mixed according to an initial Ca/P ratio equal to 1.5. The chemical reaction took place between calcium and phosphorus ions under controlled temperature and pH value of the solution. The alkalinity and reaction temperature were fixed at pH 8 and 60°C for the preparation of BCP respectively. A part of the precipitated powder was dried and the other part was aged overnight. All precipitated powders were then calcined for 2hrs at 1000 °C. Both heating and cooling rates were 20 °C/min during the calcination process. The calcined powders were analyzed by X-Ray Diffraction (XRD) and Scanning Electron Microscopy (SEM).

RESULTS: The chosen pH value was optimal in order to produce BCP powders. In particular pH less than 9 favours the synthesis of TCP powders while pH value of about 9 to 10 favours the production of straight fibrous HA [1,3]. That is due to the increase of Ca/P molar ratio of the product with the increase of the pH value of starting solution. Moreover, increasing the pH induced the substitution of PO₄ groups with CO₃ groups. The effect of aging was clearly demonstrated with

XRD. The draying stops the evolution of the burshite phase and hence the as-dried and calcined powders showed higher β -TCP/HA in the formed BCP than that of the non-dried and calcined powders [Fig.1].

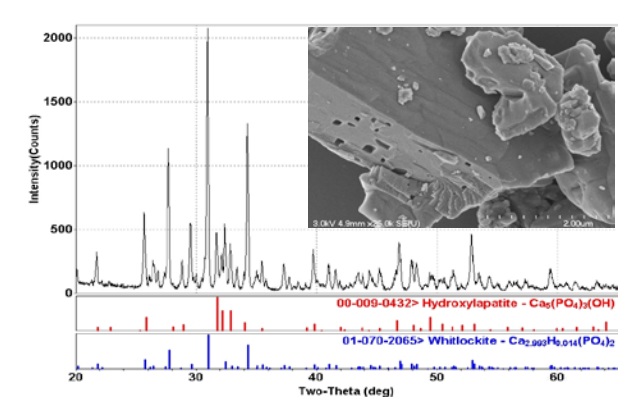


Fig. 1: XRD and SEM of as-dried and calcined BCP powder.

DISCUSSION & CONCLUSIONS: Wet process is a low cost fabrication process to synthesis HA/β-TCP via wet chemical reaction. It is also suitable for an industrial production, as it requires inexpensive reagents and BCP products with variable phase composition can be easily obtained. Yet, very few studies exist here and different compositions were investigated. In compounds, significant differences in characteristics may exist between materials of very close chemical compositions and consequently their usage in the different applications. Within these applications, the particle size, presence of substituting elements and the crystallinity strongly affect resorbability. Thus, the ability to prepare biphasic mixtures with controlled crystallinity, size and phase composition will be of our future studies.

REFERENCES: ¹ S. Kannan, A.F. Lemos and J.M.F Ferreira (2006) *Chem Mater* **18**:2181-2186. ² S.V. Dorozhkin (2010) *J Funct Biomater* **1**:22-107. ³ I.R. Gibson, I. Rehman, S.M. Best et al (2000) *J Mater Sci MaterMed* **11**(**12**):799-804.



Prophylactic Vertebral Augmentation

L Manfrè

Deptartment of Minimal Invasive Spine Therapy, AOE Cannizzaro, Italy

Prophylactic vertebral augmentation (PVA) is a new challenge for adjacent vertebral fractures (AVF) after PMMA vertebroplasty (VP) for vertebral compression fracture (VCF). The not treatment of patients with a VCF by vertebral augmentation (VA) has the risk of complications in patients forced to stay in bed. Among such risks there is cardiovascular distress related to increasing kyphosis, worsening of Altzheimer symptoms and muscles and bone Rehabilitation of osteoporosis Program Exercise (ROPE) is a valid tool in prophylaxis. Patients who undergone VA + ROPE treatment showed a new AVF only 20.4 versus 4.5 months for patients with simple VA, respectively. PVA is preferred as VCF is responsible for spine changes involving ligaments, muscles, disc, joints and sagittal balance. A need for stiffness in restoration is mandatory to prevent new AVF. In order to predict the fracture, global and local factors such as the degree of osteoporosis, bone mineral density (BMD), other concurrent diseases, the position of a vertebra into the spine architecture, the degeneration of adjacent disc, and endplates fracture and deformation are to take in account. S pectroscopy, perfusion MRI, High resolution MRI scanning and Diffusion MRI help in finding out vertebra-at-risk for fracture. However, the disc seems to play a master role in increasing AVF. For a VCF with regularly hydrated disc, the axial load is mainly distributed on the anterior 2/3 of the vertebra, the posterior arch being compressed for 8% and 2% only in the erect position and forward bending, respectively. In VCF a degenerated disc, despite a dramatic increase of the axial stress load on the posterior 2/3 or a vertebra, there is evident increase, up to 59%, in anterior endplates portion on forward bending. This could explain the involvement of bone under endplates, with new AVF clustered at the endplates closest to the previously treated vertebra. Finite Element analysis (FEA) on CT scans helps to better understand the area-at-risk for fracture. FEA before VA can predict the local area of vertebral bone weakness and the area supposed to fracture in the adjacent vertebra. A protective effect of VA has demonstrated on adjacent vertebras. In fact, in case of AVF, new fractures were depicted only

in area above adjacent endplates without PMMA under, while no fracture where depicted when endplates below were above PMMA. Moreover. in contrast to the decrease in bulge of the augmented vertebra endplates, the bulge of the adjacent endplates substantially increased, by as much as 17%. The number of incident fractures is not as many as that of prevalent fractures after bone augmentation in osteoporotic patients [1]. Consequently, VA do not increase the real risk of fracture, but the risk of AVF only, as 54% incident fractures in 934 patients after PMMA were AVF. When performing VA, distribution of PMMA, as the augmentation under the endplates seems to be the key to prevent AVF. PVA can be nowadays justified by the fact that the height loss of intact vertebra adjacent to a 2-level VA was smaller than the one adjacent a 1-level augmentation [2]. Recent studies demonstrated that restoring normal load sharing, VP has potential to decrease the risk of recurrent and adjacent level fractures [3]. Besides, PMMA distribution, changing the modulus of injected material could prevent AVF. In the past, morphological changes of injected calcium phosphate cement (CPC) in osteoporotic compressed vertebral bodies have been studied, demonstrating that CPC only is not sufficient for increasing the stiffness of a fractured vertebra. Recently, osteo-cundiction with 60 % α-Calcium Sulphate (α-CaS) and 40 % hydroxyapatite (HA) showed good capability in treating a VCF. New silicones as the VK100 are able to adhere to bone, and act as shock absorbers. Moreover, osteo- induction with recombinant human Bone Morphogenetic Protein-2 and CPC showed degradation happening simultaneously to bone regrowth, without gaps, inflammatory reaction, fibrous capsule, connective tissue or scars.

REFERENCES: ¹ K. Chosa et al (2011) *Jpn J Radiol* **29(5)**:335-341.. ² J. Luo et al (2010) *J Osteoporosis* doi:10.4061/2010/729257. ³ F. Zhao et al (2005) *Spine* **30(23)**: 2621-30.



Does balloon kyphoplasty deliver more cement safely into osteoporotic vertebraes with posterior wall defects compared to vertebroplasty?

ZM Sardar¹, W Aldebeyan¹, J Ouellet¹, T Steffan², P Jarzem¹

¹ McGill Scoliosis & Spine Centre, McGill University Health Centre, Montreal, Canada. ² Orthopaedic Research Lab, McGill University Health Centre, Montreal, Canada

INTRODUCTION: Kyphoplasty and Vertebroplasty are commonly used tools for providing pain relief in fractures due to osteoporosis or cancer. However, cement leakage during these procedures, especially in the cases of posterior vertebral wall defects, can be a major source of morbidity and degraded outcome [1].

METHODS: Forty artificial vertebral analogues made of polyurethane with osteoporotic cancellous matrix representing the L3 vertebrae were used for this study that were divided into 4 groups of 10 vertebrae each. The 4 groups tested were: Low viscosity cement injected using vertebroplasty, High viscosity cement injected vertebroplasty, Low viscosity cement injected using balloon kyphoplasty, and High viscosity cement injected using balloon kyphoplasty. The procedures were carried out under fluoroscopic guidance. Injection was stopped when the cement started protruding from the posterior wall defect. The main outcome measured was the volume of cement injected safely into a vertebra before leakage through the posterior wall defect.

RESULTS: The highest volume of cement injected was in the vertebroplasty group using high viscosity cement which was almost twice that injected in the other 3 groups. One-way ANOVA comparing the 4 groups showed a statistically significant difference (P < 0.0001). Post-hoc analysis showed a statistically significant difference in the volumes when comparing the high viscosity vertebroplasty groups with all the other 3 groups respectively. However, there was no statistically significant different in the volume of cement injected between the other 3 groups.

DISCUSSION & CONCLUSIONS: High viscosity cement injected using vertebroplasty delivers significantly more cement and fills the vertebral body more uniformly when compared to balloon kyphoplasty in osteoporotic vertebrae with a posterior wall defect [2].

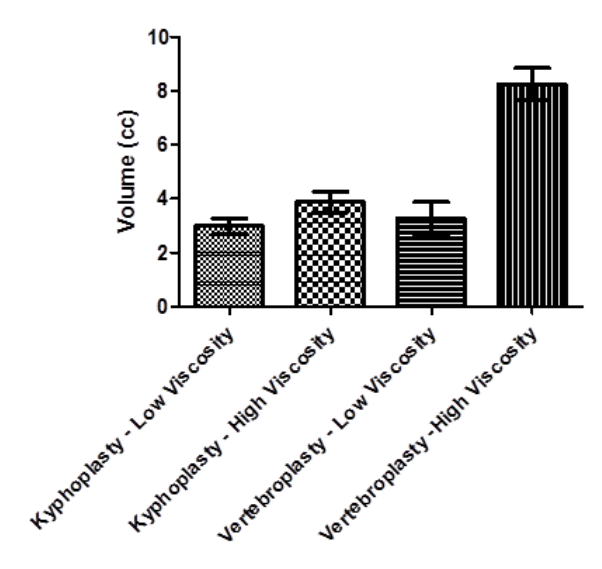


Fig. 1: Volume of cemented injected.

Table 1. Results for volume of cement injected into the vertebrae.

	Cement volume injected (ml)	Cement volume Injected (ml)
	 Calculated from vertebral 	 Calculated from Length of
	weight pre- and post- filling	bone filler devices used
Vertebroplasty – Low viscosity	3.3 (SE: 0.6, Range: 0.7 - 6.0)	3.4 (SE: 0.6, Range: 1.1 - 5.9)
(V1)		
Vertebroplasty – High	8.2 (SE: 0.6, Range: 3.7 - 10.2)	8.0 (SE: 0.6, Range: 4.1 - 10.5)
viscosity (V2)		
Balloon Kyphoplasty – Low	3.0 (SE: 0.3, Range: 1.0 - 4.3)	3.2 (SE: 0.2, Range: 1.8 - 4.3)
viscosity (K1)		
Balloon Kyphoplasty – High	3.9 (SE: 0.4, Range: 2.5 - 6.0)	4.3 (SE: 0.3, Range: 2.9 - 6.3)
viscosity (K2)		
P Value	< 0.0001	< 0.0001
and the second s		

SE indicates Standard Error of Measurement

REFERENCES: ¹ J.S. Yeom, W.J Kim, W.S. Choy et al (2003) *J Bone Joint Surg Br* **85(1)**:83-89. ² A. Krüger, L. Oberkircher, M. Kratz et al (2012) *Int J Spine Surg* **6(1)**:115-123.

ACKNOWLEDGEMENTS: The authors would like to thank Lorne Beckman and Rajashree Sen for their time, expertise and resources.



Cement augmented anterior screw fixation of odontoid type II fracture and presence of osteoporosis

M Scholz, A Pingel, F Kandziora

Center for Spinal Surgery and Neurotraumatology, Berufsgenossenschaftliche Unfallklinik Frankfurt, Germany

INTRODUCTION: Anterior screw fixation is the "gold standard" of surgical treatment of an uncomplicated Anderson D'Alonzo type II odontoid fracture [1]. Insufficient bony screw hold can cause severe procedure-related complications and result in screw breakouts with secondary fracture dislocation [2]. Therefore a posterior atlantoaxial fusion is recommended in case of severe osteoporosis [3]. However, the posterior approach is associated with a higher morbidity and a significant loss of cervical spine mobility [4]. The aim of this study was to evaluate whether an additive cement augmentation of the C2 body will increase the screw hold and lead to a safe fracture after anterior screw fixation of Anderson type II fracture and osteoporosis.

METHODS: Between 2009 and 2010 5 patients (Ø 87 years) with a displaced odontoid Anderson type II fracture and osteoporosis were treated using anterior odontoid screw fixation. After closed reduction patients received a standard anterior screw fixation using two screws. Thereafter an additional anterior vertebroplasty of the C-2 corpus with an average amount of 2.5 cc PMMA bone cement was performed using conventional bone filler. Care was taken that the bone cement completely surrounds the screws. Postoperatively, patients were advised to carry a soft collar within six weeks. Patients were followed clinically and radiologically using plain x-rays and computed tomography.

RESULTS: All patients survived the operation and the postoperative course was uneventful. Due to the additional vertebroplasty, operation time was increased by 11 minutes on average. The postoperative CT scan showed in all cases a cement layer embracing the screws. In two patients there was a slight leakage of bone cement laterally across the fracture line without clinical relevance. A 90 years old patient died 4 months after the operation by cardiac cause and was therefore not available for follow-up. 4 out of 5 patients were available for a follow-up with an average followup time of 23 months. These patients were free of neck pain and showed adequate rotation of the upper cervical spine. Computed tomography was able to detect in 3 out 4 patients (one patient denied a radiological examination on follow-up) solid bony fusion without implant complications.



Fig. 1: Patient example 32 months after the operation: X-ray and 2D-CT reconstruction after cement augmented anterior screw fixations of the dens axis showing bony fusion.

DISCUSSION & CONCLUSIONS: Cement augmented anterior screw fixation in case of unstable odontoid fractures Anderson D'Alonzo type II and prevalence severe osteoporosis results in a safe bony healing. Compared with posterior atlantoaxial spondylodesis, a cement augmented anterior odontoid screw fixation might lead to a lower morbidity and maintenance of the upper cervical spine mobility.

REFERENCES: ¹C. Klöckner (2010) *Orthopaede* **39**:432-6. ² M. Osti, H. Philipp, B. Meusburger et al (2011) *Eur Spine J* **20**:1915-20. ³ J. Stulík, P. Sebesta, T. Vyskocil et al (2008) *Acta Chir Orthop Traumatol Cech* **75**:99-105. ⁴ C. Steltzlen, J.Y. Lazennec, Y. Catonné et al (2013) *Orthop Traumatol Surg Res* **99**:615-23.



Rescue from the cut-out: Cement augmentation of a gamma nail

JM Trigueros, F Del Canto, F Ardura, DC Noriega, A Vega University Clinic Hospital, Valladolid, Spain

INTRODUCTION: Rates as high as 16% of Cutout has been reported as a major complication after intramedullary nailing stabilization of a pertrochanteric fracture [1, 2]. Recent studies of cement augmentation of the cephalic screw has shown no cases of cut-out [3, 4], but there is no reports on rescue of a cut-out with a new cement augmentation. The aim of this paper is to report a case of a rescue from a cut-out with an augmentation of a gamma nail and ultra-high density cement COHESION (VEXIM©) for filling the gap.

METHODS: An 87 women suffered pertrochanteric fracture 31A2 after a casual fall. She was operated in the first 48 hours with a Gamma Nail and she was discharged 8 days latter to a residence. 1 month after the operation the patient joined again in our institution with a cutout of the Gamma Nail. We planned the surgery for avoiding previous mistakes (lack of reduction, tip-apex distance > 2cm). We remove the previous nail and improve the reduction of the fracture using a reduction clamp or a Hoffman retractor place on the anterior side of the femoral neck and implanting a new Gamma Nail and cementing the bone gap with COHESION through a trocar as in the fashion of kyphoplasties, whose density allowed us to control the cement distribution without intra-articular penetration

RESULTS: The patient was allowed for full weight bearing with two crutches after 6 weeks and radiographic consolidation was at last revision 10 months after surgery no other complications have been found and the patient recovered her previous walking status.

DISCUSSION & CONCLUSIONS: Cut-out is a major complication after an intramedular nailing of a perthrocanteric fracture and in many cases a hip arthroplasty is needed to solve the problem, as in many cases there is no bone purchase of another cephalic screw [5, 6]. Otherwise augmentation with other kind of cements cannot be used in case of intra articular penetration as leads to cement leakage due to the lack of control of the cement distribution [3, 4]. With COHESION cement through a trocar and controlling the implant,

manipulation and stabilization times we can direct the cement wherever we need to fill the bone loss, improving bone purchase with no additional risk of intra-articular cement. This technique can be considered as a new option for the treatment of the cut-out with severe bone loss and an alternative to the arthoplasty.

REFERENCES: ¹ J.O. Anglen and J.N. Weinstein (2008) *J Bone Joint Surg Am* **90(4)**:700-7. ² P. Mattsson and S. Larsson (2004) *Scand J Surg* **93(3)**:223-8. ³ C. Kammerlander, F. Gebhard, C. Meier et al (2011) *Injury* **42**:1484-1490. ⁴ C. Dall`Oca, T. Maluta, A. Moscolo et al (2010) *Injury* **41(11)**: 1150-1155. ⁵ G.J. Haidukewych and D.J. Berry (2003) *J Bone Joint Surg Am* **85(5)**:899-904. ⁶ G.Z. Said, O. Farouk, A. El-Sayed et al (2006) Injury **37(2)**:194-202.



Cement distribution after percutaneous unilateral transpedicular balloon kyphoplasty for the mid and upper thoracic spine.

G Vastardis^{1, 2}, B Dial¹, M Stojanovich¹, A Marjan¹, T Potluri², G Carandang², A Hadjipavlou³, L Voronov^{1, 2}, ¹M Zindrick¹, A Patwardhan^{1, 2}.

¹Loyola University Chicago, Maywood, IL, USA. ²Edward Hines Jr. VA Hospital, Hines, IL, USA. ³University of Crete, Greece

INTRODUCTION: A bilateral approach ensures a maximum cement distribution in transpedicular kyphoplasty (KP). Augmenting only a single half of the vertebral body could lead to deformation of the vertebral body [1]. Balloons that fit an 11guage (11G) trocar, with an outer diameter (OD) of 3.0mm, and the curved tipped cement applicator, AVAflex (CareFusion, McGaw Park, IL), the ipsilateral and contralateral regions of the mid to upper thoracic vertebral bodies can be augment by an unilateral approach. The use of a small gauge needle decreases the surgical risk and the surgical time of the KP procedure [2,3]. This study aimed to define the general morphology of the T1-T12 thoracic pedicles; to perform unilateral transpedicular KP from T1-T12, and to assess the placement of cement in the various compartments of the vertebral bodies.

METHODS: Four fresh frozen human osteoporotic thoracic specimens (74 \pm 1.8 years) with intact rib cages and skin were screened to exclude pre-existing fractures and then scanned using Computed Tomography (CT). The CT images were uploaded into a software (Mimics, Materialize Inc, USA) where the pedicle height, width, and angulation in sagittal and axial planes were measured. Measurements were made for all specimens by 4 observers. Inter- and intraobservation scheme were separated by 1 week. The KP procedure was performed at T1-T12 levels on the same specimens using the 11G trocar for pedicle insertion, followed by the use of the 11G AVAflex curved applicator and 11G AVAmax balloon for vertebral body cavitation, and 11G AVAflex curved applicator for cement injection. The transpedicular approach was conducted through the right pedicle under C-arm fluoroscopy to facilitate the alignment of the trocar with the pedicle axis. Qualitative observations of cortical wall encroachment and fracture of the pedicle were made by observing post-op CT scans. Postoperative CT scans and 3D reconstructions of T1-T12 vertebral bodies were performed and imported into MatLab (Mathworks, USA) for volumetric analysis. Vertebral bodies were divided into 12 zones to assess the distribution of the injected cement. The augmentation in each zone was determined and a percentage was calculated comparing the volume of cement and the total volume of the vertebral body in each zone.

RESULTS: The height anatomically-limiting parameter was in the upper levels (T1-T4) at 5.38 ± 1.08 mm, highlighting a linear trend from T1 to T12. The width was most limiting in the middle levels (T5-T8) at 2.46 ± 0.32 mm, which emphasizes a parabolic trend from T1-T12. The absolute minimum height was at T1 with 3.80 mm (left) and 3.87 mm (right) at the pedicles. The minimum for width was at the left pedicle of T4 (2.10 mm) and right pedicle of T5 (2.00 mm). KP was successfully performed in T1 (1 specimen), T2 (3 specimens), and T3-T12 (all specimens). needle applicator allowed The augmentation in all zones of the vertebral body. 43.22 % of the vertebral body volume was augmented with cement at T2-T12 levels.

DISCUSSION & CONCLUSIONS: The OD of the trocar exceeded the isthmus in the upper $(2.68 \pm 0.50 \text{ mm})$ and middle levels $(2.46 \pm 0.32 \text{ mm})$. CT indicated no fracturing of the pedicles in the upper and middle thoracic levels or any vertebral levels. This indicates the potential elastic properties inherent to cortical bone and/or angular leeway allowing fractureless trocar penetration. The ipsilateral and contralateral regions of the mid to upper thoracic vertebral bodies were augmented by the curved tipped cement applicator. It is critical to target the desired cement location. The instrumentation was shown to be effective in percutaneous transpedicular balloon KP of the thoracic spine using a unipedicular approach.

REFERENCES: ¹ M. Liebschner, W. Rosenberg and T. Keaveny (2001) Spine **26(14)**: 1547-1554. ² H.S. Kim, S.W. Kim and C.I. Ju (2007) *J Korean Neurosurg Soc* **42(5)**: 363-366. ³ B. Chen, Y. Li, D. Xie et al (2011) Eur Spine J **20(8)**, 1272-1280.

ACKNOWLEDGEMENTS: US Department of Veterans Affairs; CareFusion McGaw Park, IL.



Beyond the beginning - Cervial kyphoplasty

S Moerk, KC Taeubel, C Ulrich

ALB-FILS-KLINIKEN, Klinik am Eichert, Goeppingen, Germany

INTRODUCTION: Cervical osteolytic metastasis is a problem for every spine surgeon. It leaves us to either large procedures with ventral or dorsal stabilisations or conservative treatment with immobilisation of the cervical spine for a prolonged time. In our clinic we do approx. 60 cases of kyphoplasty on the thoracic or lumbar spine per year and since being comfortable with ventral approaches to the cervical spine with started doing cervical kyphoplasty as a palliative procedure for those suffering from cervical osteolytic metastasis.

METHODS: A literature research came up with only a few reported cases and one case report [1-3]. We started to establish our own protocol. Indications were strict: destabilising osteolysis of the cervical spine (mostly C2) without a defect of the corticalis and no prior operations on the cervical spine. We used a standard ventral approach to the cervical spine over a small incision positioning the patient in backrest and reclined cervical spine. Blunt preparation to the spine and access of the vertebral body with a shard guide wire. Followed by a regular kyphoplasty using a 10mm balloon under continuous fluoroscopic control.

RESULTS: From September 2011 to December 2012 we treated a total of 15 patients with osteolytic metastasis of the cervical spine. 12 patients were treated on C2, 2 patients on C3 and 1 patient on C4. No neurological complications postoperative, one patient suffered from mild difficulties while swallowing for a few days. Average discharge from the hospital was 3 days after the procedure. All patients reported a significant decrease of neck pain.



Fig. 1: postOP X-Rays (C2 Kyphoplasty)

of the cervical spine is a easy, quick and safe procedure for the treatment of osteolytic metastasis of cervical vertebral bodies, especially C2. It should only performed by an experienced surgeon doing ventral cases of the cervical spine on a regular basis. Compared to a dorsal stabilisation is has a significantly lower rate of complications, especially wound infections, neurological complications etc)

REFERENCES: ¹ B. Blondel, T. Adetchessi, J. Demakakos et al (2012) *Orthopaedics & Traumatology: Surgery and Research* **98(3)**: 341-345 ² D.A. Monterumici, S. Narne, U. Nena et al (2007) *Spine J* **7(6)**:666-70. ³ C. Druschel, K. Schaser, I. Melcher et al (2011) *Archives of Orthopaedic and Trauma Surgery* **131(7)**:977-981.



Osteoplasty of the pelvis

PL Munk, PI Mallinson

Vancouver General Hospital, University of British Columbia, Canada

A variety of diseases of the osseous pelvis have proven very challenging to treat by conventional methods. Amongst the most common of these is metastatic disease. Traditionally most cases of bone metastases at this site have been treated with radiotherapy often in combination chemotherapy. Although very useful treatment failure often occurs and onset of pain relief can at times take weeks. Very occasionally, especially in the case of isolated disease surgery is performed, but can involve considerable morbidity and expense. The introduction of cementoplasty has provided a new useful palliative treatment which provides rapid onset of pain relief with a single treatment. It may be combined with thermo ablative techniques (radiofrequency ablation or cryoablation). Addition of thermoablation extends the region of tumor treatment beyond the region reached by cement in many instances allowing destruction of more tumor and potentially improves the durability of treatment (pain relief and non-recurrence of tumor locally)

Over the past several years new technical advancements have appeared to facilitate treatment of tumors at this anatomic site. This includes cryoablation with small bore probes as well as steerable curved needles which allow previously difficult to reach lesions to be injected. Examples of tumors treated using these techniques will be shown and discussed.



Vertebroplasty with chemotherapeutic agents: An experimental study in pigs

M Alfonso¹, A Silva², R Llombart¹, C Villas¹

¹ Orthopedics Department, University Clinic of Navarre, Spain. ² Orthopedics Department, Clínica Alemana, Santiago de Chile, Chile

INTRODUCTION: The possibility of performing vertebroplasty (VP) with the use of cement containing antineoplastic agents implies the potential to perform a local metastasis control together with stabilization of the fracture. In vitro studies have shown that cement containing methotrexate (MT), doxorubicin, or cisplatin (CP) maintains its mechanical characteristics, allows diffusion of the active form of these agents from the cement, and is able to inhibit growth of breast carcinoma cells, particularly in the first 24 h and up to 15 days following exposure [1, 2]. The aims of this study were: 1) to investigate the feasibility of performing percutaneous VP with MT-loaded and CP-loaded cement in a porcine model; 2) to determine the concentration of MT and CP in blood following VP and 3) to study the clinical and histological changes outcome mieloradicular structures and perivertebral muscles alter VP with polymethyl-metacrilate (PMMA) loaded with antiblastic drugs in pigs.

METHODS: In the Control group in 5 pigs received VP of two vertebrae using VP cement, provoking an anterior leak to the psoas and another leak to the vertebral canal. In the MT Group, VP of two vertebrae was performed in ten female pigs using VP cement to which 1 g of powdered MT had been added. After creating the mixture, the monomer was added and cement was injected in two vertebrae, provoking an anterior leak to the psoas and another leak to the vertebral canal. MT concentration in blood following cement administration was measured serial determinations during 1 week. In the second group the same procedure than group 1 was performed on 11 female pigs using VP cement to which 0.5 g of powdered CP had been added. CP blood concentration was measured during one week too. Three weeks later the pigs were put to death. We did a histological study of the soft tissue that came into contact with the cement.

RESULTS: In the Control group there were no cord lesions. In the MT group there were no major incidents associated with the technique and none of the animals had cord lesions following cement

leakage. Diffusion to the blood was detectable at 3

days, in some cases up to 7 days. In the group CP four animals presented paraparesis (1 immediate and 3 later). Mean CP values in blood were found up to 3 days. Histological results: Control and MT group: Normal spinal cord. In duramater inflammatory infiltrate and synovial metaplasia were found. Sligth muscle necrosis was found. CP group: Spinal cord necrosis was observed in 7 pigs. Wide areas of muscular necrosis were observed.

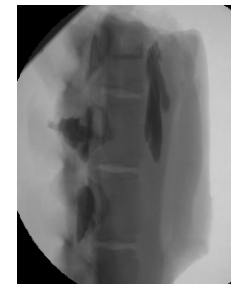




Fig. 1: (left) Lateral X-Ray showing anterior and intracanal leakage and (right) Images of PMMA with CP surrounding the spinal cord.

DISCUSSION & CONCLUSIONS: The use of MT-loaded cement is feasible in a porcine model. Despite massive epidural leakage, no neurological compromise was observed in MT group. Also no changes in the spinal cord were observed; it is likely that the dura and the cerebrospinal fluid are enough to isolate the neural structures from the cement. In CP group we observed extensive areas of cord and muscle necrosis associated with slight inflammatory reaction. The use of CP-loaded cement in this porcine model did not yield favorable results in presence of massive leakage because of the incidence of late paraparesis, probably due to the neurotoxic potential of this agent.

REFERENCES: ¹ M.A. Rosa et al (2003) *J Bone Joint Surg (Br)* **85**:712-6. ² Y. Tahara and Y. Ishii (2001) *J Orthop Sci* **6**:556–565.



New Augmentation devices and regulatory hurdles

EW Gilbert

Benvenue Medica, Inc, Santa Clara, CA, USA.

Since 2007, regulatory hurdles have increased requiring randomized clinical data for innovative products. Benvenue Medical's flagship product is the Kiva VCF Treatment System which features a proprietary flexible implant made from PEEK-OPTIMA®. The implant is designed to function as a mechanical support structure and a reservoir to contain and direct the flow of bone cement. It is currently engaged in its FDA clearance trial, KAST, which is a randomized, controlled trial of Kiva versus the current gold standard of care, balloon vertebral augmentation. Additionally, in the February edition of Spine, an independent, prospective, randomized study of patients with vertebral compression fractures (VCFs) comparing the effectiveness of balloon kyphoplasty with the Kiva VCF Treatment System found that only the Kiva system significantly restored vertebral body wedge deformity, Gardner angle. The Kiva system also resulted in significantly lower rates of extravasation and cement volume than balloon kyphoplasty.



Percutaneous vertebral augmentation assisted by peek implant in osteolytic vertebral metastasis: Experience on 40 patients

GC Anselmetti

Interventional Radiology, GVM Care & Research, Maria Pia Hospital, Turin, Italy

INTRODUCTION: Vertebral metastases are associated with significant pain, disability, and morbidity. Open surgery for fracture stabilization is often inappropriate in this population due to a poor risk-benefit profile, particularly if life expectancy is short. Vertebroplasty and kyphoplasty are appealing adjunctive procedures in patients with malignancy for alleviation of intractable pain [1, 2]. However, these patients have higher risk of serious complications, notably cement extravasation [3-6].

We prospectively evaluated clinical results of PEEK implant assisted vertebroplasty (KIVA, Benvenue Medical) performed in malignant painful osteolytic lesions at risk for cement extravasation due to vertebral wall involvement.

KIVA was performed in 40 consecutive patients suffering from back pain due to malignant vertebral involvement failing conservative therapies and without surgical indications. Follow-up was prospectively evaluated in all patients after KIVA with clinical interviews.

METHODS: 40 patients (22 females; mean age 66.8 ± 12.4), suffering from a painful spine malignancy with vertebral wall involvement not responding to conventional therapies and without surgical indications, underwent to KIVA for pain palliation. Procedure was performed in local anesthesia under combined digital fluoroscopy and computed tomography guidance. After the coilshaped polyetheretherketone implant was deployed within the vertebral lesion, bone cement was injected under continuous digital fluoroscopic control. Patients were discharged from the Hospital the next procedural day. The Visual Analog Scale (VAS) for pain, Oswestry Disability Index (ODI), analgesic requirement and use of external brace support evaluated efficacy. The main end-point was safety and efficacy at 1 month after the procedure. Furthermore, all the patients were scheduled to be followed-up at month 3, 6, and every 6 months thereafter.

RESULTS: Median pre-treatment VAS of 10 (range 6 - 10) significantly (p < 0.001) dropped to 1 (range 0 - 3), with all patients achieving a clinically relevant benefit on pain at 1 month.

Differences in pre- and post-treatment analgesic therapy were significant (p < 0.001). All patients no longer use external brace after KIVA. In 7 out of 43 (16.3 %) treated vertebrae a bone cement leakage was detected.

DISCUSSION & CONCLUSIONS: The Kiva System represents a novel and effective minimally invasive treatment option for patients suffering from severe pain due to osteolytic vertebral metastases.

REFERENCES: ¹ A. Weill, J. Chiras, J.M. Simon et al (1996) *Radiology* **199**:241-247. ² A. Cotten, F. Dewatre, B. Cortet et al (1996) *Radiology* **200**:525-530. ³ H.M. Barragan-Campos, J.N. Vallee, D. Lo et al (2006) *Radiology* **238**:354-362. ⁴ J.D. Laredo and B. Hamze (2004) *Skeletal Radiol* **33**:493-505. ⁵ D.H. Choe, E.M. Marom, K. Ahrar et al (2004) *Am J Roentgenol* **183**:1097-1102. ⁶ K.Y. Yoo, S.W. Jeong, W. Yoon et al (2004) *Spine* **29**:E294-E297.



One year results from a US IDE trial evaluating the OsseoFix implant for treatment of vertebral compression fractures

M Lorio¹, D Beall², R Eastlack³

¹Neuro-Spine Solutions, Bristol, TN, USA. ²Clinical Radiology of Oklahoma, Oklahoma City, OK, USA. ³Scripps Clinic, La Jolla, CA, USA.

INTRODUCTION: Vertebral compression fractures (VCF) are a burgeoning problem for the aging spine [1]. Previous kyphoplasty type treatments have been shown effective for pain relief but have also reported endplate fractures and cement leakage [2]. An expandable titanium mesh device has been designed to provide surgeon directed control in the reduction of the VCF and to facilitate cement delivery (OsseoFix®, Alphatec Spine, CA) [3]. OsseoFix® is not approved in US but CE mark clearance in Europe. The implant was designed to treat symptomatic patients suffering from VCF between T6-L5 by providing internal structural fixation prior to cement delivery (unlike a balloon type device). This minimally invasive (one or two level) procedure takes about 30 minutes per vertebra. The purpose of this study is to present data of a prospective multi center clinical trial from three sites treating patients presenting with one or two VCFs that were treated with the implant and PMMA.

METHODS: This study was a prospective multi center clinical trial. Patients enrolled were limited to those exhibiting painful vertebral compression fractures between T6-L5 which required surgical treatment after failing conservative care. The outcome variables in the study were changes in pain (VAS), Oswestry Disability Index (ODI), and adverse events. These data are the one year results from the prospective, multi-centered clinical study. Pain (VAS) and function scores (ODI) were collected starting pre-operatively with follow-up visits at four weeks, three months, six months and one year. Data were pooled from three surgical sites involved in the ongoing study. All available data are presented with 13/15 patients with a twelve month end point analysis.

RESULTS: Fifteen patients (11 females, 73.3 % and 4 males, 26.7 %) with an average age of 80.5 ± 8.0 years were treated for one level (14/15 or 93.3 %) or two level (1/15 or 6.7 %) VCF. At 12 months, improvement of VAS exceeded more than 51 points on average, demonstrating a dramatic and sustained relief in pain. At 12 months, improvement of ODI exceeded more than 40 % change on average, demonstrating a dramatic and sustained improvement in function. A one-way

ANOVA with a Tukey's post hoc test found a statistically significant improvement in pain (VAS p < 0.0001) and function (ODI p < 0.0001) at 4 weeks compared to pre-op which was maintained out to one year with no statistical difference between 4 week and subsequent time points. There were no device related adverse events demonstrating a risk profile lower than that previously reported.

DISCUSSION & CONCLUSIONS: Although these results are promising--we are not implying a definitive difference rather simply presenting a limited analysis for a small incomplete cohort. There were no device related complications that required intervention, nor were there observed endplate fractures. There was one instance of an asymptomatic cement leakage. Preliminary analysis shows OsseoFix augmentation for VCF decreased pain and improved function. The one or two level minimally invasive surgical procedure is a new option for the aging population that most often suffer from VCF. The surgical technique allows the surgeon to place and expand the device where desired as opposed to other pneumatic systems that do not allow for surgeon directed control. Further study and completion of the full enrollment is necessary prior to definitive confirmation of success [4].

REFERENCES: ¹ E. Truumees (2011) Kyphoplasty in *The comprehensive treatment of the aging spine: Minimally Invasive and Advanced Techniques* (Eds. J.J. Yue, R.D. Guyer, J.P. Johnson et al) Elsevier, pp 207-213. ² S.R. Garfin, R.A. Buckley, J. Ledlie et al (2006) *Spine* 31(19):2213-2220. ³ V.V. Upasani, C. Robertson, D. Lee et al (2010) *Spine* 35(19):1783-1788. ⁴ S.A. Ender, G. Gradl, M. Ender et al (2014) Rofo 186(4):380-387

ACKNOWLEDGEMENTS: Authors thank Alphatec Spine for its sponsorship



Initial clinical experience using novel radiofrequency systems for targeted ablation and augmentation of spinal tumors

RD Poser¹, BA Georgy², JW Jennings³

¹ DFINE Inc., San Jose, CA, USA. ²University of California San Diego, San Diego, CA, USA. ³Washington University, Seattle, WA, USA.

INTRODUCTION: It is estimated that 10% to 20% of the 1.64 M patients annually diagnosed with cancer will develop symptomatic spinal metastasis [1, 2]. Less than 10% of patients with painful spinal metastatic lesions are referred for vertebral fracture repair. Use of radiofrequency (RF) ablation, first described by Rosenthal *et al.* [3], has been limited in spinal metastatic disease due to requirement of targeted ablation in close proximity to neural elements and challenges navigating the unique anatomy of the spine. Treatment of painful spinal lesions using novel RF technology is described.

METHODS: Image guided targeted RF ablation (t-RFA) was performed with the STAR Tumor Ablation System (DFINE Inc.), which includes a robust articulating, navigational, bipolar electrode containing two active thermocouples (TC) along length of electrode to permit real time monitoring of peripheral edge of ablation zone (Fig. 1).

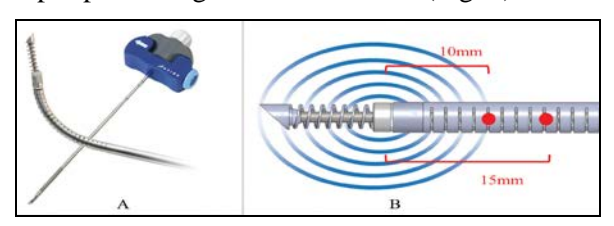


Fig. 1: (A) SpineSTAR Instrument, 10-G, articulated, extendable bipolar electrode and (B) Distal end of SpineSTAR containing 2 TC (red dots), located at 10 and 15 mm from center of ablation zone.

Over 100 lesions in 76 minimally invasive t-RFA procedures were performed. Pre-procedural planning was based on cross-sectional imaging to determine number of targeted ablations based on lesion size and thermal distribution curves. Treatment was controlled by adjusting power monitoring TCtemperature in-situ. Augmentation using high viscosity RF warmed high viscosity cement (StabiliT System) was performed via same guiding cannula in vertebrae with pathologic fractures or where structural integrity was significantly compromised. In select cases, post-procedural contrast enhanced magnetic resonance imaging (MRI) was performed to assess

ablative zone and post-op metastatic lesion status. In a subset of patients at one institution, pain was assessed by Visual Analogue Scale (VAS).

RESULTS: t-RFA procedures were successfully performed in all 76 procedures. Cement augmentation was performed in majority of cases. Lesion etiology included wide variety metastatic lesions involving T2 to S2, ilium and sternum. Post-ablation MRIs demonstrated discrete ablation zones consistent with thermal monitoring by TCs during the ablation. Ablation zone morphology was typically 3:2 length to width aspect ratio. TCs were used to confirm reestablishment of physiologic temperature in-situ cement augmentation. prior augmentation following RF ablation was efficient and resulted in predictable cement filling. Average VAS improved from 7.0 pre to 3.3 post t-RFA (53% improvement). No device related adverse events were observed.

DISCUSSION & CONCLUSIONS: The STAR Tumor Ablation System, a bipolar RF device, purpose built for targeted ablation of spinal malignant lesions, was successfully used to navigate and treat spinal malignant lesions. Postablation MRI's confirmed lesion necrosis. Ablation size was accurately determined by monitoring TCs on articulating electrode and morphology was similar to that extrapolated from thermal distribution curves. The navigational ability allowed for easy access to posterior vertebral body lesions, previously difficult to access with other ablation devices. Further, use of RF energy to modulate cement viscosity permitting delivery of ultra-high viscosity cement over an extended period of time proved useful in vertebrae with large cortical destruction.

REFERENCES: ¹ N. Howlader, A.M. Noon, M. Krapcho et al (2012) *SEER Cancer Statistic Review 1975-2009* Table 1.1; National Cancer Institute. ² K.D. Harrington (1997) *Cancer* **80(8)**:1614–1627. ³ D. Rosenthal and M.R. Callstrom (2012) *Radiology* **262(3)**: 765-80.



A novel device for radiofrequency ablation of bone metastases

M Gofeld^{1,2}, P Pezshki², CM Whyne², MK Akens², J Woo³, AJM Yee²

¹University of Washington, Seattle, WA, USA. ²University of Toronto, Toronto, Canada. ³Baylis Medical Company, Montreal, QC, Canada.

INTRODUCTION: More than 50% of cancer patients suffer from skeletal metastases that may cause significant pain, fractures, and compression leading to increased morbidity and mortality. Existing radiofrequency ablation (RFA) devices have been optimized for tumor ablation in soft tissue such as liver. However, the insulating properties of bone and close proximity to neighboring vital structures make it difficult to safely generate sufficient heat and achieve successful ablation [1]. This work investigates the physics and validates performance of a novel RF ablation system that is designed to treat spinal metastases. First technical clinical experience is also presented.

METHODS: The OsteoCoolTM RF Ablation System contains a 17G internally cooled coaxial bipolar probe which is designed for optimal performance in bone. The bipolar design provides localized and optimal energy delivery in bone, while internal cooling allows more significant ablation volumes conducive to vertebral body anatomy. The efficacy of the system was evaluated in 6 New Zealand rabbits whereby VX-2 tumor cells were injected into the femoral canal. RF treatment was administered 2 weeks later. The effect of RF ablation was determined by histology analysis. Treatment localization was characterized by MRI analysis immediately after treatment. Animals were euthanized 0 days (N=4) or 2 weeks (N=2) post-treatment. The safety of the system was evaluated by RF treatment in 5 healthy pigs, using a transpedicular approach with a 13G bone access needle. MRI scans of the resulting treatment area were analyzed at 0 day and 2 weeks following Neurological treatment. examination conducted before and after treatment, and prior to euthanasia (0 days: N=2, 2 weeks: N=3).

RESULTS: For efficacy and safety, all RF procedures produced the desired controlled temperature response. MRI analysis showed uniform ellipsoid lesions of approximately 3cm x 2cm, while histology revealed corresponding tumor cell death (Fig. 1). Tissue temperature immediately outside the cortex remained normal. Post-treatment MRI at 0 day and 2 weeks revealed clinically and anatomically relevant lesions spanning half the vertebrae (average 25mm x 13

mm) (Fig. 2). No neurological deficit was observed post-treatment. For clinical experience, RF was performed in a total of 8 patients with or without supplemental cementoplasty under FDCT guidance. Vertebral and non-vertebral (rib, pelvis, femur) tumors were treated.

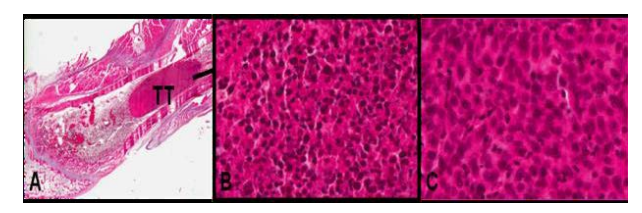


Fig. 1: H&E staining showing treated tumor (TT) region in the femur (A). RF ablated tumor cells in the treated tumor (B) is shown in contrast to untreated tumor cells (C).

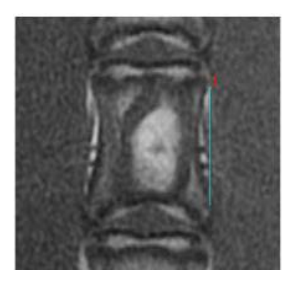




Fig. 2: MRI performed two weeks after procedure demonstrated bone marrow signal consistent with controlled damage.

DISCUSSION & **CONCLUSIONS:** The internally cooled bipolar OsteoCoolTM RF Ablation System, designed for ablation in bone, was shown to be consistent in creating lesions in diseased and healthy bone. Bipolar localization of RF energy and heat shielding by the vertebral cortex resulted in preservation of sensitive neural structures adjacent to the spine. The OsteoCoolTM RF Ablation System may represent a suitable option for vertebral tumor ablation and pain palliation.

REFERENCES: ¹ D.E. Dupuy et al (2010) *J Vasc Interv Radiol* **116:**989-97.



Surgical management of vertebral traumatic fractures

C Bono

Orthopaedic Spine Service, Brigham and Women's Hospital, Harvard Medical School, Boston, MA, USA

While low-energy mechanism, osteoporotic compression fractures can be effectively treated with vertebral augmentation if nonoperative treatment has failed, traumatic fractures of the thoracic and lumbar spine require a different set of principles. In general. management is targeted towards achieving three goals: stabilization, neurological decompression, and realignment of deformity. There is a wide array of injury patterns that can arise following high-energy trauma, each with unique treatment requirements. While there remains controversy and ongoing discussion about the ideal thoracolumbar fracture classification system, there a few widely recognized injury patterns that can help formulate a surgical treatment plan: burst fractures, seat-belt injuries, and fracture-dislocations.

There is a large body of literature regarding treatment of thoracolumbar burst fractures. In general, surgery is indicated in patients who have disruption of the posterior ligamentous complex (PLC) or neurological deficit. With PLC disruption without neurological deficit. posterior instrumented fusion is the most common method of surgical treatment. For cases in which deficit is associated with canal compromise, an anterior corpectomy is the most reliable method of decompression. This is followed by reconstruction of the anterior column with a strut graft or cage and instrumentation. Supplemental posterior instrumentation and fusion can also be performed. Seat-belt injuries occur from a flexion-distraction mechanism and thus inherently disrupt the PLC. They are rarely associated with canal compromise from vertebral comminution and are thus usually treated with a short-posterior instrumented fusion. Fracture-dislocations occur from very-high energy mechanism and are usually associated with severe neurological deficits, particularly in the thoracic spine. Canal compromise is usually the result of misalignment of the spine. These injuries are uniformly unstable and are best treated by an open reduction followed by long posterior instrumented fusion [1].

REFERNCES: ¹ K. Wood, G. Buttermann, A. Mehbod et al (2003) *J Bone Joint Surg Am* **85A**:773-81.



Clinical outcome after the use of a new cranio-caudal expandable implant for vertebral compression fracture treatment: 1-year results from a prospective multicenter study

D Noriega¹, F Ardura¹, J Beyerlein², N Hansen-Algenstaedt², F Hassel³, X Barreau ⁴

¹Spine-Unit, University Hospital Valladolid, Valladolid, Spain; ²University Medical Center Hamburg-Eppendorf, Hamburg, Germany; ³Loretto-Krankenhaus, Freiburg, Germany. ⁴

Interventional Neuroradiology Department CHU, Bordeaux, France.

INTRODUCTION: This study aims to evaluate the use of a cranio-caudal expandable intravertebral implant in combination with a new high viscosity PMMA cement (Fig. 1) as well as to determine whether this treatment provides good clinical and radiological results for vertebral compression fractures.

METHODS: A prospective international observational multicenter study was designed and set up. In the reported four study centers a total of 28 patients were enrolled (26 female, 2 male; mean age 70.2 ± 10.7 years). 22 osteoporotic and 6 traumatic fractures were treated. The clinical parameters pain (VAS), functional capacity (Oswestry Global score, ODI), quality of life (EQ-5D) and analgesic intake were assessed, along with radiological parameters. All data was collected prior to surgery and after surgery, at 6 months and at 12 months postoperatively. The rate of cement extravasation was analyzed using postoperative CT scans.

RESULTS: The results for patients followed up until 12 months postoperatively (n = 21) showed a 12-month mean reduction in VAS pain score of 6.2 from mean 7.4 ± 2.4 pre-op to 1.2 ± 1.9) at the 12 months follow up visit. The ODI score also decreased from 69.2% at baseline to 10.7% after 1 year. The EQ-VAS, measuring the self-rated health state, was 34.8 ± 22.8 preoperatively and increased to 77.3 ± 11.2 . The number of patients requiring moderate to strong analgesics dropped from 66.7% at pre op to 9.6% at 12 months. All changes in clinical parameters (VAS, ODI, EQ-VAS) were statistically significant (p<0.001). postoperative CT scans showed a cement leakage in 28.5% of vertebrae treated, all of which were asymptomatic. Adverse events were documented during the whole study period. None of the six serious adverse events reported (including 2 deaths - metastatic disease and heart disease-, 1 degenerative lumbar syndrome, 1 paralysis of the diaphragm, 1 hypophysis adenoma and 1 cerebral infarction) were device or procedure related. 6

technical incidents occurred, none of which led to a serious adverse event.



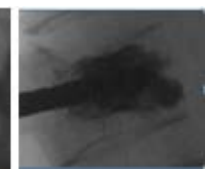


Fig. 1: SpineJack® procedure. Controlled fracture reduction with SpineJack® 5.0 implant followed by stabilization with high viscosity PMMA cement.

DISCUSSION & CONCLUSIONS: Results demonstrate that all clinical outcome scores (patients' pain, functional capacity, quality of life) were significantly improved one year after patients were treated using this new surgical procedure. The cement leakage rate (28.5%) is comparable to the 27% showed in the FREE study, especially considering that CT scans were used to identify cement leakages as opposed to less sensitive radiographs in the FREE study [1]. Earlier publications have shown that more leaks are identified by CT scans than in radiographs by a factor of 1.5 [2].

REFERENCES: ¹ D. Wardlaw, et al (2009) *Lancet* **373**:1016-24. ² J.S. Yeom, et al (2003) *J Bone Joint Surg* **85**:83-89.



A fully automated algorithm for measuring 3D anatomical restoration of fractured vertebrae across longitudinal CT scans

PA Dufort

Joint Department of Medical Imaging, University Health Network, Toronto, Canada

INTRODUCTION: We describe a new technique for performing longitudinal comparisons of vertebral shape from CT scans taken before and after surgery. Following a single click to locate the target vertebrae in pre-op and post-op scans, the program automatically computes a full 3D reconstruction for each vertebra, as well as a pretrauma reconstruction predicting the shape of the vertebra prior to injury. The three reconstructions aligned and used to compute shape measurements and 3D visualizations of the vertebra at each stage (Figure 1). The program is being used to measure 3D anatomical restoration following surgery to repair vertebral compression fractures using the SpineJackTM (Vexim, France) device. The details of the algorithm are described, as well as the results of a validation study comparing the measurements of the program against trained experts.

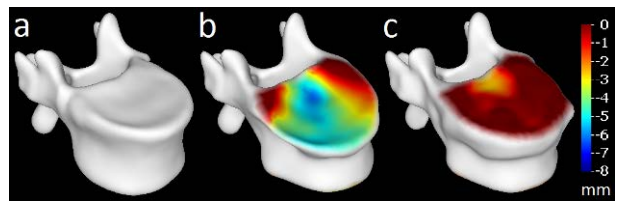


Fig. 1: 3D reconstructions of injured T12 vertebra. (a) pre-trauma, (b) pre-op and (c) post-op. Colour indicates the height difference from pre-trauma

METHODS: The user clicks on the approximate centre of the target vertebra and the two adjacent vertebrae in the pre-op scan, and on the target vertebra in the post-op scan. The software then proceeds in four stages: (i) vertebral models in the form of point clouds of oriented features are deformably registered with each of the selected vertebrae to segment them [1]. This is achieved by optimizing a dense correspondence field between the oriented features from the model and a corresponding set on the outer surface of the vertebrae in the CT scan; (ii) the segmentations are used to isolate the posterior, uninjured region of the target vertebra in both the pre-op and post-op scans and to rigidly register them; (iii) between the two adjacent uninjured pre-op vertebrae, a deformable interpolation is performed in order to compute the pre-trauma reconstruction; and (iv) a set of regional height change measurements over the upper and lower endplates are computed and displayed, along with 3D visualizations of the reconstructions. In order to validate the method, a set of 24 vertebrae each scanned at 4 longitudinal stages were selected, and height measurements using the standard six-point method were performed by 8 trained experts [2]. The software was then used to produce the same measurements from the computed correspondence fields.

RESULTS: For each of the 288 individual expert measurements (24 x 4 x 3 heights), the mean and standard deviation were computed. These were used to convert each software measurement into a Z-score. Over 288 measurements, the average Z-score was 0.03 ± 0.07 (mean \pm SEM). In physical units, this corresponded in most cases to errors well under 1 mm.

DISCUSSION & CONCLUSIONS: The fully automated software produces 3D reconstructions of the vertebra from scans before and after surgery, and also computes a predicted reconstruction approximating the target vertebra prior to injury. It has been validated against human experts and is in production use at Vexim SA, where it has been used to successfully process several hundred vertebrae.

REFERENCES: 1 P. Xiao et al (2009) *DICTA* **9**:387-94. ² G. Guglielmi et al (2009) *Eur J Rad* **70**:142-8.

ACKNOWLEDGEMENTS: This work was sponsored in part by Vexim SA, Toulouse, France.



Biodegradable cement to replace PMMA cement in management of VCF

AK Agarwal¹, M Kodigudla¹, D Desai¹, A Jones¹, B Lin^{1, 2}, VK Goel¹, B Schlossberg³

¹E-CORE, Department of Bioengineering and Orthopaedic Surgery, The University of Toledo, Toledo, OH, USA. ²Department of Biological Sciences, The University of Toledo, Toledo, OH, USA. ³Pioneer Surgical, Marquette, MI, USA.

INTRODUCTION: Kyphoplasty (KP) vertebroplasty (VP) procedures use PMMA to treat the fractured vertebrae. Bone erodes with time around the cement due to osteoporosis and inhibits bone remodeling due to the cytotoxicity. setting temperature and non-resorbability of PMMA [1, 2]. Thus, alternative cements are being explored. Calcium phosphate cements (CPC) have been explored due to their properties [3, 4]. However, the mechanical properties of CPC are questioned [1, 4]. A new polymerized CPC (pCPC) which is not brittle like traditional CPCs was evaluated. Mechanical properties of pCPC alone and of vertebral bodies augmented with either PMMA or pCPC after fracture were assessed.

METHODS: Spines were classified either normal (N) or osteoporotic (OP). Vertebral body (VB) height was measured as well as the mid sagittal plane distance (MSPD) and medial lateral distance (MLD) of the superior and inferior endplates. The MLD was measured at the halfway point of the MSPD of the superior and inferior endplates. Specimens were fractured by a transverse slit made with a hand saw blade width of 1.5mm in the middle of the VB. Specimens were restored with PMMA or pCPC. A MTS machine applied a compressive force, up to 50% of sample height, 10 mm anterior to the geometric center of the superior endplate. Endplates were leveled and aligned before compression. Loads were applied at 5mm/min and recorded to calculate the maximum cyclic load for the dynamic testing (DT). Height restoration of the fractured samples was performed using the Osseoflex® SN+ and Osseoflex® SB tools (Osseo, USA). Fluoroscopic images were used to monitor the location of the balloon in the vertebrae. The balloon was inflated at a given restoration height and cement was injected until extravasation. Samples were cured for 24 hours in water at 37°C. Height was measured before and after restoration. Static testing was performed on 15 samples, 5 from N group and 10 from OP group (5 for PMMA and 5 for pCPC). Compressive loads (5Hz, 100K cycles) of 25, 50, and 75% of the mean failure load (MFL) were applied. Augmentation for DT included pCPC in N and OP samples and PMMA in OP samples. pCPC in N vertebrae was not tested under the 75% of fracture load condition. Displacement was recorded for the DT and superior and inferior endplate height was measured pre- and post-fatigue.

RESULTS: N vertebral samples had a MFL of 9 ± 2 kN; N-pCPC augmented specimens of 9.2 ± 1.8 kN (p=0.853) and OP samples of 2.8 ± 1.4 kN. pCPC increased the failure load to 5 ± 2.7 kN (p=0.008) and PMMA to 7.2 ± 1.3 kN (p=0.049). DT revealed that at 25% MFL, OP PMMA and pCPC samples performed similarly with a mean displacement (MD) of 6.86 mm and 7.62 mm, respectively (p=0.739). For 50% MLF, PMMA had a MD of 8.60 mm and pCPC 16.46 mm (p=0.070). For the 75% MFL, PMMA had a MD of 13.81 mm and pCPC 17.12 mm. At 75% MFL one PMMA sample failed prematurely. Deformation during DT between OP and N specimens augmented with pCPC was no statistical different.

DISCUSSION & **CONCLUSIONS:** statistical difference between pCPC augmented and intact VBs for N specimens was observed. PMMA and pCPC improved the mechanical compressive strength of OP bodies with no significant difference between their augmentations (p=0.327). The similar performance between N and OP vertebrae under cyclic loading conditions could be due to part in the difference of value of the maximum load between the two vertebral conditions. For the 50% and 75% pCPC and 75% PMMA test groups, displacements up to 7mm occurred within the first 200 cycles before data This could be due collection began. deterioration of samples over time as these were unfrozen for multiple days before DT began. Quasi-static strength data and cyclic loading data suggest that pCPC could be a used in kyphoplasty.

REFERENCES: ¹ I.A. Grafe, M. Baier, G. Nöldge et al (2008) *Spine* **33**:1284-1290. ² S. Tomita, A. Kin, M. Yazu et al (2003) *J Orthop Sci* **8(2)**:192-197. ³ R. Rotter, R. Pflugmacher, F. Kandziora et al (2007) *Spine* **32(13)**:1400-1405. ⁴ T. Blattert, L. Jestaedt and A. Weckbach (2009) *Spine* **34(2)**:108-114.



Injectable peptide/glycosaminoglycan hydrogels and their potential use for minimally invasive nucleus pulposus augmentation

DE Miles^{1, 2}, E Mitchell¹, N Kapur³, RK Wilcox¹, A Aggeli²

¹Institute of Medical and Biological Engineering, University of Leeds, Leeds, UK. ²School of Chemistry, University of Leeds, Leeds, UK. ³School of Mechanical Engineering, University of Leeds, Leeds, UK

INTRODUCTION: Low back pain is strongly associated with degeneration of the intervertebral discs. Current surgical treatments for low back pain are highly invasive and have relatively low long term success rates [1]. The present work aims to develop a novel, minimally invasive therapy for nucleus replacement without the need for surgical incision using a versatile class of synthetic tapeforming, self-assembling peptides based on natural amino acids [2]. Peptides can be further optimised by mixings with GAGs found naturally in the disc.

METHODS: The peptides were analysed using a series of complementary analytical techniques (NMR, FTIR, CDUV & TEM) to determine their behaviour at the molecular and nanoscale levels and their mechanical behaviour was characterised using rheometry. A range of systematically varying peptide:GAG solutions were then injected in a bovine caudal disc model to assess the potential to remain at the treatment site and to restore disc mechanics.

RESULTS: These patented materials harness the intrinsic ability of peptides to self-assemble into micron-sized aggregates, which establish a nanostructured network and cause gelation of physiological solutions. Systematic changes in peptide structure led to aggregates with different morphologies, self-assembly profiles and mechanical properties (Fig.1).

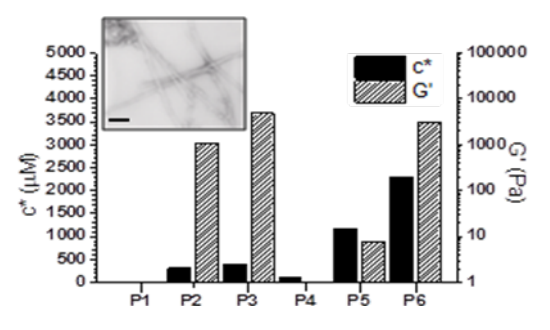


Fig.1: Critical concentration for self-assembly and elastic modulus for six peptides with differing primary structures. Inlay: TEM image of 20 mg/ml P3 fibrils in PBS, scale bar = 100 nm.

Another exciting finding was strong evidence that the mechanical properties of the gels can be controlled by peptide design and GAG ratio, allowing up to a 10,000 fold variation in the stiffness. The presence of the peptide greatly reduced the leakage of injected GAG and a denucleated disc repaired with a peptide:GAG gel was found to restore the mechanical behaviour to that of a disc with a healthy nucleus intact (*Fig.*2).

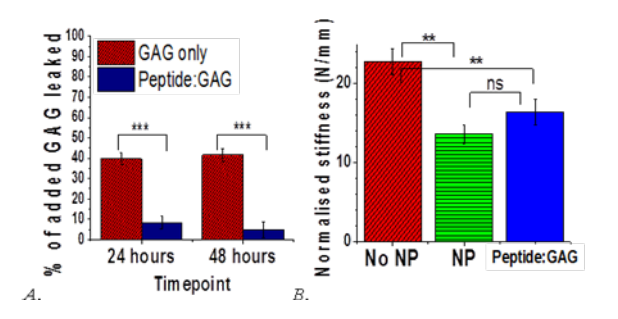


Fig. 2: A. Comparison of injected GAG leaked with and without injected peptide. B. Plot of normalized stiffness for each sample type under static compressive loading.

DISCUSSION & CONCLUSIONS: In summary although further optimisation is still required a gel material has been developed that has triggerable gelation and therefore is injectable and minimally invasive as a treatment. It forms a stable hydrogel with mechanical properties similar to that of the natural tissue and contains a high GAG content to aid in maintaining the swelling pressure and vital osmotic pumping action of the disc. The work presented here is the first step to the development of an improved nucleus augmentation treatment. If successful, it could improve the quality of life for patients and reduce the economic burden of disc degeneration.

REFERENCES: ¹ B.R. Whatley and X.J. Wen (2012) *Mater Sci Eng C Mater Biol Appl* **32**:61-77. ² R.P. Davies, A. Aggeli, A. J. Beevers et al (2006) *Supramol Chem* **18**:435-443.

ACKNOWLEDGEMENTS: The authors would like to thank the EPSRC Challenging Engineering Grant (EP/F010575/1) for funding this work.



Potential of fibre reinforced calcium phosphate cements for load bearing orthopaedic applications

N.J. Dunne, R. O'Hara, I. Palmer, S.A. Clarke, F.J. Buchanan

School of Mechanical and Aerospace Engineering, Queens University Belfast, UK

INTRODUCTION: CPC systems demonstrate poor tensile and shear properties due to their brittleness, limiting their application to non-load bearing defects. A successful improvement of the mechanical properties could significantly broaden the applicability of CPC, *e.g.* potential treatment of burst fractures. Reinforcement of CPC with natural fibres could potentially provide this improvement; therefore making possible the use of CPC systems in load bearing applications. This study aimed to incorporate collagen (Col) from different sources into a CPC system to compare their physical, mechanical and biological properties.

METHODS: CPC consisted of alpha tricalcium phosphate (TCP) and di-sodium hydrogen phosphate solution (Na₂HPO₄) using a liquid to powder ratio of 0.35mL/g [1]. Three types of Col were then incorporated into the CPC system, i.e. type I bovine fibres (BF) [2], marine fibres (MF) and marine particles (MP), these were added at 1 wt. %. Unreinforced samples were used for comparison (C). Routine tests to determine the static mechanical properties, injectability and setting properties were used [1, 2]. Biological in vitro evaluation of the Col-CPC composites was conducted using human bone marrow stromal cells (hBMSCs) seeded at a density of 5 x10⁴ cells/cm². a commercially available PMMA cement was used as a control. Cytotoxicity, proliferation and differentiation, were determined using lactate dehydrogenase (LDH), PicoGreen® and alkaline phosphatase (ALP) activity assays, respectively. Biological in vivo evaluation of the Col-CPC composites was performed in a NZW rabbit model (female/28 weeks old). Conical implants (Ø=4mm; L=8mm) were press-fitted into a defect in the distal femoral condyle. All defects were randomly assigned an implant type or no implant. Femora were retrieved in two groups; 5 and 10 weeks postimplantation. Histological analysis was conducted to determine the biocompatibility and bioactivity of each implant. Bone apposition, mineral apposition rate (MAR) and osteoclast activity were assessed.

RESULTS: Addition of 1 wt. % MF significantly increases the compressive strength to 37.8 ± 6.4 MPa, which is within the range stated for vertebroplasty (30MPa) [3]. BF (13.6 \pm 2.3MPa)

and MP (19.6 ± 3.6MPa) significantly reduced compressive strength. Adding MF showed no significant effect on injectability (55.9 \pm 9.0%); BF $(10.4 \pm 1.5\%)$ and MP $(20.2 \pm 4.4\%)$ significantly reduced the injectability. The reduction in injectability of MP could be due to a tendency for the particles to agglomerate; BF could hence, restrict the flow through the syringe and reduce cement extrusion. Introduction of all forms of Col reduced the setting times. Comparable times were found for 1 wt. % MP (13.5 \pm 1.6min) and MF $(15.5 \pm 0.5 min)$. Times were within the recommend setting time for vertebroplasty [3]. Cytotoxicity for all cements was similar and was considered not to be clinically relevant. SEM showed cells adhering and proliferating onto all cement types. Cells proliferated equally well on all the cements up to the final time point. Cell differentiation increased with time: differentiation was higher for the CPC sets. No significant difference in differentiation observed between the CPC, MP-CPC and MF-CPC sets. BF into the CPC significantly lowered the differentiation. All implants were well tolerated in vivo with little inflammatory response. Bone apposition onto the CPC was higher than on the PMMA. Bone grew very close, but was not apposed to the PMMA. The effect of Col incorporation on bone apposition significant within the first 10 weeks as no significant difference was observed between any of the CPC at either time point. No significant differences in MAR between any of the implant sets or time points were observed. The presence of positive TRAP staining within the CPC suggested active osteoclasts present and taking part in the remodelling process.

DISCUSSION & CONCLUSIONS: Mechanical and setting properties of CPC were improved, by adding MF, for load bearing applications. MF into the CPC did not compromise the biological properties. Thereby highlighting the potential for a marine fibre reinforced CPC as a minimally invasive solution for burst fracture treatment.

REFERENCES: ¹ R. O'Hara et al (2010) *J Mater Sci Mater Med* **21(8)**:2299-305. ² R. O'Hara et al (2012) *Acta Biomater* **8(11)**: 4043–4052. ³ J. Jansen et al (2005) *Orthop Clin N Am* **36**: 89-95.



Vertebral microstructure, failure and augmentation

EF Morgan

Departments of Mechanical Engineering, Biomedical Engineering, and Orthopaedic Surgery, Boston University, MA, USA

Although vertebral fractures are the hallmark of osteoporosis, their pathogenesis remains poorly understood [1]. In contrast to osteoporotic fractures in the hip and wrist, those in the spine often have a slow onset and evade clinical detection for long periods of time. Clinical and biomechanics studies have identified many factors contributing to vertebral strength and fracture risk [2]. These factors include the macro- and microstructure of the vertebra, distribution of mineral density within the vertebral body, properties of the mineralized tissue, and nature of the in vivo loading. With recent advances in the ability to quantify, or at least estimate, all of these properties, there is now tremendous opportunity to integrate this information towards a better understanding of vertebral failure. This talk will review some of the key findings from the body of literature on the contribution of vertebral microstructure to bone failure. Subsequently, recent work on direct, three dimensional visualization of vertebral failure will be presented [3]. Applications of this work and implications of the findings for vertebral augmentation will be discussed.

REFERENCES: ¹ T.W. O'Neill, D. Felsenberg, J. Varlow et al (1996) *J Bone Miner Res* **11**:1010-8. ² B.A. Christiansen and M.L. Bouxsein (2010) *Curr Osteoporos Rep* **8**:198-204. ³ A.I. Hussein, P.E. Barbone and E.F. Morgan (2012) *Procedia IUTAM* **4**:116-125.

ACKNOWLEDGEMENTS: The support provided by the NIH grant AR056420; International Osteoporosis Foundation and Servier; the support provided by the NSF grant BES 0521255.



Effect of cement injection on mechanical properties in fractured and prophylactically augmented multiple myeloma vertebrae

DM Skrzypiec¹, O Holub¹, VH Borse¹, AM Liddle¹, N Brandolini¹, A Bou Francis¹, J Timothy², G Cook³, N Kapur¹, RM Hall¹

¹ iMBE, University of Leeds, Leeds, UK. ² Department of Neurosurgery, Leeds Teaching Hospitals Trust, Leeds, UK. ³ Institute of Oncology, St James's University Hospital, Leeds, UK.

INTRODUCTION: Over 85% of patients with multiple myeloma (MM) have bone disease, mostly affecting thoraco-lumbar vertebrae [1]. Vertebral fractures can lead to pain and spinal deformities requiring application of vertebroplasty (PVP). Possibly prophylactic augmentation can be performed to minimize fracture of weak vertebrae occurring. Additionally application of Coblation to dissolve lesions, using radiofrequency energized plasma, from compromised MM vertebrae prior to cement injection (C-PVP) could help with cancer management. The aim of this study was to evaluate biomechanical effects of augmentation in fractured and intact MM vertebrae, using PVP and C-PVP augmentation techniques.

METHODS: 57 single vertebrae with lesions were dissected from 9 MM cadaveric spines. 29 MM vertebrae were initially fractured up to 75% of its original height on a testing machine using modified test set-up [2], with rate of 1mm/min. Load was applied at 25% of AP-diameter, from anterior. The remaining 28 intact MM vertebrae were used for prophylactic augmentation. Two augmentation procedures were investigated in both groups: PVP and C-PVP. All vertebrae were augmented with 15% of the vertebral volume using PMMA cement. Augmented MM vertebrae were fractured, following the same protocol as for initial fracture. Failure load (FL) was defined as 0.1% offset evaluated from slope fitted to the linear region (Stiffness) of load displacement curves. The load at the end of the tests was compared.

RESULTS: There were no statistically significant differences between the PVP and C-PVP augmentation techniques; hence the data was pooled for further analysis (Fig 1). The FL of augmented-initially-fractured vertebrae was 32% higher than for initial fracture (p=0.028, repeated ANOVA). There was no significant difference in FL of prophylactically augmented vertebrae. The end of test load for initial fracture was 55% and 49% lower than for augmented-initially-fractured and prophylactically augmented vertebrae, respectively (p<0.001). Stiffness of augmented-

initially-fractured vertebrae was 50% and 59% lower than for initial fracture and prophylactically augmented vertebrae, respectively (p<0.001).

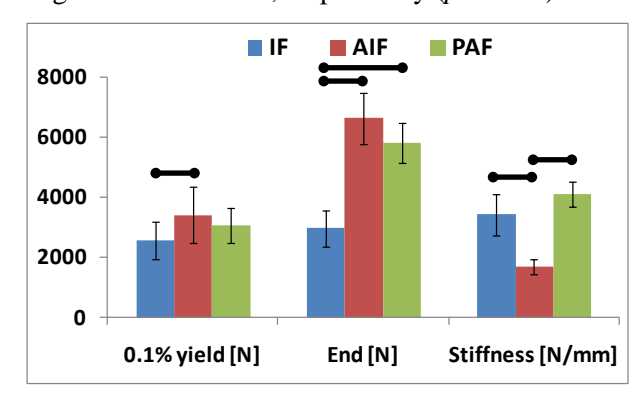


Fig. 1: Mean data \pm 95% confidence interval, with marked significant differences (IF – initial fracture; AIF – augmented-initially-fractured; PAF - prophylactic augmentation fracture).

DISCUSSION & CONCLUSIONS: Increase in FL and reduced stiffness of augmented-initially-fractured vertebrae is related to relatively small percentage fill (15 %). In earlier study it was shown that smaller PMMA cement volumes are required to restore strength but larger volumes are needed to restore stiffness [3]. Prophylactic augmentation changed pattern of failure: initially it was similar to initially fractured vertebrae but at the End of test similar to augmented-initially-fractured vertebrae. Coblation treatment did not compromise stiffness or strength of augmented MM vertebrae and can be an important tool for surgeons to treat MM infiltrated vertebrae.

REFERENCES: ¹ L.J. Melton et al (2005) *J Bone Miner Res* **20**:487-93. ² E. Dall'Ara et al (2010) *J Biomech* **43**:2374-80. ³ S.M. Belkoff et al (2001) *Spine* **26**:1537-41.

ACKNOWLEDGEMENTS: Study was funded by EPSRC (EP/H013385/1). AthroCare provided Coblation, cement and injection equipment.



Is morphology alone an effective indicator when planning prophylactic vertebroplasty in multiple myeloma patients?

O Holub¹, D Skrzypiec¹, J Timothy², N Kapur¹, RM Hall¹

¹ University of Leeds, Leeds, UK.² Leeds General Infirmary, Leeds, UK.

INTRODUCTION: Multiple myeloma (MM) is a neoplastic pathology resulting in structural weakening of a bone due to lytic infiltration to the bone. Minimally invasive operation techniques such as vertebroplasty (PVP) show great potential to prevent debilitating fractures in weakened bone. Previous studies indicated possible efficacy of prophylactic PVP [1, 2]. However, non-destructive assessment of the vertebral body remains a key factor. The unique morphological character of bone affected by MM cancer hampers use of approaches defined for osteoporotic pathology. This study was performed to identify suitable methods for assessment of cancer samples prior to prophylactic augmentation.

METHODS: Forty-three samples from three MM spines were disarticulated, cleaned of soft tissue and underwent CT scanning ([microCT80, Scanco medical AG], voxel size 70.8µm3), followed by uni-axial eccentric compression test to induce the anterior wedge fracture. The failure load (Fu) was defined as the first zero slope on the load displacement curve. Bone density images were binarized with the threshold value based on an iterative selection method [3], The microstructural quantified morphology was using Processing Language (IPL, [Scanco Medical AG]). Trabecular Spacing (Tb.Sp and $Tb.Sp_VB)$, thickness (Tb.Th), number of trabeculae (Tb.N), bone mineral density (BMD), bone fraction (BVTV and BVTV_VB), degree of anisotropy (DA), structural model index (SMI) and connectivity density (Conn.D) were assessed in representative cylinder inside the vertebral body and for whole vertebral body (_VB). Subsequently, the weakest slice and the minimal fracture load (Fz) was estimated using an analytical beam theory applied on CT images [4, 5]. Trabecular microarchitecture indices and the predicted Fz were compared to experimental data.

RESULTS: Morphometry indices (*BMD*, *Tb.Th*, *DA*, *BV/TV*, *Tb.Sp*, *Tb.N*, *SMI* and *Conn.D*) showed low or no correlation with Fu; varying from r=0.06(BMD) to r=0.44(Conn.D). Only min.CSA(r=0.69) and Fz(r=0.91) was found as good standalone predictors in all 43 samples.

Furthermore, traditionally good predictors of strength (BMD and BV/TV) appeared to be successful in two out of the three spines (r=0.12, r=0.70 and r=0.73 for BMD and r=0.30, r=0.63 and r=0.72 for BV/TV). Where Fz remained consistently high regardless the difference between spines (r=0.86, r=0.85 and r=0.95). The product of microstructure indices and min.CSA was found to increase the correlation; this varied from r=0.39 (min.CSA*Tb.Sp) to r=0.76 (min.CSA*Conn.D).

Table 1 Coefficient of determination (R^2) of Failure load (Fu) versus Predicted failure load (Fz) and selected morphometric indices.

	Spine1	Spine2	Spine3	All spines
Beam theory(Fz)	0.74	0.73	0.9	0.82
BMD	0.01	0.49	0.53	0.003
min.CSA*BVTV	0.40	0.66	0.22	0.36
min.CSA*BVTV_VB	0.58	0.70	0.55	0.56
min.CSA*BMD	0.34	0.67	0.27	0.25
min.CSA*DA	0.35	0.29	0.72	0.48
min.CSA*Conn.D	0.17	0.51	0.20	0.58

DISCUSSION & CONCLUSIONS: Prior to conducting a study on the effectiveness of prophylactic augmentation in a MM cancer patient a detailed morphometrical assessment of this pathology had to be conducted. Results suggest that the lytic nature of the disease and interspinal variability (including due to treatment history) hampers using the conventional approach in benchmarking the cancer specimens. Next to a detailed morphological assessment of MM samples the results show that combination of both the geometric distribution and measure of bone deterioration is needed for reliable assessment of strength.

REFERENCES: ¹ N. Kobayashi *et al* (2009) *Acad Radiol* **16**:136-143. ² R.J. Oakland et al (2008) *J Neurosurg Spine* **8**:442-449. ³ T.W. Ridler and S. Calvard (1978) *IEEE Systems, Man and Cybernetics* **8**(**8**):630-632. ⁴ K.M. Whelan et al (2000) *J Bone Joint Surg Am* **82**:1240-1251. ⁵ T.S. Kaneko et al (2004) *J. Biomech* **37**:523-530.

ACKNOWLEDGEMENTS: EU funded project. Grant Agreement n° PITN-GA-2009-238690-SPINEFX.



Investigation of facet joint model properties for the assessment of interventions in the functional spinal unit.

SM Tarsuslugil, RM Hall, RK Wilcox

University of Leeds, School of Mechanical Engineering, United Kingdom.

INTRODUCTION: The complex motion and geometry of the spine in the cervical region make it difficult to determine how loads are distributed through adjacent vertebrae or between the zygapophysial (facet) joints and disc. Spinal interventions such as vertebroplasty disc/nucleus replacement have been reported to affect this load distribution [1] and have highlighted a requirement for finite element modeling to more fully investigate how the biomechanics in the functional spinal unit (FSU) is affected by such interventions. The aim of this study was to develop a method to validate specimen specific FE models of FSUs prior to spinal intervention, using local measurements as well as the overall stiffness.

METHODS: Three FSUs were excised from three-year old ovine spines from within the cervical region. Small markers were then affixed to the facet joints to track motion. The vertebrae were mounted in PMMA cement. Another marker disc was fixed to the upper PMMA surface to indicate the position of load application for the experiments and the corresponding FE models. The specimens were then μ CT imaged (μ CT100, Scanco, Switzerland).

Prior to testing, the facet joint capsules were cut, allowing a thin film pressure sensor (6900, Tekscan, USA) to be positioned between the cartilage surfaces. The specimens were then tested under axial compression, using a materials testing machine (Instron 3365, USA). A loading rate of 1mm/min was applied, and halted after 2mm of deflection had been reached. Photographs were taken at every 0.5mm of deflection using a tripod mounted camera (Canon 550d, Japan).

To determine the material properties of the disc, the specimen was then retested following removal of the posterior elements and facet joints. The μ CT image data was used to create specimen specific FE models of the FSUs. The models were generated using image processing and meshing software (ScanIP, Simpleware, UK). Bone material properties were determined by the image grayscale obtained from the μ CT [2] Cartilage material properties such as friction and Young's modulus were varied to investigate the models sensitivity to

these parameters. The intervertebral disc was assigned material properties in the form of nine engineering constants [3] following a process of tuning specimen specific FE models (without posterior elements) to the corresponding experimental data.

RESULTS: Load displacement data from a single specimen is presented in Figure 2. The optimum value for friction coefficient for the cartilage interaction (μ_c) was 0.05; this corresponds well to values found experimentally for cartilage on UHMWPE [4].

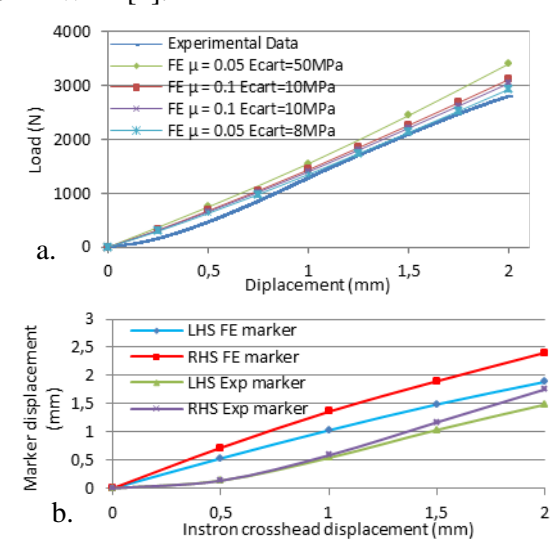


Fig. 2: a) FE vs. Experimental data showing model sensitivity of E_{cart} & μ_c . b) FE predicted vs. experimental marker position (E_{cart} =50MPa, μ_c =0.05).

DISCUSSION & CONCLUSIONS: The models appeared to be more sensitive to the Young's modulus of the cartilage surface compared to the friction coefficient. Models predict the overall stiffness of the FSU and marker location well. This technique will now be used to investigate how the influence of spinal interventions affects natural FSU biomechanics.

REFERENCES: ¹ J. Luo et al (2007) *J Bone* **40**:1110-1119, ² S. Tarsuslugil et al (2010) *Proc* 9th symp CMBBE. ³ D.M. Elliott and L.A. Setton (2001) *J. Biomech Eng* **123**:256-263. ⁴ S.M.T. Chan et al (2011) *J Tribol* **133**(**4**):041201-7.

ACKNOWLEDGEMENTS: Authors thank the funding provided by the EPSRC (EP/G012172/1).



Simulation of patient variance in computational models of the spine

AC Jones¹, S Rehman¹, VN Wijayathunga¹, KA Robson Brown², RK Wilcox¹

¹ Institute of Medical and Biological Engineering, University of Leeds, Leeds, UK. ² Imaging Laboratory, Department of Archaeology and Anthropology, University of Bristol, Bristol, UK.

INTRODUCTION: Back pain remains a major clinical and societal problem. One barrier to the successful development of spinal interventions has been the lack of robust methods of testing new treatments before they are introduced clinically. Testing tends to be undertaken on standardised laboratory or computational models, or on small numbers of in vitro specimens. Our previous work on vertebroplasty has highlighted the difference in mechanical behaviour between patients after cement augmentation because of their different anatomies [1]. In order to improve preclinical testing tools, there is therefore a need to be able to represent these variances across the patient population. The aim of this work was to characterise the differences in vertebral anatomy, architecture and properties and to develop computational models that represent variances.

METHODS: Fifty human cadaveric vertebrae (T12-L1) were imaged using microCT (uCT80, Scanco Medical, CH; Sykscan 1172, Skyscan, BE). The images were segmented using a consistent threshold and smoothing procedure. A new algorithm was developed to extract the cortical shell region. Both the shell and the trabecular bone regions were then divided into subregions and characterised using standard morphometrical measurement algorithms. Finite element (FE) models were generated from the segmented images (ScanIP, Simpleware, UK). The models had a maximum element size of 1mm and the material property of each element was based on the bone volume fraction (BV/TV) of the underlying image. Standardised loads and boundary conditions were applied and the models were solved to predict the vertebral stiffness (Abaqus, Simulia Corp, USA). Validation of the method along with sensitivity and convergence studies has been reported previously [1, 2].

RESULTS: Large differences in both the vertebral morphology and the internal bone structure were found, even in the same age group and spinal level. An example for the BV/TV is shown in Figure 1. Some regional trends were observed in terms of BV/TV distribution and cortical shell thickness, but not across all the spinal levels. The FE results

demonstrated a large range in specimen stiffness, with a twofold difference even at the same level and in the same age group (Fig 2).

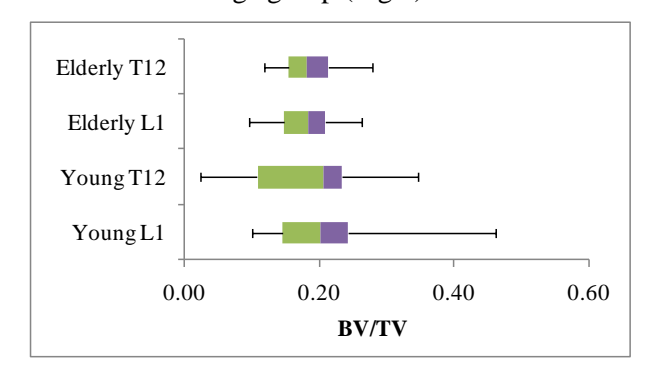


Fig. 1: Box plots of BV/TV across whole trabecular region for four subsets of the vertebrae.

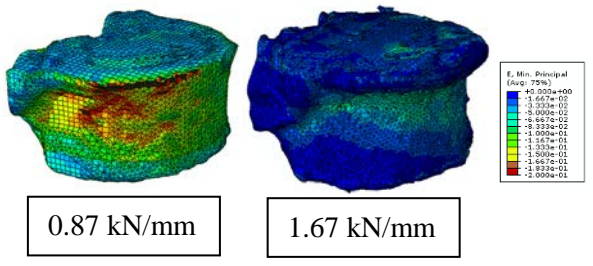


Fig. 2: Maximum compressive strain distribution on two example T12 models from the elderly population group. The stiffness values are shown.

DISCUSSION & CONCLUSIONS: Large variations in the geometry and bone properties from one vertebra to another were found. The FE results illustrate how these variances lead to big changes in the structural behaviour. The results highlight the need for treatments to be assessed across a clinically relevant range of specimens, rather than in a standardised model. This model dataset provides a potential tool, and further work is now underway using principal component analysis techniques generate to models representing specific variances in the patient population.

REFERENCES: ¹ A.C. Jones, V.N Wijayathunga, S. Rehman et al (2012) *Patient-Specific Modeling in Tomorrow's Medicine* (Ed A. Gefen), Springer, pp 133-154. ² A.C. Jones and R.K Wilcox (2007). *J. Biomech. Eng.* **129:**898-903.

ACKNOWLEDGEMENTS: Funded by EPSRC Challenging Engineering grant EP/F010575.



Novel 2D bone surrogate models for assessing cement injection behaviour in vertebroplasty

A Bou Francis, N Kapur, RM Hall

School of Mechanical Engineering, University of Leeds, Leeds, UK.

INTRODUCTION: Concerns related to cement extravasation, embolism, irregular or insufficient filling in vertebroplasty provide the motivation for the development of methodologies for assessing new cements and delivery systems [1]. Reproducible and pathologically representative two-dimensional flow models are used to understand the influence of cement properties on injection behavior.

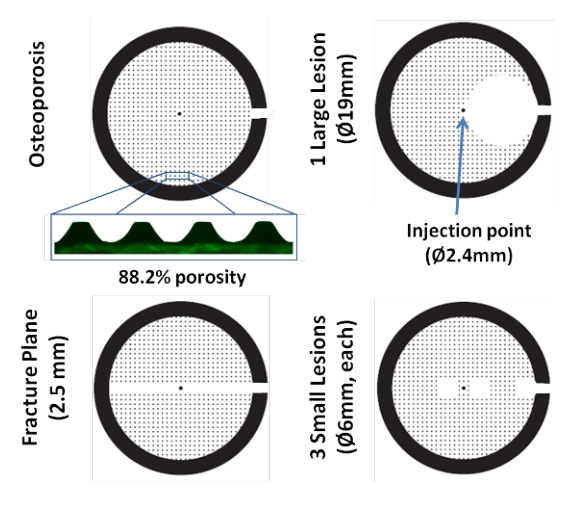


Fig. 1: Manufactured using photolithography, the 2D models have 1mm channel spacing, 0.25mm column thickness, 40mm outer diameter, and a solid boundary with 2.5 mm opening.

METHODS: A profile projector was used to test model variability. The 2D models, sandwiched between an upper glass window and a lower aluminium plate, were filled with bone marrow substitute (Carboxymethyl cellulose 1.25 % in water) then 1mL of PMMA bone cement (cold cure / rapid repair, WHW Plastics, UK) 1-to-1 liquid-to-powder ratio was injected (3, 5, 7, 9, 11 and 14 min) after cement mixing at a constant flow rate (3mL/min) using a syringe pump. Experiments were repeated three times. Labview (National Instruments, UK) was used to control the syringe pump and acquire LVDT, load cell and video data. The LVDT was used to measure the displacement of the syringe plunger. The load cell was used to measure the force applied on the plunger. The video data were analyzed in Matlab (MathWorks, UK) to quantitatively describe the resulting flow patterns and calculate parameters including the time to reach the opening in the boundary, the % filled area and the roundness.

RESULTS: The inter- and intra-model variability was very low. The pressure in the system was below 2 MPa for all injections. All parameters used to quantify the resulting flow patterns increased with the time of injection and reached an asymptotic behavior at 11 min after cement mixing.

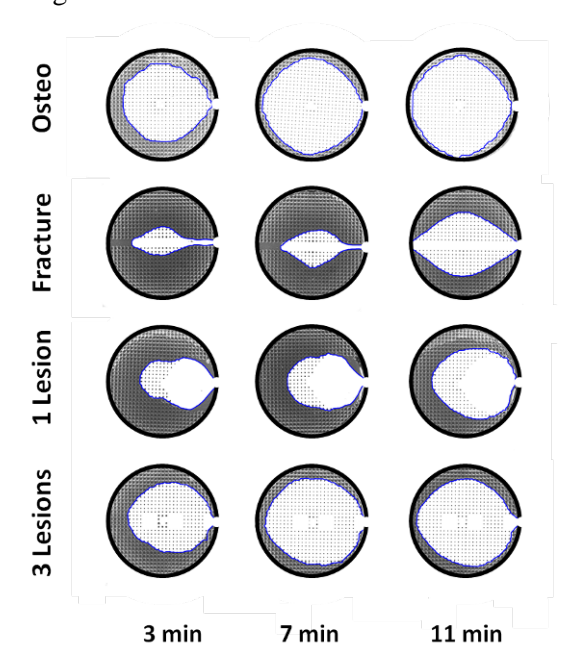


Fig. 2: Flow contours when the cement reached the hole in the boundary at various injection times after cement mixing.

DISCUSSION & CONCLUSIONS: There is a critical upper viscosity at which the injection pressure remains clinically relevant while the cement spreading is uniform and not affected by variations in the geometrical structure. The models provide a tool for quick, robust differentiation between various cement formulations, quantitative analysis of cement spreading at each time point until the cement reaches the boundary and prediction of the uniformity of cement distribution.

REFERENCES: ¹ J.D. Laredo and B. Hamze (2004) *Skeletal Radiol* **33**:493–505.

ACKNOWLEDGEMENTS: Funding was provided by the EU under the FP7 Marie Curie Action (PITN-GA-2009-238690-SPINEFX).



Mechanical and *in vitro* evaluation of low-modulus bone cement - Osteopal[®]V modified with linoleic acid

A López¹, G Mestres¹, M Karlsson Ott¹, H Engqvist¹, S J Ferguson², B Helgason², C Persson¹

Div. of Applied Materials Science, Department of Engineering Sciences, Uppsala University, SE.

Institute for Biomechanics, Swiss Federal Institute of Technology Zurich, CH

INTRODUCTION: Adjacent vertebral fractures are a common postoperative complication upon vertebroplastv Some clinical [1]. biomechanical investigations associate the risk for adjacent vertebral fractures with the usage of high stiffness bone cements [2]. The development of viable low-modulus cements has been a major challenge, since modification of commercial formulations typically results in poor cell viability or particle release [3]. Literature concerning in vitro evaluation of acrylic cements is scarce. In this work, we evaluate the mechanical behaviour of a commercial bone cement that, with minimal modification, can reach more bone-compatible mechanical properties. In addition, we report indirect cytotoxicity in vitro using a human osteoblast-like Saos-2 cell line.

METHODS: Osteopal[®]V (OP, Heraeus Medical, Hanau, Germany) cement was used as a base and modified with 9-cis,12-cis-linoleic acid (LA) dissolved in the liquid component. The following concentrations, with respect to the total weight of material, were analysed: 0 (OP), 0.75 (OP-0.75), and 1.50 (OP-1.50) wt% LA. Six groups of 14 specimens (\emptyset =10 mm, h= 20 mm) were prepared. Three groups consisted of cement only, whereas the other three consisted of cement-augmented bovine bone cores. The stress-strain behaviour was determined by uniaxial compression testing using an Instron machine at a crosshead speed of 6 mm/min. For the cytotoxicity assay, three groups of 15 specimens (Ø=12 mm, h=2 mm) were prepared. Extracts were prepared by placing specimens in cell medium at 3 cm²/ml [4]. Every 1, 6, 12 and 24 h, extracts were collected and medium was refreshed. Cells were seeded at 20000 cells/cm² and after 24 h, extracts were added undiluted or 4-fold diluted [4]. The cells were incubated with extracts or complete media for 24 h or 72 h. Cell viability was quantified using the AlamarBlue assay.

RESULTS: Figure 1 illustrates the general stressstrain behaviour of all cement groups. The Young's modulus (*E*-modulus) and yield strength (σ_v) decreased as the LA concentration increased up to 1.50 wt%. For the cement-only group, the E-modulus and σ_y decreased by 74% and 83%, respectively. For the bone-cement group, the E-modulus and σ_y decreased by 33% and 47%, respectively.

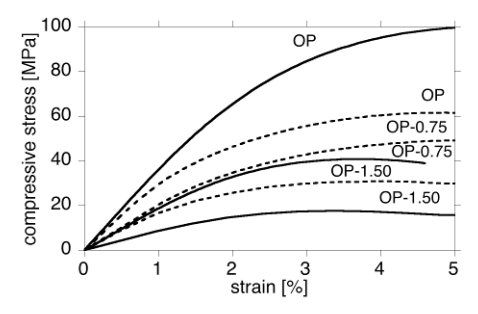


Fig. 1: Stress-strain curves for the cement-only (full) and bone-cement (dashed) groups.

Regarding cytotoxicity, for undiluted extracts, cell viability decreased for LA-modified cements in a dose-dependent manner. However, no significant differences were observed for LA-modified cements in 4-fold diluted extracts. In diluted extracts, the cells proliferated over time.

DISCUSSION & CONCLUSIONS: The addition of very small concentrations of LA can significantly reduce the *E*-modulus of commercial bone cement making it more bone-compatible. This is accompanied by a reduction of the *E*-modulus of the treated bony structure. The change in properties is thought to occur due to incorporation of LA into the polymer network by methacrylation via chain transfer mechanism. Although LA reduced the cytocompatibility of Osteopal[®]V, it is expected that fluid exchange would compensate this effect as observed for diluted extracts.

REFERENCES: ¹ F. Grados, C. Depriester, G. Cayrolle et al (2000) *Rheumatology* **39**:1410-4. ² A.A. Uppin, J.A. Hirsch, L.V. Centenera et al (2003) *Radiology* **226**:119-24. ³ S. Beck and A. Boger (2009) *Acta Biomater* **5**:2503-7. ⁴ ISO stardard 10993-11, 1993.

ACKNOWLEDGEMENTS: Funding by the EC (project FP7-ICT-223865-VPHOP and SPINEGO), STINT, VINNOVA, and the Swedish Research Council is gratefully acknowledged.



Compressive fatigue properties of acrylic bone cement for vertebroplasty

I Ajaxon, C Persson

Div. of Applied Materials Science, Dept. of Engineering Sciences, Uppsala University, SE

INTRODUCTION: Acrylic bone cements based on poly(methyl methacrylate) (PMMA) commonly used for the fixation of joint prostheses as well as for vertebroplasty. Fatigue properties of the cement are important to the long-term success of the implant. The ASTM F2118-03 standardoriginally developed for cements used in joint fixations - specifies a fully reversed tensioncompression test. However, the same standard is commonly used for testing of cements intended for vertebroplasty, despite the fact that vertebrae mainly experience compressive loads. Until now, purely compressive fatigue studies of PMMA are scarce [1, 2]. Studies on vertebroplastic cement, which may contain a higher amount of radiopacifier, are none. The aim of this study was to evaluate the compressive fatigue properties of vertebroplastic cements, as well as the effect of frequency on these properties. Due to the time consuming character of fatigue tests – the standard cites a frequency of 2 Hz - there is a desire for increasing the frequency to higher values.

METHODS: A commercial acrylic cement for vertebroplasty, Osteopal V® (Heraeus Kulzer GmbH) was used. The powder phase contains 45 wt% of ZrO₂ as a radiopacifier. Powder and liquid phases were manually mixed, and moulded in cylindrical moulds ($\emptyset = 6 \text{ mm}$ and 12 mm height). The specimens were cured at ambient temperature. Prior to fatigue testing, specimens were visually radiographically examined. Samples containing defects greater than 1 mm were discarded. Fatigue testing was performed under ambient conditions with a constant-amplitude sinusoidal wave profile, at 2 or 10 Hz, using a dynamic material testing system (MTS Axial 858 Mini Bionix II). Each specimen was subjected to a small pre-load of 20 N, and run-out was set at 5 million cycles. Failure was defined to occur at a strain of cumulative 15%, as compression fractures are detected at a vertebral height reduction of 15-25% [3].

RESULTS: The S-N curve for the experimental data together with fits to an Olgive-type equation are shown in figure 1. The statistical analysis of the fatigue results showed significant differences between the tested frequencies at stress levels of 55 and 60 MPa. However, at higher stress levels

the diffferences between 2 and 10 Hz were no longer significant. The estimated fatigue limits from the Olgive equations were 54.5 and 41.3 MPa, for 2 and 10 Hz, respectively.

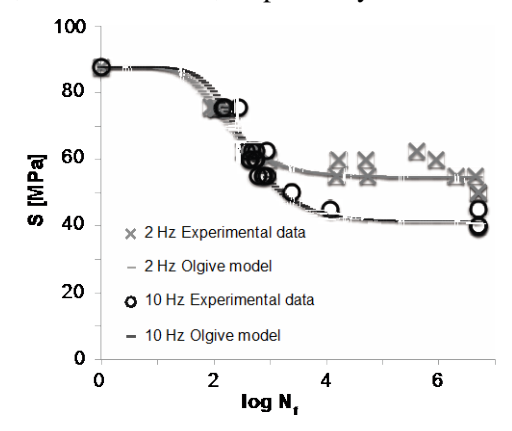


Fig. 1: Applied stress (S) as a function of the number of cycles to failure (N_f) .

DISCUSSION & CONCLUSIONS: The fatigue strengths presented here are lower than previous findings for acrylic cement in compression (CMW1®) [2]. However, the cement composition differs and this will influence the mechanical properties. The results presented here also show significant differences in fatigue properties at different frequencies. It has previously been shown that localized thermal heating of PMMA may shorten the fatigue life of the specimen [1], and increasing the frequency increases the thermal softening of the material. Hence an increase from 2 to 10 Hz may lead to an apparent decrease in fatigue life of acrylic bone cements under compressive loading. The estimated fatigue limit is approximately five times as high as that for the same cement (to the authors' best knowledge) in full tension-compression at 2 Hz [4]. This indicates that tension-compression fatigue testing may substantially underestimate the performance of cements intended for vertebroplasty.

REFERENCES: ¹ D. Rittel (2000) *Mech Mater* **32**:131–147. ² K. Serbetci et al (2004) *Polym Test* **23**:145–155. ³ E.N. Schwartz and D. Steinberg (2005) *Curr Osteoporos Rep* **3**:126–135. ⁴ G. Lewis (2000) *J Biomed Mater Res* **53**: 119-130.

ACKNOWLEDGEMENTS: Funding from VR – Swedish research council, Vinnova and EU is gratefully acknowledged.



Augmentation of cadaveric vertebrae with an α -TCP/ α -CSH ceramic cement: A biomechanical study on the effect of injected volume

O Holub¹, A Kasioptas², N Brandolini¹, N Kapur¹, E Lidén², RM Hall¹

¹ School of Mechanical Engineering, University of Leeds, Leeds, UK, ² BONESUPPORT AB, SE

INTRODUCTION: More than two million vertebral compression fractures (VCF) occur annually in the EU [1], with increasing health-care costs currently exceeding 30 billion €year[2]. Percutaneous vertebroplasty (PVP) as a cheaper and minimally invasive treatment tool shows promising results in improving patients' quality of life. Predominantly there are two types of materials used in PVP, biocompatible calcium-based materials (CaP) and acrylic PMMA materials that lack osseointegration. The injectable biphasic α -TCP (Tri-Calcium Phosphate) / α -CSH (Calcium Sulfate Hemihydrate) material used in this study is osteoconductive and resorbable, thus possessing a bone remodelling capacity. This biomechanical study provides evaluation for the initial stages after implantation with focus on optimization of cement volume.

METHODS: Thirty samples from three osteoporotic spines were disarticulated, cleaned of soft tissue and underwent CT scanning ([microCT80, Scanco medical AG], voxel size 70.8µm³). Samples were allocated to three equal groups (A, B, C) using a beam-theory based fracture prediction method.

Samples underwent an eccentric axial compression at 25% of vertebral body depth, at 1mm/min rate to induce a wedge fracture. Stiffness was defined as the maximum slope on the load-displacement curve. Strength was estimated based on the proof load at 0.5% apparent strain offset. Groups A, B and C were injected bi-pedicularly with the ceramic cement with 10, 20 and 30% of vertebral body volume, respectively. The augmented samples were soaked in 0.04% sodium azide solution and left to cure for 72h, at 37°C, with sequential re-fracturing. Pre/post augmentation strength and stiffness were compared.

RESULTS: Groups A, B and C were injected with 2.1 ± 0.7 , 4.3 ± 1.2 and 6.4 ± 2.0 ml of cement, respectively. No significant difference was found in either strength or stiffness between the groups (p>>0.05). Initial stiffness was higher for all groups (box plot in fig.1). Combining all data, the initial strength $(1.05\pm0.61\text{kN})$ increased to $2.02\pm1.0\text{kN}$, whilst the stiffness was found to

decrease from 1.98±1.66kN/mm to 1.18±0.55kN/mm (fig.2).

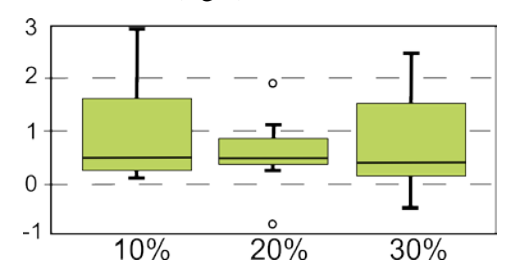


Fig. 1: Difference between stiffness pre and post augmentation [kN/mm] grouped by filling volume.

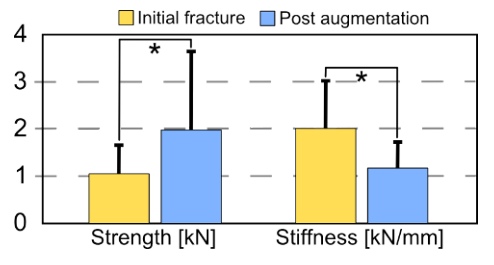


Fig. 2: Pre and post augmentation comparison.

DISCUSSION & CONCLUSIONS: The results of this study show that this ceramic cement almost doubled the strength of the cadaveric vertebrae, while stiffness was almost halved when compared to pre-augmentation values, which is in agreement with previous studies [3, 4, 5]. Regarding the effect of different cement volume, the reported results indicate that even the smaller volumes (~2ml, 10% of vertebral body volume), may be sufficient to stabilize the fracture suggesting that the volume of introduced cement is not crucial in terms of biomechanical improvement. The findings imply that volume is not a crucial factor in enhancing vertebral strength and stiffness. Hence, the volume can be adjusted rather according to the bioactive character of the cement to achieve the optimal bone-healing conditions.

REFERENCES: ¹ O. Strom et al (2011) *Arch Osteoporos* **6:**59-155. ² J.A. Kanis et al (2005) *Osteoporos Int* **16:**229-238. ³ S. Tomita et al (2003) *J Orthp Sci* **8:**192-197. ⁴ T.H. Lim et al (2002) *Spine* **27(12):**1297-1302. ⁵ S. Tomita et al (2004) *Spine* **29(11):**1203-1207.

ACKNOWLEDGEMENTS: EU funded project Grant Agreement n° PITN-GA-2009-238690-SPINEFX.



Novel resorbable calcium phosphate putty for bone tissue engineering

C Sfeir^{1,2,3}, A Roy^{1,2,3}, S Zaky^{1,2,3}, S Yoshizawa^{1,2,3}, B Costello^{3,4}, PN Kumta^{1,2,3}

¹Center for Craniofacial Regeneration, School of Dental Medicine, University of Pittsburgh, Pittsburgh, PA, USA. ²Department of Bioengineering, University of Pittsburgh, Pittsburgh, PA, USA. ³McGowan Institute for Regenerative Medicine, University of Pittsburgh, Pittsburgh, PA, USA. ⁴Department of Oral and Maxillofacial Surgery, University of Pittsburgh, Pittsburgh, PA, USA.

INTRODUCTION: There is a need to develop safe and effective craniofacial/orthopedic bone regeneration material. The objective of this study is to determine the efficacy of a novel biodegradable nano-structured Calcium Phosphate (CaP) based putty for bone regeneration. This putty will contain nano-sized CaP nanoparticles (NanoCaPs), as carriers, with or without BMP-2 to enhance bone regeneration in a critical sized bone defect model.

METHODS: Nano-structured porous calcium phosphate based putty carrying nanosized CaPs nanoparticles (NanoCaPs) were prepared and characterized prior to their in vivo use. Critical size defects (CSD) in rabbit ulnae (1.5-cm segmental defect) and a 15mm diameter rabbit craniofacial defect were created to test the regeneration potential of the putty alone or with BMP-2. X-rays were taken immediately following the surgery as well as 2, 8 and 26 weeks post-op. Rabbit specimens were harvested at designated time points and Micro-CT as well as histological, and histomorphometry analysis were performed to quantify bone regeneration.

RESULTS: The putty shows excellent cell attachment and cellular migration. The nanostructured nature and the high specific surface area of the HA formed as a result of the setting reaction are added factors contributing to the likely observed faster resorption kinetics of the implanted putty. Our results of the radiographical, micro-CT and histological/histomorphometrical assessment of the new regenerative bone showed that with or without BMP-2 addition to the CaPputty yielded higher bone regeneration compared to the control groups.

DISCUSSION & CONCLUSIONS: Our results to date thus indicate that the CaP-putty with or without the incorporation of BMP-2 does yield bone healing enhancement compared to controls. Our current on-going research is focused on exploring further the development of resorbable

putties that are amenable to the addition of growth factors.



Injectable, settable lysine-derived polyurethane grafts for bone regeneration

SA Guelcher

Vanderbilt University, Nashville, TN, USA.

INTRODUCTION: Within the US more than 650,000 bone grafting procedures are performed each year. Although autologous bone grafts have the best capacity to stimulate healing, explantation risks donor-site morbidity. Thus, the development of synthetic therapeutics exploiting minimally invasive surgical techniques has substantial benefits for treatment of orthopaedic injuries. We are developing biodegradable bone grafts and drug delivery systems comprising two reactive liquid components that harden in situ as an injectable alternative to autograft [1, 2]. These materials cure in <10 min and support infiltration of cells and ingrowth of new tissue in vivo. The injectable grafts are also an efficient delivery system for biologics, including antibiotics and growth factors such as recombinant human bone morphogenetic protein (rhBMP-2). We aim to create a family of injectable grafts for treatment of orthopaedic conditions that are difficult to heal, such as tibial plateau fractures in which articular congruence must be maintained as well as open extremity fractures contaminated with bacteria.

METHODS: Polyurethane (PUR) biocomposites were prepared from a lysine triisocyanatepoly(ethylene glycol) prepolymer, a polyester triol (70% caprolactone, 20% glycolide, 10% lactide polyol, M_n 300 - 900 g mol⁻¹), triethylene diamine catalyst in dipropyl glycol, and a particulated matrix, such as allograft bone, calcium phosphates, bioactive glass, or sucrose. BG particles were functionalized surface by grafting polycaprolactone (PCL) to enhance interfacial bonding [3, 4]. Compression and torsion testing were performed on cylindrical specimens. For the in vivo study, a 3mm x 5mm unicortical defect was created in the diaphysis of the rat femur. Biocomposites were injected into the defect and allowed to cure in situ for ~5 min followed by wound closure. Rats were sacrificed 4 and 8 weeks after implantation (n=5). After harvesting the defects, µCT images were taken and radial analysis was conducted for µCT evaluation. Specimens were embedded in PMMA, ground-sectioned (~50 um), and stained with Sanderson's Rabid Bone Stain in conjunction with Von Gieson Solution.

RESULTS: Under static compression, surface-modified BG/PUR biocomposites have static compressive and torsional strengths of 68 and 28

MPa, respectively (Fig. 1A-B), which are twice those of unmodified BG composites (C-BG) and substantially greater than those of host bone. After 8-weeks implantation time, cellular infiltration and new bone formation were observed throughout the entire BG/PUR biocomposite (Figure 1C-D). No signs of prolonged negative inflammatory response that hindered bone growth were observed. Both radial histomorphometric and μ CT quantification of bone within the biocomposite showed a comparable increase in amount of new bone between the 4- and 8-week time points.

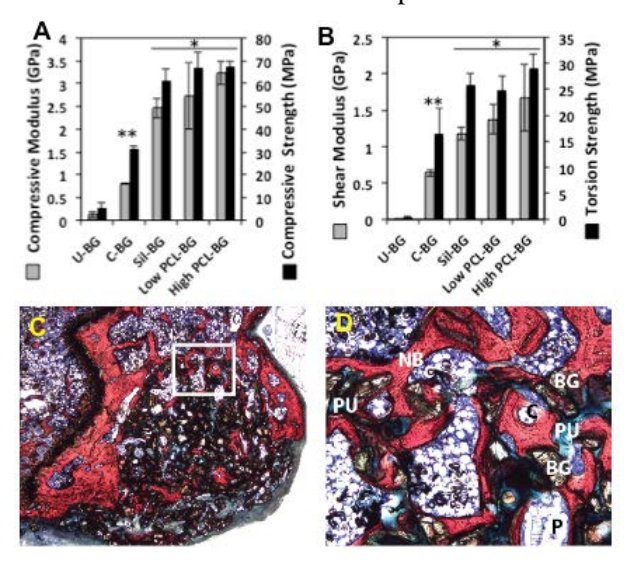


Fig. 1: (A) Compressive and (B) torsional properties of BG/PUR composites. (C) 1.25X and (D) 10X images of histological sections showing new bone (red, NB) and cellular infiltration (C), as well as resorption of residual polymer (PU) and bioglass (BG) at 8 weeks implantation time in rats.

DISCUSSION & CONCLUSIONS: Composites fabricated from surface-modified BG particles exhibited compressive and torsional strengths exceeding those of unmodified BG and host trabecular bone. After 8 weeks implantation time, the biocomposites supported balanced remodeling, as evidenced by histomorphometric and μ CT analysis of new bone growth.

REFERENCES: ¹J.E. Dumas et al (2010) *Tissue Eng Part A* **16(8)**:2505-18. ² J.E. Dumas et al (2012) *Biomed Mater* **7(2)**: 024112. ³ C. Kunze et al (2003) *Biomaterials* **24**:967-974. ⁴E. Verne et al (2009) *J Biomed Mater Res A* **90A**:981-992.

ACKNOWLEDGMENT: NSF DMR0847771.



A clinical case study: Using a strontium substituted bioactive glass -Stronbone®to fill alveolar sockets

R Hill, S Rawlinson, G Davis, S Nehete, S Shahdad

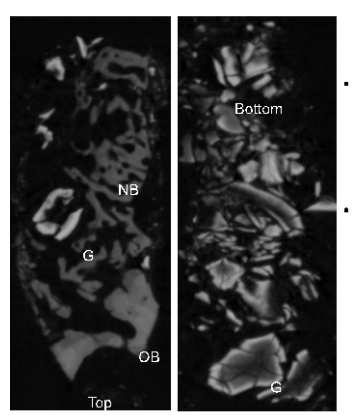
Dental Institute, Barts and The London School of Medicine and Dentistry, Queen Mary University of London, London, UK.

INTRODUCTION: Strontium is known to stimulate osteoblasts and inhibit osteoclasts Strontium Ranelate is used as a drug for treating osteoporosis and the active component is the Sr²⁺ cation. Stronbone® is based on the 45S5 bioactive glass composition, but where 10 mole percent of the Calcium is replaced by Strontium. Substitution of Sr for Ca in bioactive glasses is known to expand the glass network and result in faster glass dissolution, faster hydroxycarbonated apatite formation and improved bioactivity as well as the release of strontium [1, 2].

METHODS: Stronbone® which consists of irregular shaped glass particle 100-800 microns in diameter was mixed with the blood of the patients and packed into alveolar sockets following tooth extraction. Three sockets were filled with Stronbone®, i.e. an upper canine, an upper premolar and a lower premolar. Following implantation a membrane was placed over the top of the implant sites prior to suturing. After two months the lower premolar socket site was trevined with a core drill and a sample obtained. A titanium dental implant was then placed. The same process was repeated for the two other sockets at three months. The alveolar socket model is one of the few ways histological material from bone substitutes can be obtained clinically. The trevined cores were fixed with formalin and then examined by X-ray Microtomography (XMT) using our in house built muCAT Scanner. Following the XMT the samples were embedded and sectioned for histology.

RESULTS: The two month implanted core showed little evidence of new bone formation, though there was extensive evidence of glass dissolution and apatite formation on the surface of the glass particles. The histology showed only a fibrous matrix surrounding the particles. The upper premolar (Fig. 1 and 2) at three months showed extensive new bone formation and almost complete dissolution of the bioactive glass particles in the upper halve but there was limited new bone in the lower halve of the core and many residual glass particles.

DISCUSSION & CONCLUSIONS: Strontium containing bioactive glass has the capability to stimulate new bone formation but the results obtained probably depend on the size geometry of the socket and time of placement. New bone formation and osseo-integration of Stronbone is much slower than found in a previous ovine implant study into the femur.



- On Left, Original bone OB can be seen with new trabecular bone (NB) forming. Most of the glass particles have disappeared.
- On the Right the bottom halve contains lots of glass particles (G) and relative little new bone. The strontium substituted apatite can be seen forming on the glass particles

Fig. 1: XMT slices of Stronbone® implanted upper premolar.

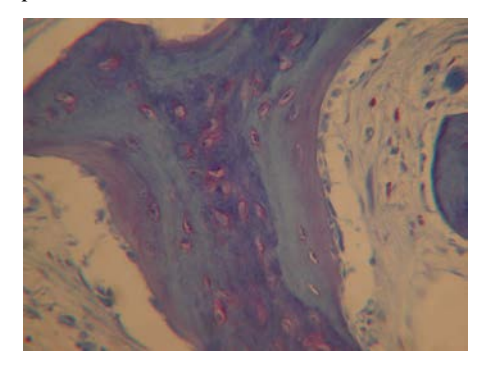


Fig. 2: Light Histology of an Eosin Stained Section of an upper premolar socket showing new bone formation.

REFERENCES: ¹ F.C. Fredholm, N. Karpukhina, R.V. Law et al (2010) *J Non-Cryst Solids* **356**:2546-2551. ² F.C. Fredholm, N. Karpukhina, D.S. Brauer et al (2012) J R Soc Interface **9**:880-889.



In vivo rhBMP-2 release from degradable polyurethane biocomposites

AD Talley¹, KJ Zienkiewicz¹, SS Funk², J Dasgupta³, JM Davidson³, GE Holt², SA Guelcher¹

Dept of Chemical and Biomolecular Engineering, Vanderbilt University, Nashville, TN, USA. ²

Dept of Orthopaedics and Rehabilitation, Vanderbilt University Medical Center, Nashville, TN, USA. ³ Dept of Pathology, Vanderbilt University Medical Center, Nashville, TN, USA.

INTRODUCTION: Growth factors incorporated into scaffolds for tissue engineering promote the infiltration of cells and tissue. Recombinant human morphogenetic protein-2 (rhBMP-2) bone stimulates osteoblast differentiation and new bone formation. Biodegradable polyurethane (PUR) biocomposites incorporating allograft particles have been reported to be effective carriers for rhBMP-2 and support new bone growth [1]. However, delivery of even a low dose of rhBMP-2 combined with allograft can result in transient resorption [2]. Mastergraft (15% hydroxyapatite, 85% tricalcium phosphate) and sucrose beads are biocompatible substitutes for allograft. In the present study, we investigated the in vivo release of rhBMP-2 from PUR biocomposites containing Mastergraft or sucrose and compared this to new bone formation at 8 weeks.

METHODS: The rhBMP-2 was radiolabeled with 2 mCi Na¹²⁵I prior to use and mixed with nonlabeled protein at a hot:cold ratio of 1:8. The biodegradable polyurethane (PUR) synthesized from a lysine triisocyanate (LTI) prepolymer and polyethylene glycol (PEG), a polyester triol (900 g/mol), and triethylene diamine catalyst. The lyophilized rhBMP-2 was hand mixed into the PUR and injected into bilateral, non-critical defects of approximately 5mm diameter by 11mm depth made in the metaphysis of the distal femurs of New Zealand White rabbits. Treatment groups included a collagen sponge (positive control) and the PUR with 45% Mastergraft or 40% sucrose all with a dose of 35µg rhBMP-2 per defect (n=4 defects per group). Porosity of the PUR samples was 40-50%. Release profiles of rhBMP-2 were measured with a scintillation probe collimated by a 3cm hollow tube wrapped in leaded tape and were normalized to initial data and decay. The animals were sacrificed at 8 weeks and new bone formation and polymer degradation evaluated by µCT, histology, and histomorphometry.

RESULTS: The rhBMP-2 release profiles for both PUR groups were significantly different than the collagen sponge group (Fig. 1). Within the first two days, almost 90% of the rhBMP-2 released

from the sponge whereas about only 20% is released from the PUR groups. The release profile from the PUR scaffolds does not change based on the type of filler even though the sucrose dissolves within the first few days based on *in vitro* data.

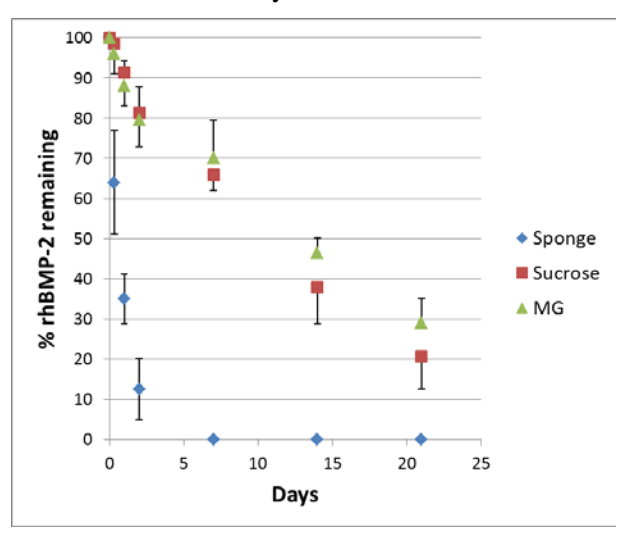


Fig. 1: rhBMP-2 release profile for the collagen sponge, PUR with sucrose, and PUR with Mastergraft (MG) groups

proups extend the release of rhBMP-2 when compared to the collagen sponge. In addition, the filler type does not change the release profile, which alludes to the fact that the rhBMP-2 release is controlled by diffusion from the PUR. In ongoing experiments, we are testing the effect of different molecular weight polyester triols on PUR degradation and new bone formation. We aim to tailor the degradation rate of the PUR by changing the molecular weight and composition of the polyesterol triol to match the rate of cellular infiltration.

REFERENCES: ¹ B. Li, T. Yoshii, A.E. Hafeman et al (2009) *Biomaterials* **30**:6768-79. ² O. Belfrage, G. Flivik, M. Sundberg et al (2011) *Acta Orthopaedica* **82**:228-233.

ACKNOWLEDGEMENTS: This work was supported by the Armed Forces Institute of Regenerative Medicine (W81XWH-08-2-0034).



Effects of rhBMP-2 and mineralized matrix composition on osteoclastic differentiation and resorptive activity

EM Prieto, SA Guelcher

Chemical and Biomolecular Engineering, Vanderbilt University, Nashville, TN, USA

INTRODUCTION: Settable biocomposite (BC) bone grafts of polyurethane/mineralized matrices, with the potential of maintaining initial bone-like strength during healing, undergo balanced remodeling when injected into femoral plug defects in rabbits. Grafts with recombinant human (rhBMP-2) Bone Morphogenetic Protein-2 reduced gaps between newly formed bone and the resorbing matrix. Delivery of rhBMP-2 at low (L) and high (H) doses increased new bone formation at 6 and 12 weeks. However, it also increased polymer degradation and matrix resorption at 6 weeks, which suggests osteoclast activation. The aim of the present study was to investigate the of rhBMP-2 delivery and matrix composition on the differentiation and function of osteoclast-like cells.

METHODS: Mouse bone marrow cells positive for CD11b were seeded on bioglass, tricalcium phosphate (TCP) and dentin. The cells were then treated with nuclear factor kB ligand (RANKL, 50 ng/ml), macrophage colony stimulating factor (M-CSF, 25 ng/ml), and rhBMP-2 (50 ng/ml) for up to 28 days. Cellular attachment and differentiation into osteoclast precursors was verified by intracellular TRAP staining. The effect of rhBMPmatrix composition 2 on differentiation was monitored through the gene expression of osteoclast specific markers (TRAP, Cathepsin K, Atp6v0d2 proton pump). Resorptive activity of the cells was quantified by measuring secreted TRAP into the culture medium, as well as number and area of resorption pits generated on the materials imaged using SEM.

RESULTS: Cells seeded on mineralized matrices differentiated into osteoclast precursors positive for intracellular TRAP. After 7 days of culture without rhBMP-2, dentin promoted significantly higher gene expression of osteoclastic markers than all the other groups. When rhBMP-2 was added to the culture, the expression of osteoclastic gene markers changed most significantly in dentin (Fig. 1). Resorptive activity, which correlates to TRAP secreted into the extracellular media, was initially lower than dentin for both TCP and bioglass (day 7) [1]. However, after 15 days of

culture, osteoclasts were activated on the synthetic matrices and had higher activity than the dentin control (Fig. 2).

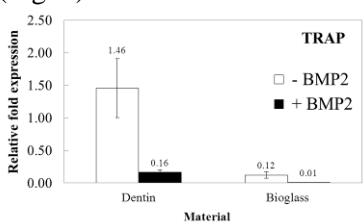


Fig. 1: TRAP gene expression normalized to GAPDH after 7 days of culture. Cathepsin K and ATP6v0d2 followed the same trend.

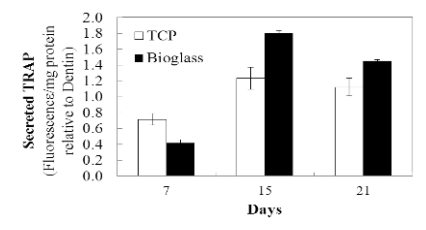


Fig. 2: TRAP produced by osteoclasts and secreted into the media as a measure of resorptive activity. Bars represent values relative to dentin and error bars represent standard error of the mean.

DISCUSSION & CONCLUSIONS: The results above suggest a combined effect between substrate composition and rhBMP-2 delivery on the differentiation and activity of osteoclasts, and support the observations of other groups related to osteoclasts expressing rhBMP-2 receptors [2]. Additional longitudinal studies of the gene expression of cells seeded on the different matrices is required to verify the suggested lag in differentiation/activation generated by synthetic matrices (ongoing studies in our lab). This work underscores the importance of taking into account changes in the differentiation process of cells due to their interaction with synthetic vs. natural matrices during the design of functional scaffolds for bone tissue engineering.

REFERENCES: ¹ B. Kirstein et al (2006) *J Cell Biochem* **98**:1085-1094. ² E. Jensen et al (2010) *J Cell Biochem* **109**:672-682.

ACKNOWLEDGEMENTS: This work is supported by the NSF under Grant No. DMR0847711.



In vivo ovine animal study of bioglass-based calcium phosphate cement

NW Kent¹, RG Hill¹, G Davis¹, I Gharib¹, G Blunn², N Karpukhina¹

¹Dental Physical Sciences, Barts and The London School of Medicine and Dentistry, London, UK.
²Institute of Orthopaedics & Musculoskeletal Science, UCL Medical School, London, UK.

INTRODUCTION: The first successful calcium phosphate cement (CPC) was developed by Chow and Brown [1]. This was based on a composition of Ca₄(PO₄)₂O and CaHPO₄ salts that formed apatite. This study investigates CPCs produced using melt derived bioactive glasses as one of the initial reagents. These cements are produced through reactions between bioactive glass (Table 1) and Ca(H₂PO₄)₂. Three bioglass cement compositions were implanted with a commercial composition HydroSet®. Three bioglass cement compositions of two forming octacalcium phosphate $(Ca_8(HPO_4)_2(PO_4)_4.5H_2O)$ cements $(PaG04)_4.5H_2O$ & PaG15) and the third containing fluoride (PaG08). Fluoride was added in order to produce a fluorapatite cement which would potentially be osteoinductive but non-resorbable.

METHODS: Glasses were produced via the meltquench route [2]. The glass powder and Ca(H₂PO₄)₂ powders were mixed together to give an overall calcium to phosphate ratio of 1.67. The cement powders were then mixed with a 2.5% Na₂HPO₄ solution to give a liquid to powder ratio of 0.6. The cement paste was then mixed for 30 s. A six week (n=1) and twelve week (n=6) ovine animal study was conducted. Four cement compositions (PaG04, PaG08, PaG15, and HydroSet) were implanted into proximal and distal femur sites. Cement compositions were chosen based upon working and setting times, compressive strength, and cements phase formed. Distal and proximal sites were drilled into the right a left femur, the size of the defect was 8 mm diameter and a depth of 15 mm. After implantation tetracycline labelling was injected into each animal at eight weeks. X-ray microtomography (XMT) using an in-house built MuCAT scanner, with time-delay integration and a voxel size of 30 µm, was conducted on the harvested samples.

Table 1. Glass compositions of produced glasses (mole %).

Name	SiO ₂	P_2O_5	CaO	Na ₂ O	CaF ₂
PaG04					
PaG08	36.80	6.00	49.23	5.47	2.50
PaG15	42.00	4.00	39.00	15.00	0.00

RESULTS: Cements were all implanted without complication and no infection was witnessed in any of the animals. All animals had mobility within two hours of the operation. XMT showed new bone formation surrounding the implant site was at six weeks on all compositions, there was also new bone beginning to form over the top implant. Clear interdigitation with

trabecular bone was identified with a clear bond between the cement and host bone.

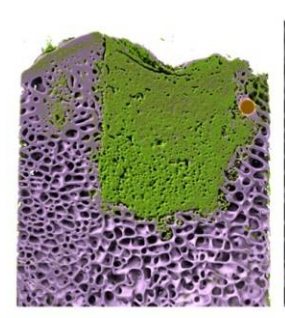




Fig. 1: 3D Reconstructed XMT images of implant at six weeks showing the cement PaG04 (left) and HydroSet (right). Green shows cement implant and new bone formation pink shows host bone.

be more interdigitation associated with the bioglass based compositions compared to HydroSet®. The bioglass compositions showed a higher degree of apparent osseointegration compared to the HydroSet®, where there was a distinguishable gap between the trabecular bone and the cement. It appeared the PaG08 cement showed increased resorption and increased bone formation compared to the other compositions. The results indicated that all the cement samples studied are osteoconductive and are able to osseointegrate with host bone. The developed bioglass cements showed potentially improved osseointegration with host bone compared to HydroSet® cement.

REFERENCES: ¹ W.E. Brown and L.C. Chow (1983) *J Dent Res* **62**:672. ² D.S. Brauer, N. Karpukhina, M.D. O'Donnell et al (2010) *Acta Biomaterialia*, **6**:3275–3282.

ACKNOWLEDGEMENTS: Authors would like to thank QM INNOVATIONS for financial support.



Effects of an osteoporotic condition on the biological performance of injectable calcium phosphate/PLGA cements

JJJP van den Beucken¹, FCJ van de Watering¹, P Laverman², VM Cuijpers¹, M Gotthardt², EM Bronkhorst³, OC Boerman², JA Jansen¹

¹ Dept. of Biomaterials, RUNMC, Nijmegen, NL. ² Dept. of Nuclear Medicine, RUNMC, Nijmegen, NL. ³ Department of Preventive & Curative Dentistry, RUNMC, Nijmegen, NL.

INTRODUCTION: Calcium phosphate cements (CPC) are promising candidates for bone regenerative applications due to the control over degradation by a platform based on poly (lactic-coglycolic acid) (PLGA) microspheres [1]. The PLGA microspheres (PLGA-u) are prone to rapid hydrolytic degradation, which creates porosity within the CPC matrix and increases the surface area in contact with the biological surroundings to allow faster degradation of the CPC. With an increasing elderly world population, the number of osteoporotic patients is rapidly rising [2]. For the treatment of bone defects in osteoporotic patients, no data are available regarding the biological performance of synthetic bone substitute materials. The aim of the present study was to comparatively evaluate the biological performance of CPC/PLGA in healthy and osteoporotic rats using a femoral condyle defect (FCD) model.

METHODS: PLGA (Purasorb®; Purac BV, The Netherlands) was used for the preparation of PLGA-µ as described previously [3]. PLGA-µ were combined with CPC at 30 wt.% in a 2 ml syringe (containing 1 g CPC/PLGA) and sterilized using gamma irradiation (>25 kGy; Synergy Health BV, The Netherlands). Female Wistar rats were used for pre-clinical experiments after ethical approval and according to national guidelines for the care and use of laboratory animals. Half of the animals underwent bilateral ovariectomy (OVX) and the other half received sham surgery (SHAM). Six weeks later, all animals were used for the creation of unilateral FCDs (Ø 2.5 mm, depth 3 mm). CPC/PLGA was injected into the bone defect and left to heal for 4 and 12 weeks. Retrieved specimens were histologically processed, embedded in MMA (n=7) or paraffin (n=1) and stained with methylene blue/basic fuchsin or HE/TRAP. The sections were histologically and -morphometrically analysed.

RESULTS: CPC/PLGA was created with PLGA- μ of 36 \pm 20 μ m and a porosity of ~75% (microporosity: ~49%). Histology analysis showed

no inflammatory responses and a faster degradation of CPC/PLGA in OVX condition. For

SHAM and OVX, new bone was trabecular-like and associated with bone marrow formation. TRAP staining revealed similar osteoclastic activity for SHAM and OVX. Quantitative measurements showed significantly faster CPC/PLGA degradation and delayed new bone formation (Fig. 1) for OVX compared to SHAM.

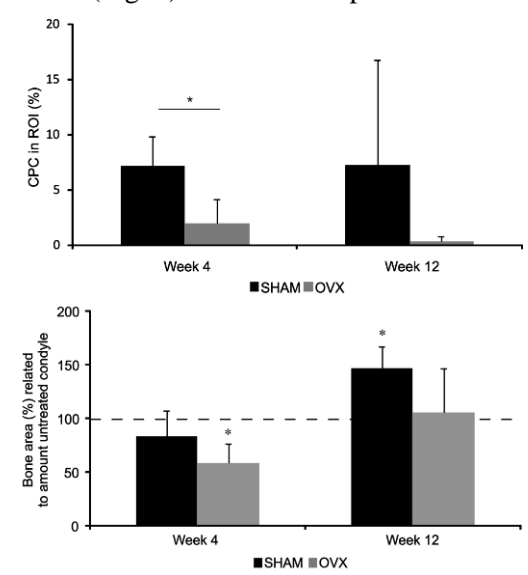


Fig. 1: Analysis of CPC (top) and new bone (bottom) in the defect area. Dashed line indicates values in untreated defects. (*p<0.05)

DISCUSSION & CONCLUSIONS: This study shows that an osteoporotic condition significantly accelerates CPC/PLGA degradation and delays new bone formation compared to healthy controls. The rat FCD model allowed screening for empowerment strategies for bone substitute materials to be used in osteoporotic conditions.

REFERENCES: ¹ R.P. Félix Lanao, S.C.G. Leeuwenburgh, J.G.C. Wolke, et al (2011) *Acta Biomater* **7(9)**:3459-68. ² Internatinal Osteoporosis Foundation (2011), http://iofbonehealth.org, L Misteli (Ed.). ³ W. Habraken, J.G.C. Wolke, A.G. Mikos, et al (2006) *J Biomater Sci Polym Ed* **17**:1057-74.



Thermoresponsive hydrogel development for the interruption of adverse remodelling processes in ischemic cardiomyopathy

WR Wagner, DM Nelson, R Hashizume, Z Ma

McGowan Institute for Regenerative Medicine and Departments of Surgery & Bioengineering, University of Pittsburgh, Pittsburgh, PA

INTRODUCTION: Ischemic cardiomyopathy is characterized by an adverse remodelling process wherein the infarcted ventricular wall thins and stiffens, while the ventricular cavity dilates. Mechanically, the thinning wall is exposed to increasing stress, which may be involved in driving further wall thinning and scar formation. It is hypothesized that reducing this wall stress during the remodelling period may serve to alter the outcome towards a more functional structure, characterized by less dilation and wall stiffening. One way this might be accomplished is through the injection of material into and around the infarct region to reduce the wall stress.

METHODS: Thermoresponsive hydrogels are a class of materials that have attractive features for ventricular wall injection. With a lower critical solution temperature below body temperature, these materials could be injected in soluble form through a small bore needle, yet gel in situ to avoid regurgitation and to provide mechanical support. A variety of synthetic thermoresponsive hydrogels have been synthesized that have tunable phase change behaviour, hydrolytic lability, as well as the capacity for serving as reservoirs for controlled release of bioactive agents [1-4]. These materials have been characterized in vitro and evaluated in a rat model of ischemic cardiomyopathy.

RESULTS: Echocardiographic assessment of rat ventricular function has demonstrated the benefit of thermoresponsive hydrogel injection versus saline control material in terms of end diastolic area and fractional area change. Histological assessment shows maintenance of a thickened wall with the injected material being infiltrated by macrophages as the degradation process proceeds.

DISCUSSION & CONCLUSIONS: The injection of synthetic thermoresponsive hydrogels into the ventricular wall has shown benefit in altering the remodelling course of ischemic cardiomyopathy, at least over the first several months following myocardial infarction in the rat model. Fundamental questions remain as to the optimal properties of such hydrogels, for instance in terms of degradation rate, stiffness, and the need for concurrent pharmaceutical agent delivery. If

this approach can be effective in the clinic, it would be attractive in that it might be accomplished in a minimally invasive manner and serve to delay or halt the progression towards end-stage cardiomyopathy, where current options remain limited to hospice care, cardiac transplantation or possibly the implantation of a ventricular assist device for chronic circulatory support.

REFERENCES: ¹ K.L. Fujimoto, Z. Ma, D.M. Nelson et al (2009) *Biomaterials* **30**:4357-68. ² D.M. Nelson, Z. Ma, C.E. Leeson et al (2012) *J Biomed Mater Res Part A* **100**:776-85. ³ Z. Ma, D.M. Nelson, Y. Hong et al (2010) *Biomacromolecules* **11**:1873-81 (2010). ⁴ D.M. Nelson, Z. Ma, K.L. Fujimoto et al (2011) *Acta Biomaterialia* **7**:1-15.

ACKNOWLEDGEMENTS: This work was supported by the National Institutes of Health (NIH), Grant No. HL105911.



Study on injectable silicates/alginate composite hydrogels

J Chang^{1, 2}, Y Han¹, Q Zeng¹, H Li¹

¹Med-X Research Institute, School of Biomedical Engineering, Shanghai Jiao Tong University, Shanghai, China. ²Shanghai Institute of Ceramics, Chinese Academy of Sciences, Shanghai, China

INTRODUCTION: Silicate based bioactive ceramics and glasses have received much attention as potential biomaterials for bone regeneration and bone tissue engineering. Recent studies showed that calcium silicate bioceramics possessed an excellent bone regeneration biodegradability and the ability to induce angiogenesis [1-3]. However, the common drawback of these bioactive ceramics and glasses is the brittleness of the materials and the difficulty in shaping. Sodium alginate (SA) hydrogel has been widely investigated for tissue engineering applications. SA has a distinctive ability to form hydrogels via ionotropic crosslinking in presence of divalent cations such as calcium [4]. However, alginate inherently lacks mammalian celladhesivity and bioactivity to stimulate cell differentiation, which hampers the applications of alginate in bone tissue engineering [5, 6]. Since calcium-containing silicate ceramics (CS) and glasses have been reported to be biodegradable and are able to release calcium ions under physiological environment, it is reasonable to assume that the addition of CS into alginate may lead to an in-situ forming and injectable CS/SA composite hydrogel, which may combine the advantages of SA and CS, especially maintaining the bioactivity of CS and the injectability and porous structure of SA hydrogel.

METHODS: Silicate bioglasses and calcium silicate bioceramic were incorporated into an alginate solution to from composite hydrogels. The gelling time, the hydrogel stability and the structure of the composite hydrogels were evaluated. The *in vitro* bioactivity of the composite hydrogels was examined by soaking in simulated body fluid. Furthermore, the effect of the composite hydrogel on cell proliferation and differentiation was evaluated by culturing the hydrogel with cells.

RESULTS: The gelling time could be controlled by the amount of the added silicates. Times could be adjusted between about 30 seconds and 10 min by varying the amount of silicates. SEM observation of the composite hydrogels showed an optimal interconnected porous structure with pore size ranging between 50 and 200µm. FTIR and

SEM witnessed that the composite hydrogels induced the formation of hydroxyapatite on the surface of the materials in simulated body fluid. In addition, rat bone mesenchymal stem cells (rtBMSCs) cultured in the presence of ion extracts of hydrogels were able to maintain the viability and proliferation. Furthermore, the ion extracts of the composite hydrogels stimulated rtBMSCs to produce alkaline phosphatase and to promote angiogenesis of human umbilical vein endothelial cells.

DISCUSSION & CONCLUSIONS: Injectable bioactive composite hydrogels were prepared. The gelling time and swelling behaviour of the composite hydrogel system could be controlled and regulated by varying the contents of silicate components. The composite hydrogels possessed good bioactivity, which was revealed by the ability to induce formation of bone-like apatite on its surface in SBF and to stimulate the osteogenic differentiation of rtBMSCs and angiogenic differentiation of HUVECs. The combination of good injectability, bioactivity and angiogenic ability suggests that silicate/SA hydrogels have great potential as injectable system for applications in bone regeneration and bone tissue engineering.

REFERENCES: ¹ H. Li, K. Xue, K. Liu et al (2014) *Biomaterials* **35**:3803-18. ² C. Wang, K. Lin, J. Chang et al (2013) *Biomaterials* **34**:64-77. ³ S. Xu, K. Lin, Z. Wang et al (2008) *Biomaterials* **29**:2588-96. ⁴ Y. Murata, Y. Kodama, T. Isobe et al (2009) *Int J Polym Sci* Article ID 729057, **2009**:1-4. ⁵ A.J. Campillo-Fernandez, R.E. Unger, K. Peters et al (2009) *Tissue Eng Part A* **15**:1331-41. ⁶ K.Y. Lee and D.J. Mooney (2012) *Prog Polym Sci* **37**:106-26.

ACKNOWLEDGEMENTS: This work was supported by the National Natural Science Foundation of China (Grant Nos. 81190132, 31200714 and 30900299), the Natural Science Foundation of Shanghai Municipal (Grant No. 12ZR1413900) and the Opening Project of State Key Laboratory of High Performance Ceramics and Superfine Structure (Shanghai Institute of Ceramics, Chinese Academy of Science) (Grant No. SKL201203SIC).



Hydrogels and musculoskeletal applications

P Weiss

University of Nantes, INSERM UMR 791, LIOAD, Faculty of Dental Surgery, Nantes, France.

Biomimetic extracellular matrices show bioactive properties, enable exchange of stimuli with its environment and induce specific cellular responses. We (INSERM U791) worked for 10 years on injectable self-crosslinking hydrogel for cartilage and bone tissue engineering. We have developed a hydrogel with great potential in bone and articular tissue engineering. It is a pH-related auto-crosslinking hydrogel that is made up of a hydroxypropylmethyl cellulose (HPMC) aqueous solution onto which silane groups are graft to enable the formation of covalent links between HPMC chains [1, 2]. This polymer is stable in aqueous solution at pH superior or equal to 12.5. Acidification of the solution results in progressive increase of the viscosity and the formation of a hydrogel.

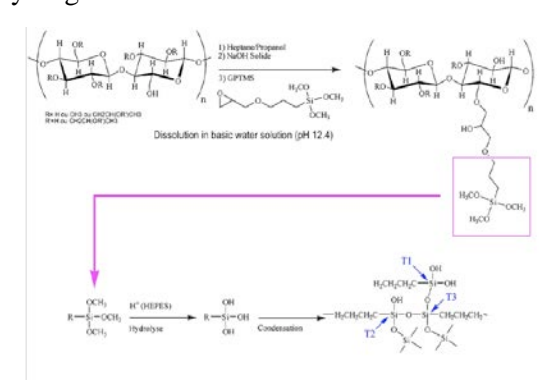


Fig. 1: Functionalization and crosslink process of silated HPMC

Hydrogels can be blended with calcium phosphate ceramics to do biomaterial composite for bone substitution or on the opposite can be used in calcium phosphate cements to make macropores pores inside the cement. Extracellular matrix is a non-uniform material combining glycosaminoglycans and fibers. Hydrogel alone is too soft if we want to use it for musculoskeletal tissue engineering with alive cells in it. engineer matrices from hydrogels made of polysaccharides, blends with polylactic fibers, calcium carbonate and phosphates or silicates nano or micro particles in a non-homogenous manner. One pot assembly of hydrogels with nano and/or microparticles of organic or mineral composition is being studied [3-5] and will provide modulation of mechanical strength and controlled release of bioactive molecules (for *i.e.* pO2 and cell adhesion) into niches within the matrices. Values of soft tissue elasticity (Young modulus E) could be in the range of 10 kPa for muscle, 20 kPa for cartilage and 30-40 kPa for precalcified bone.

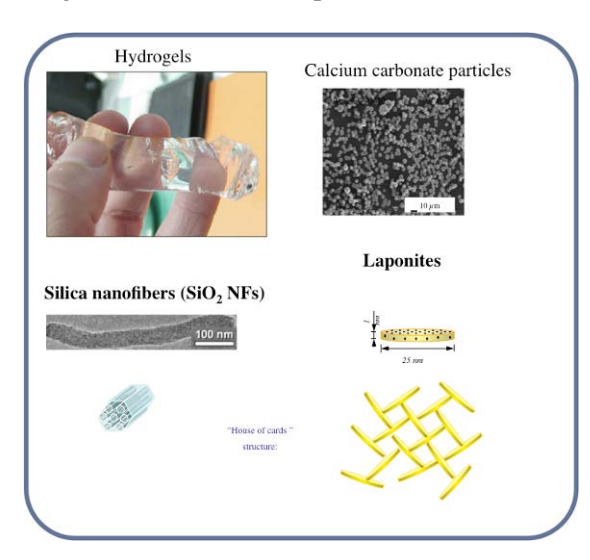


Fig. 2: Hydrogel and 3 types of particles for reinforce it : carbonates, silica nano fibers and Laponites

REFERENCES: ¹ A. Fatimi et al (2008) *Biomaterials* **29(5)**:533-43. ² X. Bourges et al (2003) *Adv Colloid Interface Sci* **99(3)**: 215-228. ³ N. Buchtová et al (2013) *J Mater Sci Mater Med* **24(8)**:1875-84. ⁴ E. Rederstorff et al (2011) *Acta Biomater* **7(5)**:2119-30. ⁵ F. Xie et al (2010) *J Mater Sci* **21(4)**:1163-8.

ACKNOWLEDGEMENTS: Authors thank the Région Pays de la Loire for Bioregos 1 & 2 fundings



Revisit immune responses to silkworm silk

Z Xia¹, X Wang¹, J Triffitt²

¹Institute of Life Science, School of Medicine, Swansea University, Swansea, UK. ²Botnar Research Centre, Nuffield Department of Orthopaedics, Rheumatology and Musculoskeletal Sciences, University of Oxford, Oxford, UK.

INTRODUCTION: Silkworm silk refers to silk produced by the domesticated silkworm, *Bombyx Mori (BM)*, or wild silkworms such as *Antheraea Perni (A P)* (Fig. 1). Both types of silk (domesticated or wild) is made of two main components: fibroin, a fibrous protein that forms the core silk filament with strong mechanical strength, and serecin a glue-like coating which surrounds the silk fiber and joins the silk filaments together. It is reported that most immune responses are from reaction to sericin with the presence of fibroin [1]. This study compared macrophage response to silks from *BM* and *AP*, and evaluated inflammatory responses elicited by raw silks and degummed silks of *BM* both *in vitro* and *in vivo*.



Fig. 1: Silkworms, cocoons and the ultrastructure of raw silks

METHODS: For *in vitro* study, we cultured murine macrophages RAW264.7 in presence of these materials. Cellular responses to silks were observed by using bright field microscopy, scanning electron microscopy and transmission electron microscopy. TNF and IL 1β mRNA expression and TNF protein level were also tested in. For *in vivo* experiment, we implanted these materials into BALB/C mice subcutaneously for 10 weeks.

RESULTS: The results indicated that undegummed *AP* silk caused macrophage cell death *in vitro* (Fig. 2); sericin-like structure appeared to exist within fibroin, which illustrated continuous macrophagic infiltration *in vivo*. For *BM* silk, macrophages do not respond to raw silks, degummed silks or white sutures tested in a short-

term *in vitro* model (Fig. 3). Throughout the *in vivo* study, the degummed silk fibres were tolerated well by the host animals. Interestingly, the degummed silks appeared to exhibit a higher degradation rate than raw silks.

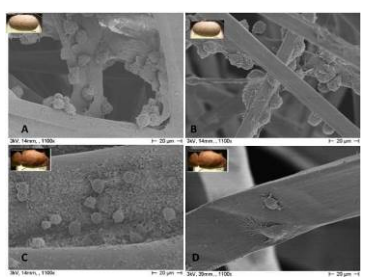


Fig. 2: Macrophages on undegummed (A), degummed (B) B M silk; and undegummed (C) and degummed (D) A P silk.

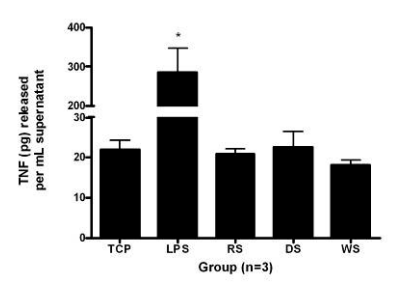


Fig. 3: TNF α release from macrophages in response to TCP (control), LPS (positive control), raw BM silks (RS), degummed silks (DS) and white sutures (WS) after 4 days in vitro exposure. Data were shown as mean \pm SE * compared with control p<0.01

DISCUSSION & CONCLUSION: There are structural differences of silk from *Bombyx Mori* and *Antheraea Perni*. Silk from *Bombyx Mori* silkworms is easier to degum (remove of sericin) and less to provoke tissue response than that from *Atheraea Perni*. *Bombyx Mori* silk is biodegradable, or slowly biodegradable material. Macrophages and foreign body giant cells actively participate on the biodegradation process, with very little evidence of consequent inflammation.

REFERECES: ¹ B. Panilaitis et al (2003) *Biomaterials* **24(18)**: 3079-85.

ACKNOWLEDGEMENTS: This work was partially supported by the Botnar Research Fellowship.



Biomimetic collagen/apatite scaffolds for bone repair and regeneration

Z Xia¹, X Yu¹, D Rowe², M Wei¹

¹Department of Materials Science and Engineering, University of Connecticut, Storrs, CT. ²Department of Reconstructive Sciences, University of Connecticut Health Center, Farmington, CT.

INTRODUCTION: In recently years, bone tissue engineering has proved to be a promising approach for repair and regeneration of damaged bone. In this process, the architecture and geometry of scaffolds and progenitor cell sources play critical roles in directing new bone formation [1]. In the study, a method combining current biomineralization gelation approach controllable freeze casting was developed to prepare a novel biomimetic collagen/apatite (Col-Ap) scaffold. The effect of scaffold structure and cell type on bone forming capability was evaluated using a two-hole mouse calvarial defect model.

METHODS: Biomimetic Col-Ap hydrogel was synthesized using a collagen-containing modified simulated body fluid. The hydrogel was frozen using two freezing regimes: 1) cooled at a constant rate in a homogenous cold environment; 2) unidirectionally cooled from bottom to top at a fast cooling rate. It was then freeze-dried, cross-linked using EDC and rinsed. The in vivo performance of the scaffold was evaluated using transgenic mice carrying a pOBCol3.6GFP transgene associated with osteoblast differentiation. The scaffolds were loaded with four different combination of osteoprogenitor cells, including mouse calvarial cells (mCalv), bone marrow cells (BMSC), mCalv+ BMSC, bone marrow stromal cells (BMSC), and tested in a two-hole calvarial defect model. Histological analysis was carried out to assess new bone formation [2].

RESULTS: Mineralized collagen hydrogel was prepared by a biomimetic gelation method. The rheological behaviour of Col-Ap hydrogel can be tailored by controlling collagen concentration in m-SBF and gelation temperature (Table 1). Freezedried hydrogels with an isotropic equiaxed structure and a unidirectional lamellar structure were prepared. The pore size of these scaffolds could be easily adjusted by controllable gelation and freeze casting. In the equiaxed regime, the average pore size of the scaffolds was ranged from 69 to 120 µm. In the lamellar regime, the interlamellar spacing of the scaffolds ranging from 7 to 340 µm [3]. The scaffolds were evaluated in vivo using a two-hole calvarial defect model, which demonstrated that both of the scaffolds well supported osteoblast activities and new bone formation (Fig. 1). Moreover, the structure of newly formed bone was closely related to the microstructure of scaffolds².

Table 1. The effect of collagen concentration and gelation temperature on the storage modulus (G').

	Collagen (g/L)	25°C (Pa)	25°C+40°C (Pa)	40°C (Pa)
Ì	2	280.9	547.2	324.7
ĺ	4	773.6	1500.1	853.9

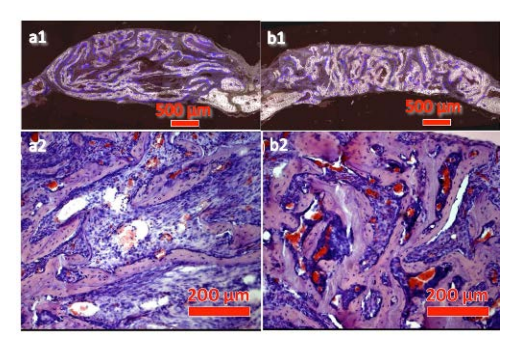


Fig. 1: Fluorescent imaging analysis of bone formation in the calvarial defects loaded with (a) lamellar scaffold+mCalv and (b) equiaxed scaffold+mCalv after 28 days of implantation.

DISCUSSION & **CONCLUSIONS:** developed a novel biomimetic gelation method to prepare mineralized collagen hydrogel with tailored properties. Freeze-dried hydrogels with an isotropic equiaxed structure and a unidirectional lamellar structure were prepared and the pore size of which could be tailored by controlling hydrogel properties and freezing regimes. In vivo evaluations have demonstrated that such prepared scaffolds have excellent bone forming capability. Also, the scaffold architecture plays an important role in guiding new bone formation. In addition, the study has demonstrated the importance of cell source in bone tissue engineering.

REFERENCES: ¹ P.X. Ma (2004) *Mater Today* **7**:30-40. ²X. Yu, Z. Xia, L. Wang et al (2012) *J Mater Chem* **22**:9721-9730. ³ Z. Xia, X. Yu, X. Jiang et al (2013) *Acta Biomater* **9**:7308-7319.

ACKNOWLEDGEMENTS: The authors would like to thank NSF (CBET 1133883) and NIH (1R21AR059962-01A1) for their support.



Novel biomimetic thermosensitive $\beta TCP/chitosan$ based hydrogels for bone tissue engineering

M Dessi¹, A Borzacchiello², TH El Massry³, WI Abdel-Fattah³, L Ambrosio²

¹ Brighton Studies in Tissue-mimicry and Aided Regeneration, School of Pharmacy & Biomolecular Sciences, University of Brighton, UK. ² Institute for composite and biomedical materials, National Research Council of Italy, IT. ³ Biomaterials Department, NRC, Cairo, Egypt

INTRODUCTION: Many of the on-going challenges in bone tissue engineering rely on invasive surgical procedures. less Injectable in situ gelling systems have gained great attention for their ability to undergo in situ sol-gel transition in physiological environments [1]. Biomimetic approach is moving toward the realization of composite materials with features resembling natural tissue [2]. In this contest, this work is aimed to realize a composite chitosan hvdrogels reinforced via physical interactions with β -tricalcium phosphate (β TCP), crosslinked with glyoxal and and glycerophosphate (BGP) to obtain injectable and thermosensitive in situ gelling hydrogels. These biomaterials have a set of transversal key features that can be successfully used as minimally invasive bone analogues.

METHODS: Two composite hydrogels containing β-TCP were realized at concentrations of 1.5% and 1% (w/w). The kinetics of sol-gel transition and the composite hydrogel properties were investigated by rheological analysis with a rotational rheometer (Gemini, Bohlin Instruments), at controlled temperature of 37°C. The time evolution of the elastic modulus has been expressed (*Equation 1*) in terms of a normalized elastic modulus G(t) given by the ratio:

$$G(t)_{red} = G'(t) - G'_{0} / G'_{f} - G'_{0}$$
 (1)

where G_0' and G_1' are the elastic modulus of the starting solution and of the formed gel, respectively. Moreover, G' and G'' moduli were evaluated in function of frequency. The chemicophysical properties were carried out by FTIR, X-Ray and thermogravimetric (TGA) studies along with morphological properties analyzed by SEM and TEM. The vitality and proliferation of osteoblasts cells was analyzed by Alamar Blue assay. MG63 were seeded on the gels at cell density of 1.7×10^4 cells/ml and on polystyrene well plates as control.

RESULTS: The results showed that gelification gelation takes place after the injection. The

materials switch from liquid state to gel state in above 5min. Chemico-physical analysis highlight that the strong network is a consequence of: chemical bonds between the amine groups of chitosan and the aldehyde groups of glyoxal, physical and electrostatic interactions among ammonium chitosan groups and phosphate groups both of βGP and βTCP, and hydrogen bonds among the macromolecules. The synergistic effect of the above mentioned interactions leads to a well-developed 3D network, with rheological strong gel behaviour and thermally stable. Composites hydrogels resemble natural bone in chemical and topological composition, with needle-like crystals shape. Biological data showed the affinity of hydrogels with natural tissue and their ability to promote and support cell growth and proliferation.

DISCUSSION & **CONCLUSIONS:** The obtained results showed that crosslinking with βGP and glyoxal is a promising strategy to develop biomimetic in situ gelling hydrogels. Composite hydrogels show a network with rheological properties typical of strong gels, able to support mechanical loads. The materials exhibit the advantage of resembling the organization of organic/inorganic natural tissue for structure and composition. These findings associated with biological results, suggest the potential of the materials as promising candidates for spongy bone regeneration.

REFERENCES: ¹ K. Song, M. Qiao, T. Liu et al (2010) *J Mater Sci Mater Med* **21**:2835-2842. ² M. Dessi, M.G. Raucci, S. Zeppetelli et al (2012) *J Biomed Mater Res Part A* **100A**:2063-2070.

ACKNOWLEDGEMENTS: This work was supported by Italy /Egypt Exchange of Researcher Program.



Effects of surface modification of 45S5 bioactive glass on dynamic compressive fatigue mechanical properties of polymeric biocomposites

AJ Harmata, S Uppuganti, JS Nyman, SA Guelcher Vanderbilt University, Nashville, TN, USA.

INTRODUCTION: Injectable, settable bone grafts that possess dynamic mechanical strength exceeding that of bone. Maintaining a strength comparable to bone while remodeling could improve the clinical management of a number of orthopaedic conditions, such as vertebroplasty. Injectable polyurethane (PUR) biocomposites are an attractive alternative to calcium phosphate cements due to their tough mechanical properties and ability to facilitate active remodeling [1]. 45S5 bioactive glass (BG) has widely been used for bone regeneration purposes due to its osteoconductivity and bioactivity [2]. Although physiological loads are generally cyclic, fatigue properties of biomaterials utilized in load-bearing applications are rarely reported. In this study, we investigated the effects of BG surfacemodification on the dynamic compressive mechanical properties of BG/PUR biocomposites. Prior to reaction with the PUR binder, BG particles were functionalized with the silanecoupling agent 3-aminopropyl-trietoxysilane (APTES), which has been shown to increase the mechanical compressive strength of BG, as well as surface grafting of polycaprolactone (PCL) to enhance interfacial bonding [3,4].hypothesized that a low-porosity **BG/PUR** biocomposite comprised of surface-modified BG would improve the fatigue properties compared to one made with cleaned BG, as well as native trabecular bone.

METHODS: Cylindrical biocomposites were prepared from a lysine triisocvanatepoly(ethylene glycol) prepolymer, polyester triol (70% caprolactone, 20% glycolide, 10% lactide polyol, Mn ~300 g mol⁻¹), triethylene diamine catalyst in dipropyl glycol, and BG (56.7 volume %). After pre-conditioning the specimen in phosphate buffer solution for 24 h, mechanical testing was completed in cyclic sinusoidal compression mode at a frequency of 5 Hz, reaching independently set physiologically relevant maximum stress levels (5, 10, and 15 MPa). Throughout the entire testing period, specimen were hydrated with water via a dripsystem, additionally an extensometer tracked the percent strain. Complete mechanical failure was

defined as strain >9%. Analysis focused on the mean fatigue life, change in modulus and residual strain, as well as mode of failure.

RESULTS: Under static compression, cleaned and surface-modified BG/PUR biocomposites have static compressive strengths of 7.9 ± 3.2 and 53.8± 6.5 MPa, respectively. Consequently, the dynamic compression fatigue properties of the cleaned-BG/PUR biocomposite cannot feasibly be evaluated at maximum stress levels of 10 and 15 MPa. Under a maximum stress level of 5 MPa, the mean fatigue life of the surface-modified and cleaned-BG biocomposites was 899,953 ± 160,471 and 197 ± 257 cycles (P<0.05), respectively. The mean fatigue life of surface-modified BG/PUR biocomposite at 15 MPa was determined to be $85,666 \pm 16,615$ cycles. As shown in Fig.1A, at a max level of 15 MPa, the compressive modulus of surface-modified BG/PUR biocomposite decreased as the number of cycles increased. Additionally. its residual strain increased throughout the testing due to plastic deformation (Fig. 1B).

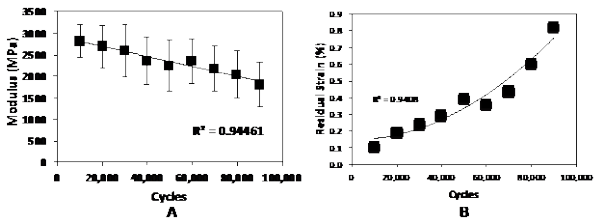


Fig. 1: Fatigue analysis of surface-modified BG/PUR biocomposite at a maximum stress level of 15 MPa. Second order polynomial fits correlate to respective R² values.

DISCUSSION & **CONCLUSIONS**: By comparing the fatigue life of PUR biocomposites made with cleaned versus surface-modified BG, we conclude that APTES-PCL surface modification significantly extends the BG/PUR biocomposite's ability to withstand physiologically relevant dynamic compressive stresses.

REFERENCES: ¹J.E Dumas et al (2010) *Acta Biomater* **6**:2394-2406. ² A.R Boccaccini et al (2005) *Expert Rev Med Devic* **2**:303-317. ³ C. Kunze et al (2003) *Biomaterials* **24**:967-974. ⁴ E. Verne et al (2009) *J Biomed Mater Res A* **90A**:981-992.



Acceleration of gelation and increased mineralization of thermosensitive chitosan hydrogels by incorporation of alkaline phosphatase

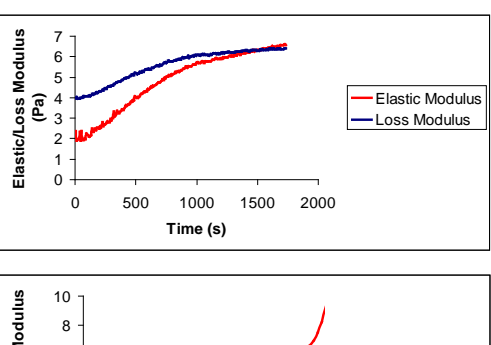
AL Skwarczynska¹, Z Modrzejewska¹, TEL Douglas², JA Jansen², SCG Leeuwenburgh²

INTRODUCTION: Chitosan has been widely applied as a biomaterial for tissue engineering due biocompatibility, non-toxicity Furthermore, biodegradability. iniectable thermosensitive chitosan hydrogels are formed by neutralization of acidic chitosan solution using beta-glycerophosphate physiological pH and temperature. Bioactive substances such as Alkaline Phosphatase (ALP), a mineralization-promoting enzvme incorporated during gelation. To promote bone regeneration, the presence of calcium phosphate (CaP) mineral is desirable. The aim of this study was to investigate the effect of ALP on mineralization and gelation of chitosan-β-GP hydrogels.

METHODS: Chitosan/β-GP injectable gels were produced according to the protocol of Chenite et al [1]. Briefly, 16ml of 2.5% (w/v) chitosan (Fluka) in 0.1 M HCl was mixed with 2ml of 1g/ml (β-GP) solution in water and 0.4 ml of an aqueous ALP solution of concentration 2.5, 1.25 or 0 mg/ml. was Hydrogel mineralization induced incubation 0.1 M (aq) calcium glycerophosphate (Ca-GP) Hydrogel mineralization characterized by monitoring mass changes, FTIR, XRD and SEM Gelation kinetics and viscoelastic properties were studied by rheometry at 37 °C, oscillatory stress of 5 Pa and frequency of 1 Hz. The gelation point was defined as the point where storage modulus (G') exceeded the value of loss modulus (G'').

RESULTS: Addition of ALP shortened gelation time. An example is given in *Fig.1*. Increasing ALP concentration led to an increase in solid mass percentage. Mineralization with CaP was confirmed by FTIR, XRD and SEM.

DISCUSSION & CONCLUSIONS: Addition of ALP to thermosensitive chitosan/β-GP hydrogels accelerates gelation at 37 °C and induces their mineralization. Acceleration of gelation is advantageous from a clinical point of view and mineralization is expected to promote bone regeneration. Addition of ALP makes chitosan hydrogels more attractive as injectable biomaterials for bone tissue engineering.



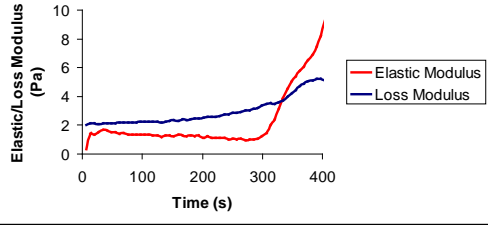


Fig.1: Determination of gelation time without ALP (top) and with ALP (0.23 mg/ml gel) (bottom) at 37°C.

REFERENCES: ¹ A. Chenite, C. Chaput, D. Wang et al (2000) *Biomaterials* **21**:2155-2161.



¹Department of Environmental Systems Engineering, Lodz University of Technology, Poland. ²Department of Biomaterials, Radboud University Nijmegen Medical Center, The Netherlands

Hydroxyapatite made easy

P Sharrock^{1, 2}, D Phan-Minh², A Nzihou²

¹ SIMAD laboratory, University of Toulouse, Toulouse, France. ² RAPSODEE Research Center, UMR CNRS 5302, Université de Toulouse Mines-Albi, Albi, France.

Hydroxyapatite (HA), the calcium salt closely resembling the minerals in bone, has been the subject of much research and controversy since its introduction in the medical field. Considered by most to be non-resorbable, difficult to manufacture and at best an inert biomaterial, others have found it to be degradable, having osteoinductive-like properties, and of easy synthesis. Some claim tricalcium phosphate is a better biomaterial with higher resorption rates, usually basing their arguments on in vitro small scale experiments. We will survey the clinical data available on these subjects, including plasma spraying of HA coatings on metal implants and review the numerous methods put forward for HA synthesis procedures including sol-gel, thermal combustion, hydrothermal, biomimetic, solid state and calcium phosphate cement processes.

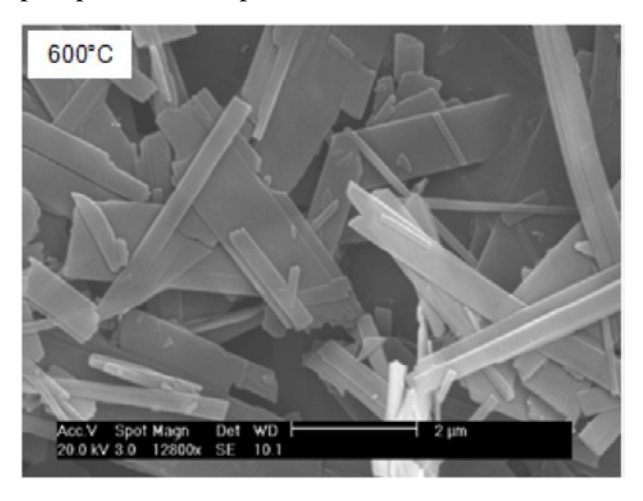


Fig.1: SEM photo of carbonated hydroxyapatite (CAP) sintered at 600° C[1] The CAP was made by heating under pressure the calcium carbonate with H_3PO_4

Recent trends on HA modification by grafting organic molecules and extended substitutions will be exposed, as well as sintering investigations in the presence of bioglass additives. We will report on various methods used to manufacture porous ceramic or composite HA implants, and show the relation between porosity and drug release properties [2]. We will end with the description of our latest results on carbonated HA synthesis at atmospheric pressure, starting with calcium

carbonate and phosphoric acid as sole reactants and describe the higher reactivity obtained with this procedure for making HA gel of nanometer scale and high specific surface area, using green chemistry [3, 4]. The advantage of using calcium carbonate as starting material stems from the absence of pollution from counter-ions.

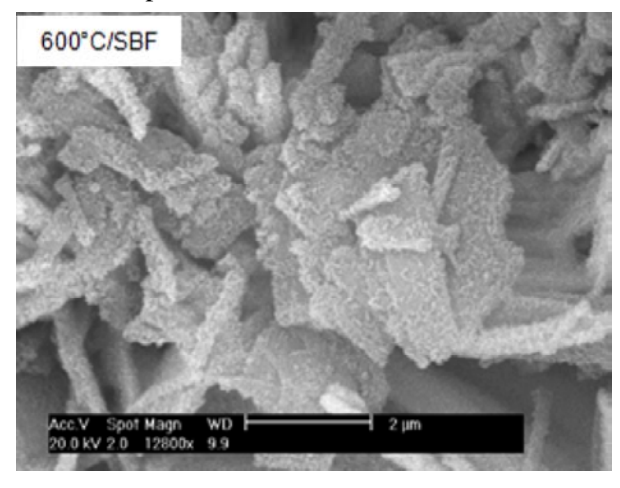


Fig. 2: SEM photo of CAP) sintered at 600°C and immersed in SBF. The CAP was rapidly covered with biomimetic HA.

REFERENCES: ¹ D. Pham-Minh, S. Rio, P. Sharrock et al (2014) J Mat Sci **49**:4261-4269. ² O. Zamoume, S. Thibault, G. Regnié et al (2011) *Mat Sci Eng C* **31**:1352–135. ³ D. Pham-Minh, N. Dung-Tran, A. Nzihou and P. Sharrock (2014) *Mat Res Bull* **51**:236-243. ⁴ D. Pham-Minh, D. Dung-Tran, A. Nzihou and P. Sharrock (2013) *Mat. Sci. Eng. C* **33**(**5**):2971-2980.

ACKNOWLEDGEMETS: We thank the Solvay company (Ms C.Tahon and Mr. G.Depelsenaire) for continued support on the subject of apatite chemistry (project APACHE).



Influence of iron oxidation state on magnetic properties of iron substituted hydroxyapatite

ME Zilm¹, M. Jain², M Wei¹

¹ Department of Materials Science and Engineering, University of Connecticut, Storrs, CT, USA.

² Department of Physics, University of Connecticut, Storrs, CT, USA.

INTRODUCTION: Materials with multifunctionality are auspicious for medical applications. Magnetic materials, in particular, are of high interest for the remote actuation. Particles injected intravenously are guided with a magnetic field to a targeted site for targeted drug delivery or hyperthermia treatments¹. Many magnetic materials lack an intrinsic biocompatibility and vice versa for biocompatible materials. Current magnetic biomaterials rely on composites of a magnetic and a biocompatible material to achieve multi-functionality. We have taken an alternative approach to this method. The properties of hydroxyapatite (HA), the mineral phase of bone, are readily modified through substitution of different atomic sites². Exploiting these properties, magnetic elements can substitute the calcium site of HA and induce an intrinsic magnetism. We have achieved fabrication of biocompatible, magnetic HA through iron substitution.

METHODS: HA was synthesized via a wet chemical method; particle size was modified by controlling solution concentration, temperature and ageing time. Iron substituted HA was fabricated via ion exchange. Briefly, HA powder was immersed in iron salt solutions containing various amounts of Fe²⁺ and Fe³⁺. Collected powders were then characterized using X-ray diffraction (XRD), Fourier-transform infra-red spectroscopy (FTIR), energy dispersive X-ray spectroscopy (EDXS) and X-ray photoelectron spectroscopy (XPS). Crystallite size of fabricated powders was calculated using Scherrer's formula, and the magnetic properties were measured by vibrating sample magnetometry (VSM).

RESULTS: The HA powders had a crystallite size of ~ 40 nm or ~ 300 nm. XRD and FTIR spectrums of iron-substituted HA are indicative of a phase of pure substitution. EDXS confirmed the presence of iron. High resolution XPS scan of the Fe 2p peak supported the observations from XRD and FTIR with observed peak positions of ~710 eV and ~712 eV, associated with iron phosphate bonding. Magnetic properties of iron substituted. HA varied based on crystal size and oxidation state. Figure 1

depicts the varying magnetic properties ranging from paramagnetic to super-paramagnetic to antiferromagnetic.

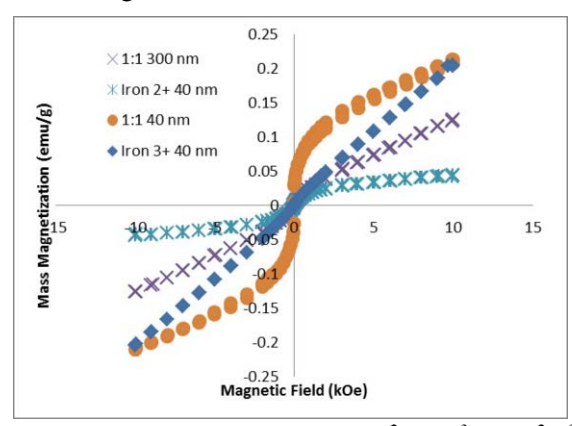


Fig. 1: Magnetic properties of Fe^{2+} , Fe^{3+} , Fe^{2+} ,

DISCUSSION & CONCLUSIONS: An intrinsic magnetic biomaterial based on iron substitution for calcium in HA has been successfully fabricated via ion exchange. Both Fe²⁺ and Fe³⁺ substituted calcium sites; the binding energy observed at ~710 and ~712 eV correspond to Fe²⁺ and Fe³⁺ bonded to phosphate. The magnetic properties can be tailored based on the oxidation state of iron. Paramagnetic properties arose from the spin-only electron contribution of Fe³⁺. Anti-ferromagnetic and super-paramagnetic properties are attributed to the exchange interactions of iron through oxygen and or phosphate atoms. Biocompatible and iron-substituted HA magnetic has successfully fabricated, which has the potential for biomedical applications, intravenous injection for targeted cancer therapy.

REFERENCES: ¹ G.F. Goya, V. Grazu and M.R. Ibarra (2008) *Curr Nanosci* **4**:1-16. ² J.C. Elliot, R.M. Wilson and S.E.P Dowker (2002) *AXA* **45**:172-181. ³ E.R. Kramer, A.M. Morey, M. Starch et al (2013) J. Mater. Sci. **48**:665-673.

ACKNOWLEDGEMENTS: The authors would like to thank NSF GK-12 program and NSF grant (CBET-1133883) for their support.



Development of ion substituted calcium phosphate cement for spinal repair

RW Ormsby¹, FJ Buchanan¹, S Best², R Cameron², NJ Dunne¹

¹ Biomaterials Research Group, School of Mechanical and Aerospace Engineering, Queens University Belfast, UK. ² Cambridge Centre for Medical Materials, Department of Materials Science and Metallurgy, University of Cambridge, UK

INTRODUCTION: Ion substituted calcium phosphate cement (CPC) offers the potential to improve the mechanical and bone remodelling properties of bone cement used in vertebroplasty [1]. Magnesium (Mg) expedites the resorption process of bioceramics [2]. Mg has also been shown to stabilise the crystal structure of tricalcium phosphate (TCP) [3]. Similarly silicon (Si) has been included in hydroxyapatite (HA) to increase the rate of bone repair [4]. The aims of this study were two-fold; (i) Synthesise Mg and Si substituted TCP powders; (ii) Use these TCP powders to produce and characterise Mg-Si substituted CPC.

METHODS: Solid-state hydrothermal reactions were used to synthesise Mg and Si substituted α-TCP. This was achieved via a stoichiometric reaction between calcium hydrogen phosphate (CaHPO₄), calcium carbonate and magnesium oxide (MgO), or CaHPO₄ and calcium silicate. Xray diffraction (XRD) was used to confirm the phase composition of the TCP powders produced. XRD also confirmed the extent of ion substitution into the crystal structure of TCP. These ion substituted α -TCP powders were mixed with disodium hydrogen phosphate producing injectable CPC, as per the methods described by O'Hara et al [1]. The weight loadings (wt %) of Si used were 1.0, 2.5, 5.0, and 10.0. The wt % of Mg used were 0.1, 0.25, 0.5, and 1.0. CPC containing Si and Mg collectively) (both individually and produced. Setting, compressive and injectability properties were characterised with CPC (100% α-TCP) used as a control. Statistical analysis using ANOVA with Gabriel's Pairwise Comparisons post hoc test was conducted (PASW Statistics 18, USA).

RESULTS: Synthesis of ion substituted α -TCP powders was confirmed via XRD. Mg substituted CPC (Mg-CPC) provided non-significant reduction in setting properties; with significant improvements in compressive strength and injectability (Table 1). Si substituted CPC (Si-CPC) showed non-significant reductions for the properties measured (Table 2).

Table 1. Percentage changes for Mg-CPC vs. Control (* denotes p<0.05, ** denotes p<0.01).

wt.% Mg	0.1	0.25	0.5	1.0
Setting Time	-2.0	-4.0	-5.0	-5.0
Injectability	7.0	7.0	14.4	26.2*
Compressive Strength	47.5**	48.0*	46.0**	33.0*

Table 2. Percentage changes for Si-CPC vs. Control.

wt.% Si	1.0	2.5	5.0	10.0
Setting Time	-3.0	-4.0	-6.0	-8.0
Injectability	-1.0	2.0	3.0	7.0
Compressive Strength	-3.0	-5.0	-4.0	-7.0

The CPC substituted with Mg and Si (Mg-Si-CPC) demonstrated no significant reductions in the setting times or extent of injectability, however significant improvements in compressive strength (43.4%) were recorded for Mg-Si-CPC containing 0.25wt.% Mg; and 10wt.% Si content (p<0.001 vs. Control).

DISCUSSION & CONCLUSIONS: Significant improvements in compressive strength were recorded for Mg-CPC and Mg-Si-CPC. It is postulated that Si ions substitute into the TCP crystal structure as Ca₃(P_{0.9}Si_{0.1}O_{3.95})₂,⁵. It is suggested that Mg is substituted into TCP in the formula Mg_xCa_{3-x}(PO₄)₂ (x=1 or 2). When Mg is substituted into TCP the Mg-O bond becomes stronger, whereas the Ca-O bonds are weakened by the increased bond length compared to the Mg-O interaction. It is hypothesised that this is the reason for the Mg stabilising the structure of TCP, and improving the compressive properties of CPC developed herein.

REFERENCES: ¹ R. O'Hara et al (2012) *Acta Biomater* **8(11)**:4043–4052. ² S. Dorozhkin (2009) *Materials* **2(2)**:399-498. ³ J. Ando (1958) *Bull Chem Soc Jpn* **31**:201–205. ⁴ E. Thian et al. (2006) *J. Mater. Sci.* **41(3)**: 709-717.

ACKNOWLEDGEMENTS: Financial support for this project is provided by Orthopaedic Research UK.



Experimental and analytical investigations into the mechanism of filter pressing of calcium phosphate pastes during injection

R O'Neill, F Buchanan, A Lennon, N Dunne

School of Mechanical & Aerospace Engineering, Queen's University Belfast, UK

INTRODUCTION: The location or mechanism by which filter pressing occurs during the injection of calcium phosphate cement (CPC) remains unknown [1]. The aim of this study was to establish if existing filtration theories correspond with experimental results obtained in order to identify the filter pressing mechanism.

METHODS: In this study beta-tricalcium phosphate (β-TCP) and deionised water were mixed to form a non-setting calcium phosphate paste (CPP), which was used to simulate the flow of CPC. The CPP was loaded into a syringe and extruded at a constant rate to a maximum force of 100 N. The variables investigated were liquid-topowder ratio, LPR, (40, 42.5 and 45 %), extrusion rate (5, 10 and 20 mm/min), needle gauge (12, 13 and 14 G) and length (3, 7.5 and 11 mm). The level of injectability and the LPR of sections of the extrudate and paste remaining in the barrel were determined[1, 2]. In order to model the filter pressing of CPP, it was assumed that the paste in the barrel acted as a compressible cake. By exerting a mechanical force on the cake, the filtrate (i.e. extruded paste) is squeezed out, which is referred to as 'expression of the cake' [3]. A derivation of Darcy's law was used (Equation 1):

$$\Delta P = \alpha_{av} \mu c_{av} \frac{Q^2}{A^2} t \tag{1}$$

where ΔP is required pressure to compress the cake, α_{av} is the average specific cake resistance, c_{av} is the concentration, and A is area of the cake. Viscosity and flow rate of the filtrate are denoted by μ and Q respectively and t represents time.

RESULTS: Comparing the LPR of sections of the extrudate and paste remaining in the barrel, it was evident that phase separation occurred from the onset of injection and continued throughout the injection process until a non-injectable portion of CPP remained in the barrel. With regards to injectability, no significant difference (*p*-value <0.05) was observed between experiments conducted with or without cannulated needles. The model provided good agreement with regards to injectability (Fig.1 and Table 1) but underestimated the extent of phase separation (Table 1).

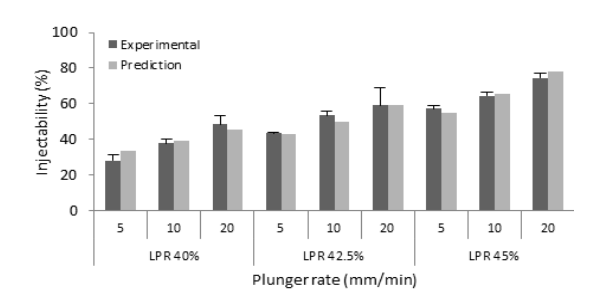


Fig. 1: Effect of plunger rate and initial LPR on injectability (Experimental and model results)

Table 1. Regression coefficients for predicted vs experimental injectability and LPR values; m and c are coefficients of the regression line and R^2 is the coefficient of determination.

	m	c	R^2
Injectability	0.99	0.36	0.96
LPR _{Extrudate}	1.37	-15.43	0.94
LPR _{Paste in barrel}	0.79	7.24	0.80

DISCUSSION & CONCLUSIONS: This study shows that the location of filter pressing is in the syringe barrel, as needle geometry does not have a significant effect on injectability. The correlation between experimental results and cake expression theory indicate that the mechanism of filter pressing is due to consolidation of particles forcing water to migrate to a region of less pressure, i.e. barrel exit. The migrating water has a lubricating effect enabling granular flow through the barrel exit. As the LPR of the paste is reduced the pressure required to induce granular flow is increased. The pressure required quickly exceeds pressure that can be produced by hand during injection. By establishing that existing filtration theory corresponds with filtration of CPP during injection this study has given a potential new insight into the mechanism of filter pressing of CPC.

REFERENCES: ¹ M. Habib *et al* (2008) *Acta Biomater* **4**:1465-1471. ² R. O'Hara *et al* (2010) *J Mater Sci Mater Med* **21**:2299–2305. ³ L. Svarovsky (2000) in *Solid-Liquid Separation, Butterworth-Heinemann* Elsevier.

ACKNOWLEDGEMENTS: The authors would like to thank DEL UK for financial support.



Injectable lubricants for prosthetic articular joints

KI Pakkanen, S Lee

Department of Mechanical Engineering, Technical University of Denmark, Kgs. Lyngby, DK

INTRODUCTION: Wear particles of orthopaedic implants have long been recognized as the principal cause of degradation and failure of the articular joint implants [1]. Thus, improvement of tribological properties of implant materials is a key requirement to improve longevity of prosthetic articular joints. The present study proposes to solve this problem by administering external lubricants to prosthetic joints.



This approach is primarily based upon recent development of lubricant additives that improve anti-wear properties of a variety of materials in aqueous solutions [2-4].

Fig. 1: A schematic illustration of conceptual approach to improve the longevity of orthopaedic implants in this work.

A most outstanding novelty of this approach is that since the external lubricants are independently administered from the implant manufacturing and surgical processes, those who have already received prosthetic joint surgeries, not only the future patients, can benefit for longer lifetime of the prosthetic implants.

METHODS: External lubricants were formulated by dissolving commercial amphiphilic triblock copolymers, PEO-PPO-PEO, in aqueous buffer solution. Pin-on-disk tribometry was employed to assess the lubricating capabilities of external lubricants for the sliding contacts between UHMWPE and CoCrMo tribopair. Various biopolymers, including hyaluronic acid (HA), bovine submaxillary mucin (BSM), bovine serum albumin (BSA) etc., have also been tested. For invitro cytotoxicity tests, cell morphology and standard MTT tests have been performed.

RESULTS: Tribological studies have shown that all the PEO-PPO-PEO copolymers tested displayed immediate reduction effects in the coefficient friction upon injection for the sliding contacts between CoCrMo pin and UHMWPE disk in calf

serum. A representative example, the case where 1 ml of F127 solution (20%) injected into 2 ml of serum is shown in Figure 2.

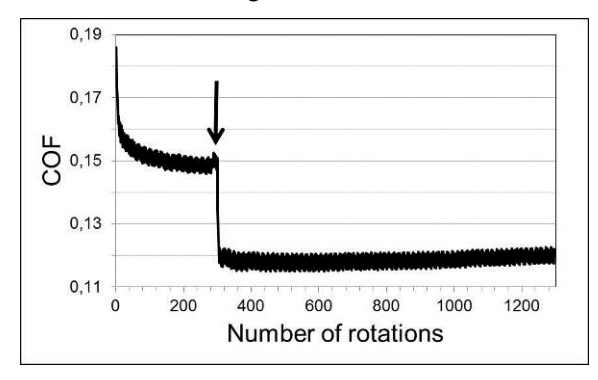


Fig. 2. 1 ml of F127 solution (20%) injected (arrow) into serum solution at 300th rotation immediately reduced the coefficient of friction, and persisted to the end of tests (1,300 rotations, ca. 38 m).

The efficacy of reducing the coefficient of friction was roughly proportional to the concentration of lubricant additives. But, none of the biopolymers tested show lubricating effects. In-vitro cytotoxicity tests have shown that more hydrophilic copolymers are more favourable in cell viability, as tested from both cell morphology and MTT tests.

DISCUSSION & CONCLUSIONS: The first test results in this work indicate that the new approach proposed i.e. injection of external lubricants to prosthetic joints, is very promising to improve the tribological properties of orthopaedic implants, thus potentially their longevity. In addition, in vitro biocompatibility tests also support that the selected lubricant additives reveal positive cell viability.

REFERENCES: ¹ S.M. Kurtz (2001) *The UHMWPE Handbook: Utra-High Molecular Weight Polyethylene in Total Joint Replacement*, Elsevier. ² S. Lee, N.D. Spencer (2007) Achieving ultalow friction by aqueous, brush-assisted lubrication in: *Superlubricity* (eds. A. Erdmir, J.-M. Marin) Elsevier, pp 365-396. ³ M. Müller, S. Lee, H.A. Spikes et al (2003) *Tribol Lett* **15**: 395-405. ⁴ W. Hartung, A. Rossi, S. Lee et al (2009) *Tribol. Lett.* **34**: 201-210.



Optimization of an acidic calcium phosphate cement with enhanced radiopacity

J Engstrand, J Jacob, H Engqvist, C Persson

Div. of Applied Materials Science, Dept. of Engineering Sciences, Uppsala University, SE

INTRODUCTION: Calcium phosphate cements (CPCs) are commonly used in biomedical applications due to their resemblance to the mineral phase of bone. However, due to this resemblance the radiopacity of CPC is very similar to that of bone. The inorganic radiopacifiers (e.g. ZrO₂ and BaSO₄) commonly used in non degradable bone cements are not water-soluble and cements utilizing these radiopacifiers have shown an increased bone resorption [1]. To overcome this problem, other radio opaque agents need to be investigated. Studies have shown that strontium can enhance the osteoblasts activity, which could lead to increased bone formation [2]. Hence, soluble strontium salts could be an alternative for enhanced radiopacity. However, additives that do not (or only partially) take part in the setting reaction may have a negative effect on the cement's mechanical properties. In this study the influence of additions of strontium chloride (SrCl₂) on various properties of a CPC is evaluated. The objective is to find an optimal composition with regards to radiopacity, compressive strength (CS), and setting time.

METHODS: A screening study was performed with three factors included; wt% sodium pyrophosphate (SPP), wt% SrCl₂ and liquid phase (phosphoric acid, citric acid, or water). The maximum amounts of SPP and SrCl₂ were fixed at 5 wt%, and 30 wt% respectively; and the concentration of the acids were kept at 2 M and 0.5 M for phosphoric acid and citric acid respectively. From the results of the screening study further testing was performed using 10 wt% SrCl₂ and varying the amount of SPP from 0.25 to 1 wt%. The CPC consisted of equimolar amounts of β-tricalcium phosphate and monocalcium phosphate monohydrate. The cement powders were mixed with the liquid in a powder to liquid ratio of 3.3 g/mL.

RESULTS: The CS measurements showed that the incorporation of 30 wt% SrCl₂ decreased the strength drastically (*Fig 1*). However, as the amount of SrCl₂ decreased, the effect on CS was not as pronounced. It was also seen that the incorporation of all additives increased the setting time remarkably. Most distinct was the increase to approximately 400 minutes for cements containing 30 wt% SrCl₂ together with 5 wt% SPP.

Furthermore, the setting of cements without any SPP or SrCl₂ is very short and molding was almost impossible. The radiopacity of the cements showed logarithmic relations, and 15 wt% and 30 wt% had a similar radiopacity of 1.4 and 1.5 mm Al/mm, respectively. To increase CS and decrease setting time it was desirable to have as low amounts of SrCl₂ as possible, which still showed radiopacity, and 10 wt% was hence chosen for further studies.

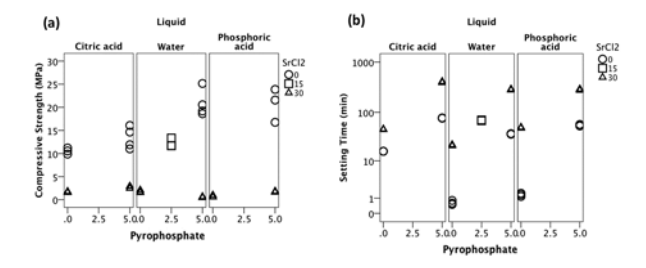


Fig. 1: (a) Compressive strength, and (b) setting time for cements investigated in the screening study. Three to four measurements were made for each group.

For cement compositions containing $10 \text{ wt}\% \text{ SrCl}_2$ in combination with varying amounts of SPP it was seen that the addition of SPP increased the CS exponentially from 4 MPa for 0.25 wt% to 20 MPa for 1 wt%. The setting time was also increased with increasing amount of SPP; however, between 0.5 wt% and 1 wt% the setting time was constant around 35 minutes.

bas shown that compositions containing 1 wt% SPP and 10wt% SrCl₂ could be a feasible alternative for cements requiring enhanced radiopacity. These cements have a setting time of approximately 35 minutes and show CS of around 20 MPa, this can be compared to cement without any SrCl₂ or SPP, but with 0.5M citric acid to make moulding possible, which had CS of around 12 MPa and a setting time of approximately 10 minutes.

REFERENCES: ¹ W Mitchell et al (2003) *Biomaterials* **5**:737–748. ² PJ Marie et al (2001) *Calcif Tissue Int* **69**:121-9.

ACKNOWLEDGEMENTS: The authors are grateful for financial support from FP7 NMP project Biodesign, STINT, Carl Tryggers Stiftelse, the Swedish Research Council and Stiftelsen Lars Hiertas Minne.



Accurate morphological characterization of βTCP scaffolds by isolating connected pores

S Jerban¹, G Baroud¹, M Bohner²

¹ Laboratoire de Biomécanique, Université de Sherbrooke, Québec, Canada. ² RMS foundation, Bettlach, Switzerland

INTRODUCTION: Macro-porous resorbable bone substitutes are employed to heal bone in large complicated and defects. **Biological** responses to resorbable bone substitutes (i.e. vascularization, scaffold resorption and bone deposition) appear to be strongly associated with microstructural parameters such as porosity, pore size, interconnection size and pores connectivity number. In connected complex void space (Fig.1a), it is not possible using previous characterization approaches to find a unique size, coordinates, volume and surface in a specific pore or interconnection¹. This abstract describes a characterization approach to identify and isolate connected pores and their shared interconnection in a morphological complex structure of high volume porosity. This approach improves not only the characterization accuracy but also opens avenues to understand the biological processes. Some algorithms were developed before to isolate connected pores in 3D µCT scanned scaffolds but they have some weak points like segmentation^{2,3}.

METHODS: To avoid over-segmentation (OvS), a marker based isolating algorithm was used which is partially similar to Watershed algorithm^{2, 3}. All local maxima of void space FDT map are labeled exclusively as initial markers for growing their associated pores¹. To avoid the OvS error, an idle marker elimination code is used in advance to exclude the redundant local maxima. Then, the isolation process is performed via a set of iterative steps (FDT= [1-FDTMAX]) by joining unlabeled voxels to the mentioned exclusively labeled markers. Finally, the probable remained OvSs are solved, by a particular merging algorithm to unite some isolated regions as one pore. To verify this combined isolating algorithm, more than 10 % of pores (randomly) in a central cube of scaffolds have been inspected visually.

RESULTS: In Fig.1 (a) and (b), connected pores before and after isolating in a small section of real scaffold are illustrated. The isolated pores and interconnections are presented by different colours (Fig.1b). In Fig.1 (c) and (d), the isolation process

is shown in a cylindrical section of the β -TCP scaffold 4 .

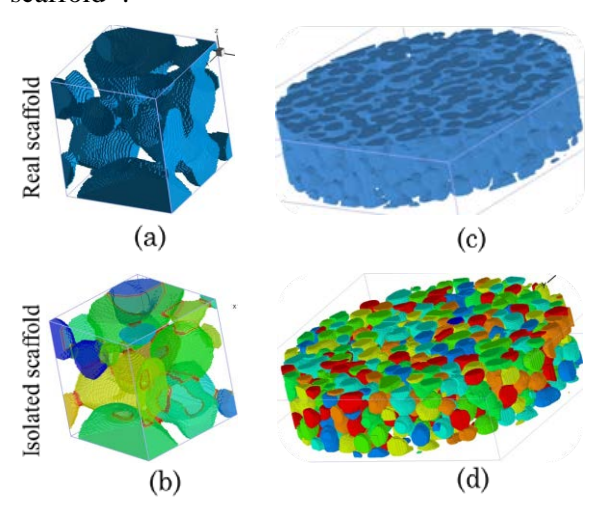


Fig. 1: Isolating pores and interconnections

The characterization results in two groups of fabricated β -TCP scaffolds, C and D are presented in Table.1⁴. The voxel size in μ CT scans was 30 μ m. Using the visual verification process, an error of less than 1 % of inspected items was found.

Table 1. Summarized characterization results

	Group C	Group D
Macro porosity [%]	52±1	53±1
Mean pore size [µm]	412 ± 3	852 ± 37
Mean interconnection size [µm]	149±7	262±17
Mean connectivity number ^a	5.5 ± 0.1	3.8 ± 0.1

^a Each shared interconnection was considered in both sides (both pores).

DISCUSSION & **CONCLUSIONS:** The proposed approach is appears accurate within 1 %. Characterization was improved strongly, *vs* old approach, particularly in interconnection size calculation¹. The understanding of biological responses can be improved via studying the derived pores network by isolating algorithm.

REFERENCES: ¹M. Bashoor-Zadeh et al (2011) *Biomaterials* **32**(27):6362-6373. ² A.C. Jones et al (2007) *Biomaterials* **28**(15):2491-2504. ³ S. Yue et al (2011) *Acta Biomater* **7**(6):2637-2643. ⁴ M. Bohner et al (2005) *Biomaterials* **26**(31):6099-6105.

